Quality of insertion in cochlear implants : a clinical and temporal bone study

Daniele de Seta

Université Pierre et Marie Curie

Sapienza Università di Roma

Ecole doctorale Physiologie Pathophysiologie et Thérapeutique

Scuola di dottorato in Neuroscienze Clinico Sperimentali e Psichiatria

Laboratoire INSERM UMR 1159 "Minimally Invasive Robot-Based Hearing Rehabilitation"

Quality of Insertion in Cochlear Implants: A Clinical and Temporal Bone Study

Daniele De Seta

Joint PhD thesis

Co-Director: Prof Olivier Sterkers

Co-Director: Prof Patrizia Mancini

Co-Encadrant: Dr Yann Nguyen

Defended in Rome, May 24 2016

Dissertation committe:

Prof Gaetano Paludetti

Prof Jean Marc Edeline

Prof Christophe Vincent

Prof Adelchi Croce

A Francesca

Aknowledgements

First of all I would like to express my sincere gratitude to my directors and coordinators

Professor Olivier Sterkers,

I am grateful to you for giving me the opportunity to work in your research unit for carry out this thesis under joint supervision and later for having me proposed to be part of your group in the hospital. Thank you for continuing to share your knowledge and for being a guide for me in this project, it is a privilege and an honor to have you as a mentor.

Doctor Patrizia Mancini,

Thank you for having introduced me in the world of the cochlear implants, and for making this joint project possible.

Doctor Yann Nguyen,

My “co-encadrant” of this thesis, thanks for everything. Your support and help in the accomplishment of this project have been essential.

Professor Roberto Filipo,

Thank you for introducing me to the otology and the cochlear implants, for guiding me during the residency and for beginning this project.

I thank the committee members

Prof Gaetano Paludetti and Dr Jean Marc Edeline that accepted to read and evaluate my work.

Prof Christophe Vincent that accepted to came in Rome just for one day to be part of the committee.

Prof Adelchi Croce that accepted to be part of the committee.

Dr Evelyne Ferrary,

Thank you for the help, for your teachings and your support given during these years spent in the lab. Thank you for all the time spent on the countless corrections and re-readings of articles, abstracts, posters and powerpoints…

Dr Isabelle Mosnier,

Thanks for your help in the writing and re-writing of the papers that finally have been accepted! Thanks for your trust and confidence.

Dr Jean Loup Bensimon,

Thank you for the cone beam CT acquisition and for your help in the analysis of the images

Prof Dominique Heymann and Jerome Amiaud,

Thank you for accepting to take part of this project giving me the possibility to perform the histologic analysis in your lab in Nantes.

My collegues and friends in the lab

Dr Renato Torres, gracias por todo amigo mio!

Dr (PhD!) Guillaume Kazmitcheff, thanks for all the time spent togheter in the lab and outside…NYC, Grenoble, you never came in Roma!

Dr Elisabeth Mamelle, when I met you in Beaujon (it was long time ago…) I never imagined to work with you in the lab and later in the hospital!

I would like to thank:

The French Society of Otolaryngology (SFORL) for the 2013 research grant that partially financed this thesis.

MEDEL company, in particular to Dr Michel Beliaeff, Dr Samia Labassi and Dr Vincent Pean, for the unconditional support of material (MedEl Flex 28 dummy arrays), the help in the statistical analysis of the data and the sponsorship for the participation to congresses.

Last but not the least, I would like to thank my family,

My father, the reference for me in ENT,

My mother, who always supported whatever the choice,

Claudia, because is my sister!

Abstract

The cochlear implantation represents the standard technique to restore the hearing in totally deafened persons, and the indications during the last years are widening also to patients with residual hearing or presenting single sided deafness. Despite the overall good to very good results after cochlear implantation reported in literature a wide heterogeneity of the hearing outcomes emerges in the single studies and poor results both in unilateral and bilateral cochlear implantation are still reported. Several patients' specific factors have been identified as affecting postimplant speech perception score, including duration of deafness, residual preoperative speech recognition, and different speech coding strategy. In this thesis the anatomy of the cochlea and the position of the electrode array in implanted patients have been studied with the attempt to identify the affecting factors that contribute to the variability of the inter- and intra-individual speech discrimination scores both in bilaterally and unilaterally implanted patients. Moreover, following the expanding indication for cochlear implantation, the preservation of inner ear structures is becoming recommended for all cochlear implant candidates, regardless of their preoperative hearing. A radio-histological temporal bone study with a motorized insertion of the array was performed in order to identify the insertion forces parameters that could predict the possible traumatism involving the inner ear. The results of this thesis showed a relationship between the intracochlear electrode position and hearing performance in the short term follow up, whereas the neural plasticity would play an important role in the adaptation of the cochlear implant to the neural structures in the long term. A correlation between insertion forces and inner ear traumatism was found in temporal bones. Two different force profiles for traumatic and atraumatic insertion were obtained; these values, if confirmed by further studies, could be useful for the development of future force feedback automated cochlear implant insertion tool in order to reduce the risk of insertion related damage and provide the best chance for an optimal hearing rehabilitation in cochlear implanted candidates.

Keywords: cochlear implants, electrode position, cochlear anatomy, insertion forces, hearing performance, long term**.**

Résumé

L'implant cochléaire représente le dispositif de référence pour réhabiliter l'audition des patients atteints de surdités sévère à profonde. Les indications se sont récemment étendues vers les patients avec une audition résiduelle avec de bons résultats. Il persiste cependant une grande hétérogénéité des résultats auditifs. Plusieurs facteurs ont été identifiés comme influençant les performances auditives: durée de la surdité, intelligibilité préopératoire et stratégie de codage. Dans cette thèse, l'anatomie de la cochlée et la position postopératoire du porte-électrodes ont été étudiés afin d'identifier les facteurs de variabilité de la discrimination vocale inter- et intra-individuelle. Les résultats de cette thèse ont montré un lien entre la position de l'électrode et les performances auditives à court terme, alors que la plasticité neuronale pourrait jouer un rôle important dans l'adaptation de l'implant cochléaire aux structures neurales à long terme. De plus, la préservation des structures cochléaires est maintenant recommandée pour tous les candidats à l'implantation, quelle que soit leur audition préopératoire. Une étude radio-histologique sur rochers avec une insertion motorisée du porte-électrodes a été réalisée afin d'identifier les paramètres des forces d'insertion qui pourraient prédire le traumatisme de l'oreille interne lié à l'insertion. Une corrélation entre les valeurs de forces d'insertion et le traumatisme cochléaire a été trouvée dans les os temporaux. Ces valeurs, serviront au développement d'outils d'insertion « intelligents » pour réduire les lésions liées à l'insertion et ainsi conduire à des conditions de rééducation auditive optimale.

Mots-clés: implant cochléaire, position de l'électrode, anatomie cochléaire, forces d'insertion, performances auditives, long terme

Riassunto

L'impianto cocleare rappresenta il gold standard per la riabilitazione dell'udito nei soggetti affetti da sordità grave e profonda bilaterale; le indicazioni durante gli ultimi anni si stanno ampliando anche per i pazienti con udito utile parzialmente conservato sulle basse frequenze o sordità unilaterali. Nonostante gli ottimi risultati uditivi postimpianto riportati in letteratura una vasta eterogeneità dei risultati emerge nei singoli studi e pazienti con scarsi risultati sia dopo impianto cocleare unilaterale che bilaterale vengono ancora riportati. Diversi fattori paziente specifici sono stati individuati nell'influenzare le performance postimpianto tra i quali la durata della sordità, l'udito residuo preoperatorio, e le differenti strategie di codifica del segnale da parte del processore. In questo lavoro di tesi l'anatomia della coclea e la posizione degli elettrodi in pazienti impiantati sono stati analizzati con il tentativo di identificare i fattori in grado di contribuire alla variabilità dei risultati di discriminazione vocale inter e intra-individuale postimpianto sia in pazienti impiantati in bilaterale che in unilaterale. Inoltre, seguendo le nuove tendenze nelle indicazioni per l'impianto cocleare, la chirurgia mininvasiva con conservazione delle strutture dell'orecchio interno e' raccomandata per tutti i candidati di impianto cocleare, a prescindere dalla funzione uditiva preoperatoria. Uno studio radio-istologico su osso temporale con un inserimento motorizzato dell'array portaelettrodi è stato eseguito al fine di identificare i parametri della forza di inserzione che potrebbe determinare il traumatismo delle strutture dell'orecchio interno (membrana basilare, legamento spirale, lamina spirale ossea). I risultati di questo lavoro di tesi hanno mostrato una relazione tra la posizione dell'elettrodo e le performance uditive nel breve periodo di follow-up, mentre la plasticità neuronale svolgerebbe un ruolo importante nell'adattamento dell'impianto cocleare alle strutture neurali nel lungo periodo. Una correlazione tra le forze di inserimento e il traumatismo dell'orecchio interno è stata identificata su ossi temporali. Due diverse funzioni della regressione lineare delle differenti curve per l'inserimento traumatico ed atraumatica sono state ottenute; questi valori, se confermati da ulteriori studi, potrebbero essere utili per lo sviluppo di futuri strumenti di inserimento automatizzato dell'impianto cocleare con controllo in tempo reale delle forze ai fini di ridurre il rischio di traumatismo dell'orecchio intero legato inserimento e fornire la migliore possibilità di una riabilitazione ottimale dell'udito nei pazienti con impianto cocleare.

Parole chiave: impianto cocleare, posizione degli elettrodi, anatomia cocleare, forze di inserzione, risultati uditivi, lungo termine

Table of Contents

Introduction

The cochlear implantation represents the gold standard technique to restore the hearing in deafened patients. The cochlear implant is able to replace the function of hair cells that are no longer able to generate electrical impulses in response to sound, representing a bionic organ able to bypass the transduction mechanism of the sound wave normally done in the outer, middle and inner ear and directly stimulate the spiral ganglion of the cochlear nerve. Nevertheless, despite the overall excellent results in speech perception among cochlear implanted patients, results are still heterogeneous with some implanted patients being poor performers after unilateral and/or bilateral cochlear implantation (Holden et al. 2013, Mosnier et al. 2009). Moreover some improvements still have to be done in the processing of signal and the stimulation strategy in order to improve the speech understanding in difficulty noisy condition and quality of the perceived sound (e.g. appreciation of music).

The classical indication for cochlear implantation was the severe to profound sensorineural hearing loss; over the past decade indications for cochlear implantation evolved and include now also the hearing loss involving only high frequencies or in some selected cases the single sided deafness. As a consequence, surgery has evolved toward a low intracochlear trauma insertion in order to maintain the integrity of inner ear structures in all cochlear implants recipients, even for those destined to electric-only stimulation. Minimizing trauma during implantation may offer several advantages. For patients with "usable" preimplant low-frequency hearing, limiting trauma can allow for the preservation of the residual hearing, allowing the electric-acoustic stimulation. For all the other patients, reducing intracochlear damage may limit the fibrosis and ossification, making easier the revision surgery for device failure or upgrade; this is becoming increasingly important as more patients are undergoing implantation during infancy and early childhood, thereby increasing the likelihood that reimplantation will be required during their lifetime. Moreover, limiting injury potentially allows for the application of future technologies, such as cellular regeneration or other novel cochlear nerve stimulation technologies (Carlson et al. 2011). The concept of soft surgery has been introduced in 1993 by Lehnhardt, and since then his technical modification is employed broadly by numerous implantation centers.

The preservation of the inner ear structures during the insertion of cochlear implant and the correct understanding of the optimal site of stimulation should permit to achieve the best hearing performance. As a consequence, the quality of insertion in the cochlear implant has been extensively studied during the last decades. In this context, three parameters have been more accurately investigated: the translocation of the array with the consequent basilar membrane rupture, the depth of insertion of the electrode array, and the proximity of the electrodes to the spiral ganglion cells. Until now, it is not clear whether the position of an electrode within the cochlea might be a prognostic factor with regard to the hearing performance results since many different factors could influence this outcome. All the different electrode arrays available have their own specific length, diameter, shape, and physical properties that influence the trajectory during the insertion and determine the final position in the cochlear lumen. The cochlear anatomy and the characteristics of the electrodes

array could influence the friction forces applied to the cochlea during the electrode array insertion and thus the insertion related traumatism to the inner ear structures (*i.e.* spiral ligament, basilar membrane, lamina spiralis ossea). Various studies have focused on measuring mechanical insertion forces and insertion trauma caused to the cochlea from different cochlear implant electrodes, and the influence of the insertion speed, use of lubricants, different electrodes array, or different insertion tools on the friction forces have been investigated and reported so far (Nguyen et al. 2015, Miroir et al. 2012, Majdani et al. 2010, Rohani et al. 2014, Roland 2005). To date, the relationship between insertion forces and histological traumatisms remains to be demonstrated.

In this thesis the quality of insertion in cochlear implants has been investigated in clinical and temporal bones studies. The objective of this research was to investigate on the role of the electrode array insertion and its final position within the cochlea on the hearing outcomes of the implanted patients and the preservation of the inner ear structures during the insertion in temporal bones with particular attention to the mechanical insertion related trauma. A secondary objective of the study was to evaluate the reliability of the cone beam CT scan (CBCT) to identify the correct scalar position of the electrode array within the cochlea.
In the first two chapters of this thesis the basics of the anatomy (chapter 1) and physiology (chapter 2) of the ear and hearing are reported. The chapter 3 is focused on the cochlear implants reporting the basics of the transduction of the signal, a brief history from the beginning to the recent advances in the new speech coding strategies and the expanding indications. The second part of the thesis reports the clinical and temporal bone studies conducted during the period 2013-2016 at the laboratory of the UPMC Paris 6 and in the hospitals of Rome La Sapienza and Paris Pitié Salpetriere. The chapter 4 reports the radio-histological study performed on temporal bones and cochlear implanted patients to validate the reliability of cone beam CT scan on the correct assessment of intracochlear positioning of the electrodes array. In chapter 5 the clinical studies performed on uni- and bilaterally implanted patients to evaluate the influence on hearing performance of the electrode placement in short and long term use are reported. Finally, in the chapter 6, the insertion related traumatism and insertion forces are investigated and the results of a temporal bone study with correlation between insertion forces and histologic traumatism are reported. The conclusion and perspective of the future research project are reported in the last chapter.

All the studies performed on temporal bones have been performed in the INSERM laboratory UMR-S 1159, University Pierre et Marie Curie – Paris 6; the fresh temporal bones were provided by the Institute of Anatomy of the University René Descartes - Paris 5. The histologic analysis was performed in the laboratory physiopathology of bone resorption INSERM UMR 957 in Nantes.
Clinical studies were performed at the cochlear implant center, Policlinico Umberto I - Sapienza University of Rome and at Pitié-Salpêtrière Hospital, Unit of Otology, Auditory Implants and Skull Base Surgery in Paris

1 Anatomy

1.1 EXTERNAL AND MIDDLE EAR

The external or outer ear is the portion of the ear lateral to the tympanic membrane. It consists of the auricle or pinna and the external auditory canal.
The auricle is a semicircular plate of elastic cartilage surrounding the concha, which is the depression posterior to the external auditory meatus.
The external auditory canal (3.5 cm in length, with a diameter of 1 cm) is bounded medially by the tympanic membrane and is lined with a thin layer of skin with little subcutaneous tissue medially, but containing laterally numerous hair follicles and ceruminous and sebaceous glands. The tympanic membrane is composed of three layers: the outer squamous cell epithelial layer, the medial mucosal layer facing the middle ear, and the fibrous layer. It is identified by a prominent landmark, the manubrium of the malleus, limited superiorly by its short process and inferiorly by a rounded end named umbus. The part of tympanic membrane superior to the short process of the manubrium lacks of the fibrous layer, this portion is hence called the pars flaccida (Shrapnell's membrane); the major or inferior portion of the tympanic membrane is referred to as the pars tensa.

The middle ear is the space between the tympanic membrane and the bony capsule of the labyrinth in the petrous portion of the temporal bone, and contains the ossicular chain with its associated muscles, the orifice of the eustachian tube, and the vascular system. The tympanic cavity is divided into the epitympanic, mesotympanic, and hypotympanic regions. The hypotympanic portion lies inferiorly to the aperture of the eustachian tube and the round window niche This portion of the middle ear contains various bony trabeculae and the bony covering of the jugular bulb. The mesotympanic portion of the middle ear is limited superiorly by the second portion of the facial canal and inferiorly by the RWN. This region contains the oval and round windows, the stapes, thestapedius muscle posteriorly, and the canal for the tensor tympani muscle anteriorly. In the oval window, the footplate of the stapes bone is held in place by the annular ligament. The RWN forms a deep recess that obscure the round window membrane (RWM). The RWM is a fibrous membrane covered with a layer of mucosa that is roughly kidney bean shaped. In the posterior mesotympanum there are two bony recesses of clinical importance: the facial recess lateral to the vertical segment of the facial, and the sinus tympani medial to the facial canal. These two recesses are important clinically as they frequently harbor chronic middle ear infection and must be controlled in surgery. The facial recess also provides access to the middle ear space and RWN in those procedures in which the ear canal wall is preserved (ie, intact canal wall mastoidectomy, cochlear implantation). A bony projection from the facial canal (pyramidal eminence) contains the tendon of the stapedius muscle before its insertion into the neck of the stapes bone. The epitympanum is the portion of the middle ear that is limited superiorly by the bony roof of the middle ear called the tegmen tympani. The medial wall of the epitympanum is formed by the bony prominence of the lateral and superior semicircular canal ampullae as well as the epitympanic portion of the facial (fallopian) canal. The head and neck of the

malleus and its articulation with the incus occupy most of the space in the epitympanum. These two ossicular masses are held in place by ligaments anteriorly and posteriorly to provide an axis of rotation for the ossicular chain. The epitympanic space communicates posteriorly through a narrow opening called the aditus ad antrum to the central mastoid tract of the mastoid cavity.

The head of the malleus and body of the incus function as a unit suspended by ligaments in the epitympanum. The tip of the long process of the incus articulates at a right angle with the head of the stapes so that the sound energy transmission initiated by medial displacement of the tympanic membrane is carried by the parallel displacement of the elongate processes of the malleus and incus to the head, crura, and footplate of the stapes. Since the surface area of the tympanic membrane is larger than that of the stapes footplate by a ratio of 25 to 1, the sound pressure density in the oval window and the inner ear fluids is similarly increased. Maintaining this ratio by various reconstructive methods constitutes an important principle in middle ear surgery. The stapes therefore acts in a piston-like fashion in the oval window. These auditory ossicles are controlled to some degree by two middle ear muscles, the tensor tympani and the stapedius. The tensor tympani muscle is housed in a bony semicanal in the anterior mesotympanum just superior to the orifice of the eustachian tube, and it is innervated by a branch of the fifth cranial nerve. Its action causes the drumhead to be pulled medially, thus raising the resonant frequency of the sound conduction system. The stapedius muscle arises within either on its own or with the fallopian canal and is accompanied by the motor portion of the facial nerve. It converges superiorly and anteriorly to form the stapedius tendon, which emerges through the pyramidal eminence to insert at the neck of the stapes. The stapedius muscle contraction displaces the stapes posteriorly and attenuates sound transmitted by the ossicular chain. Since reflex contraction of the stapedius muscle is activated by sound, it is regarded as a protective mechanism for the cochlea.

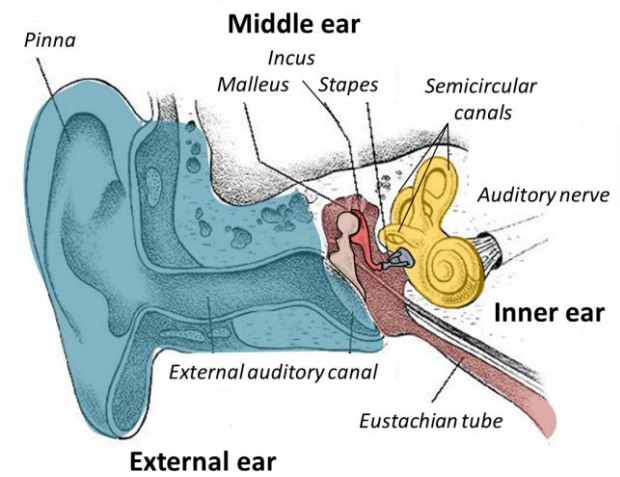

Figure 1.1 External, middle and inner ear

1.2 THE INNER EAR: COCHLEA AND POSTERIOR LABYRINTH

The inner ear is a structured fluid-filled cavity within the otic capsule of the petrous portion of the temporal bone. Within the bony labyrinth is contained the membranous labyrinth, which represents a continuous series of epithelial lined tubes and spaces of the inner ear containing endolymph and the sense organs of hearing and balance. The membranous labyrinth can be divided into three regions that are interconnected: the pars superior or the vestibular labyrinth with the exception of the saccule, the pars inferior (cochlea and the saccule), and the endolymphatic duct and sac. All of the sense organs of the labyrinth have in common that they contain hair cells with rigid cilia and are innervated by afferent and efferent neurons.

1.3 THE COCHLEA

The cochlea is a snail shaped bony structure coiled in 2 and ½ to 2 and ¾ turns. The maximal cochlear diameter is approximately 9 mm and its height about 5 mm. The cochlea is divided into three partitions or scalae. The scala media or cochlear duct is the cochlear extension of the membranous labyrinth and is filled with potassium (K+)-rich, sodium (Na+)-poor electrolyte fluid called endolymph. The other two partitions, the scala vestibuli and the scala tympani, are filled with perilymph, a Na+-rich, K+-poor electrolyte fluid and communicate in the apex of cochlea, the helicotrema (for review on inner ear fluids production and ions transport see: Sterkers et al. 1988, Coulognier et al. 2006) Figure 1.2 shows the partitions of the cochlea. The scala media is limited by the basilar membrane, superiorly by Reissner's membrane, and the stria vascularis with spiral ligament on the lateral side. When the cochlea is activated by sound, the scala media and its content bounded superiorly by Reissner's membrane and inferiorly by the basilar membrane, tend to move as a unit.

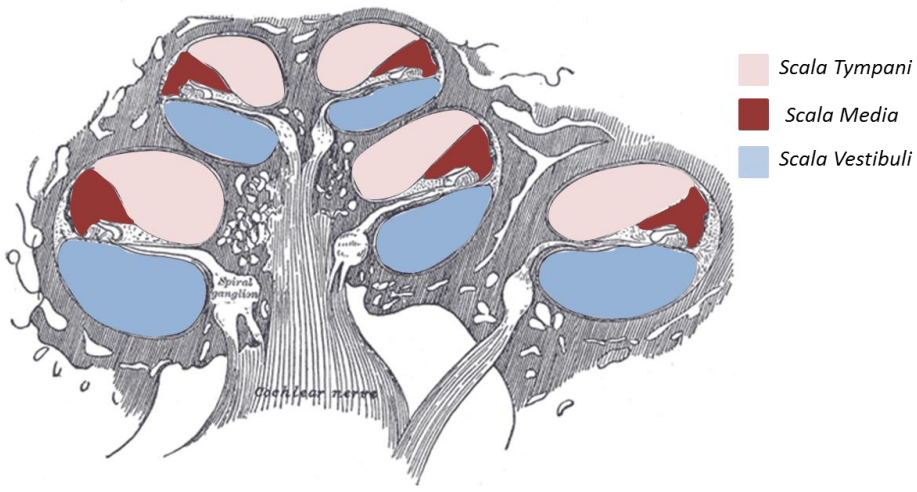

Figure 1.2. Intracochlear partitions. Modified from Gray, 1918

Organ of Corti

The organ of Corti contains many different kinds of cells. The sensory cells, the hair cells, so called because of the hair-like bundles that are located on their top, are arranged in rows along the basilar membrane. There are two main types of hair cells: outer hair cells and inner hair cells. The human cochlea has approximately 12,000 outer hair cells arranged in 3–5 rows along the basilar membrane, and approximately 3,500 inner hair cells arranged in a single row. On each outer hair cell, 50–150 stereocilia are arranged in 3–4 rows that assume a W or V shape whereas the inner hair cells stereocilia are arranged in flattened U-shaped formations. Between the row of inner hair cells and the rows of outer hair cells is the tunnel of Corti, bordered by inner and outer pillar cells. The outer hair cells are different from the inner hair cells in several ways. The outer hair cells are cylindrical in shape while the inner hair cells are flask-shaped or pear-shaped (Figure 1.3). The tallest tips of the outer hair cell stereocilia are embedded in the overlying tectorial membrane, whereas the tips of the inner hair cell stereocilia are not. Inner hair cells have similar dimension in the entire cochlea and all have approximately the same number of stereocilia (approximately 60). In addition to hair cells, other types of cells are found in the cochlea. Supporting cells of the organ of Corti are the Deiter's cells and Henson's cells, inner border and inner phalangeal cells, and the Claudius cells extending laterally toward the spiral prominence epithelium, forming the outer sulcus.

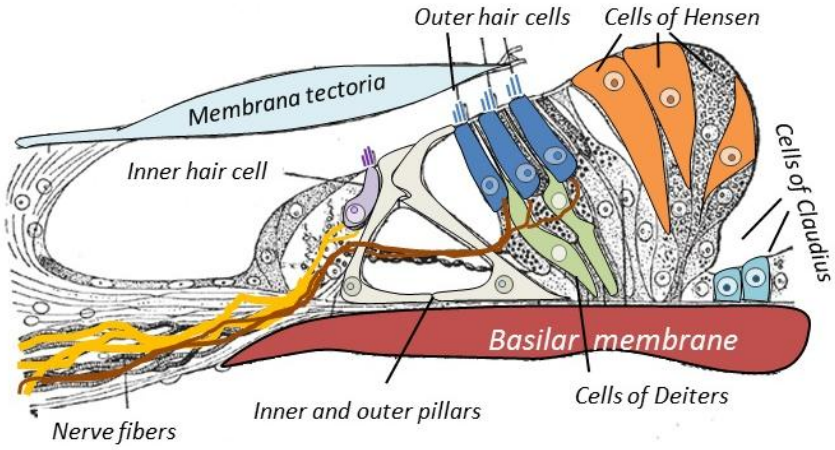

Figure 1.3. Organ of Corti.

Reissner's Membrane

The Reissner's membrane consists of an epithelial-cell layer facing the endolymph compartment of the scala media and a mesothelial facing the perilymph compartment of the scala vestibuli. RM is involved in homoeostasis and fluid transport. Integrity of this membrane is essential for hearing to maintain the endocochlear potential (80 mV). In the cochlear duct the cellular transport systems involved in the endolymph secretion may be altered by different hormones such as antidiuretic hormone and/or adrenocorticosteroid

hormones (Ferrary et al 1996). A scala vestibuli electrode insertion would probably disrupt the RM and abolish the endocochlear potential, at least locally, thereby leading to the loss of residual hearing that may have been present.

Basilar membrane

The basilar membrane consists of connective tissue and it forms the floor of the scala media. It has a width of approximately 150 μm in the base of the cochlea and it is approximately 450 μm wide at the apex. It is also stiffer in the basal end than at the apex. Due to this gradual change in stiffness, sounds that reach the ear create a wave on the basilar membrane that travels from the base towards the apex of the cochlea. This traveling wave motion is the basis for the frequency separation that the basilar membrane provides before sounds activate the sensory cells that are located along the basilar membrane. As we shall see in the next chapter the frequency analysis in the cochlea is complex, involving interactions between the basilar membrane, the surrounding fluid, and the sensory cells. The outer hair cells interact actively with the motion of the basilar membrane.

Spiral ligament

The spiral ligament anchors the basilar membrane at the lateral aspect of the cochlea. This attachment to the organ of Corti is characterized through the presence of tension fibroblasts that contain actin, myosin, and tropomyosin. Besides its mechanical function, the spiral ligament plays an important role for the supply and drainage of perilymph. The extensive capillary network suggests high level of communication between the scala tympani and scala vestibuli. The importance of this tissue for maintaining the ion balance is supported by the presence of gap junctions (connexins) and Na^+/K^+-ATPase pumps. The spiral ligament is thought to pump K^+ out of the perilymph and transport it for maintaining the high concentration of K^+ in the endolymph (Spicer and Schulte, 1991; Raphael and Altschuler, 2003). This is where the tip of the electrode first reaches the spiral ligament at the junction between the lower and upper basal turn. This is a critical step during the cochlear implant insertion with risks of perforation of this very important structure, that is, the spiral ligament. The spiral ligament supports the stria vascularis. This high metabolic tissue is served by an extensive meshwork of capillaries and forms the lateral aspect of the scala media between Reissner membrane and the spiral prominence. The stria vascularis plays an essential role for generation and maintenance of the scala media endocochlear potential. High expression of Na/K-ATPase, ionic pumps, and transporters and extensive vascularization highlights its energy consuming task.

Tectorial membrane

Tectorial membrane is an extracellular matrix that causes a shearing motion to stereocilia bundles when vibration enters the cochlea partition
The tectorial membrane is composed of radially running unbranched fibrils of type II and type IX collagen (type A) and highly branched fibers of type V collagen (type B) in which the thick fibers are embedded (Slepecky et al. 1992). The jelly-like matrix is composed of various glycoproteins, for example, the tectorins and otogelin. Mutations in human a-tectorin underlie two dominantly inherited non-syndromic deafnesses, that is, DFNA8 and DFNA12 (Verhoeven et al. 1998). Stereocilia imprints from the OHC tallest stereocilia tips indicate a rather close attachment of these structures to the tectorial membrane, while this close association between IHC stereocilia tips and the tectorial membrane remains unclear.

Spiral ganglion

The spiral ganglion contains 35,000 afferent bipolar neurons located in the helical Rosenthal's canal in the modiolus along the 1 and ¾ turns of the cochlea. The spiral ganglion terminates in a bulge containing the cell bodies of neurons innervating hair cells of the third turn. Peripheral processes run within the osseous spiral lamina to the habenula perforata to exit this bony canal and reach the hair cells.
Electric stimulation from cochlear implants evokes action potentials in remaining acoustic nerve fibers. Is not yet know where these spikes are initiated anatomically, but somas or initial axonal Ranviers nodes seem probable, indeed preserved dendrites may not seem to influence performance as evaluated histologically in patients treated with cochlear implants. Similarly, the amount of neurons necessary is not clear, but small number of neurons (10%) seem to be required to create speech performance, reflecting the redundancy present in the acoustic system (Rask-Andersen et al. 2012)

1.4 IMPLICATION OF COCHLEAR ANATOMY ON COCHLEAR IMPLANTATION

A large variation in cochlear anatomy has been described by several authors. The mean number of turns was found to be 2.6 with a range from 2.2 to 2.9 (929-degrees; range, 774-1037-degrees) (Erixon et al 2009), an extensive variation has been described in the cochlear diameter and cochlear duct length (Alexiades et al. 2014). This variation in cochlear lengths, angles between turns, and position in the skull base can influence the insertion of a cochlear implant. The basal end of the cochlea, named hook region, is of great interest for the surgical approach in cochlear implantation. The anatomy of this region varies making difficult for the surgeon to choice the optimal site of the cochleostomy and reach scala tympani without determine any inner ear structures damage (Atturo et al. 2014). Narrowings of the scala tympany have been reported in some cochlear region (Biedron et al. 2010) determinining pressure points to the basilar membrane during cochlear implantation at risk for traumatism or scalar translocation (Verbist et al. 2009).

The influence of the cochlear anatomy on the intracochear position of the cochlear implant and in potential insertion related trauma will be discussed in detail in the chapter 5.1 and 6.3.

1.5 BLOOD SUPPLY TO INNER EAR

Arterial blood supply

The cochlea and the vestibule are supplied by the labyrinthine artery. The internal auditory artery usually arises from anterior inferior cerebellar artery (AICA), a branch of the basilar artery; in some individuals, it arises directly from the basilar artery (Fig. 1.4). The labyrinthine artery follows the eighth cranial nerve in the internal auditory meatus, where it gives off the anterior vestibular artery which supplies the posterior and lateral semicircular canals, the utricle, and the posterior part of the saccule. The cochlea is supplied by the spiral modiolar artery and vestibule cochlear artery, which arise from the common cochlear artery. The common cochlear artery originates from the internal auditory artery near the site where the cochlear nerve penetrates into the modiolus; it runs through the modiolus and supplies the apex of the cochlea, the second turn, and part of the basal turn. The vestibulocochlear artery arises after the spiral modiolar artery and travels to the vestibule, where it gives off a vestibular branch and a cochlear branch. The vestibular branch supplies the posterior semicircular canal and the saccule, whereas the cochlear branch feeds the proximal part of the base of the cochlea. Thus, obstruction of the spiral modiolar artery would be expected to cause hearing loss predominating in the low frequencies and obstruction of the vestibulocochlear artery hearing loss predominating in the high frequencies and accompanied with vertigo. The arteries are terminal, forming no anastomoses.

Large arteries penetrate into the cochlea via the modiolus. The spiral modiolar artery gives off radial branches to the lateral cochlear wall, including the stria vascularis. As the arteries decrease in size, they lose their muscular layer, so that spasm necessarily causes extensive cochlear ischemia. The capillary network in the stria vascularis is extremely rich at the base of the cochlea, compared to the apex. The physiological and pathological impact of this difference in capillary abundance is unclear. The key role played by the stria vascularis in ensuring proper function of the OHC feedback loop suggests that this loop may be essential to the perception of high-frequency sounds but may be less important for low-pitched sounds.

The stria vascularis consists roughly of three cell layers: the basal layer facing the perilymphatic space, the intermediate layer, and the marginal layer facing the endolymphatic space. The basal cells are held together by tight junctions that make the stria vascularis impermeable to perilymph. Similarly, the intrastrial space is sealed away from the endolymph by tight junctions linking the marginal cells. The stria vascularis is the only structure in the body where blood vessels are isolated by completely leak-proof cell layers. However, cross-layer communication occurs via gap junctions, which allow nutrients and metabolites to travel from the perilymph. Secretion of potassium into the endolymph is ensured primarily by energydependent ion pumps coupled to ATPases. Cochlear ischemia stops ion pump function

nearly instantaneously, inducing a drop in the endolymphatic potential and thereby causing hearing loss.

Cochlear veins

Venous drainage of the cochlea occurs via the spiral modiolar vein. The venous blood empties either directly into the inferior petrosal sinus or internal jugular vein or travels through other venous sinuses via the vein of the vestibular or cochlear aqueduct. The multiplicity of venous drainage channels probably explains why resection of the internal jugular vein or sigmoid sinus does not cause hearing impairment.

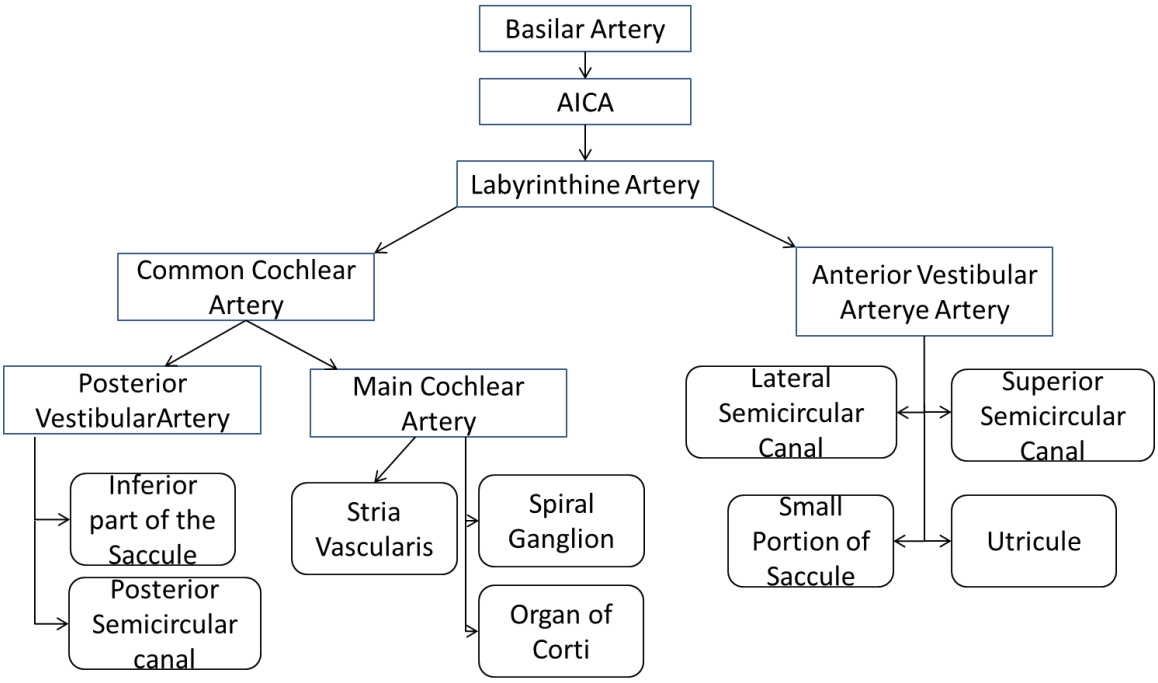

Figure 1.4. Arterial supply to the inner ear

2 Physiology and pathophysiology of the hearing

The pinna and the external auditory canal collect the sound waves and direct them to the tympanic membrane for transmission to the middle ear. The shape the pinna confers directional collector properties and the external auditory canal act as a sound amplifier. The degree of amplification varies as a function of frequency. The ear canal play the role of a resonator and the transfer function from sound pressure at the entrance of the ear canal to sound pressure at the tympanic membrane has a peak at approximately 3 kHz. At this frequency the sound pressure at the tympanic membrane is approximately 10 dB higher than it is at the entrance of the ear canal. Sound pressure energy is transmitted from the tympanic membrane across the middle ear space by the ossicular chain comprised of the malleus, incus, and stapes that act as a lever system. The tympanic membrane vibration moves the manubrium the malleus. The long process of the incus and manubrium move together because the malleoincudal joint is essentially fixed. In contrast, the joint between the incus and the stapes is flexible. Therefore, because the stapes is fixed at its posteroinferior border, movement of the tympanic membrane causes it to move in and out of the oval window. The changes in acoustic pressure caused by the stapes moving in and out of the oval window are transmitted instantaneously by the perilymph through the cochlear partition and then to the round window. This pressure transmission through the cochlear partition causes it to move either upward or downward, depending on the direction of the pressure change.

2.1 TRASDUCTION OF THE SIGNAL: FROM THE SOUNDWAVE TO THE ELECTRIC STIMULUS

The detection of the sound stimulus and its conversion to an equivalent electrical waveform, denominated mechanoelectrical transduction, occurs in the hair cells of the organ of Corti. The final mechanical event in the cochlear transduction process is the bending of the stereocilia. Basilar membrane deformation causes a shearing action between the reticular and tectorial membranes. Sound-induced motion of the basilar membrane excites the hair cells by deflecting their hair bundles to activate mechanoelectrical transduction ion channels (Hudspeth, 1989). Because the long OHC cilia are attached to both membranes, they are bent. In contrast, the IHC cilia, and possibly also the shorter OHC cilia, which are not attached to the tectorial membrane, bend in response to some mechanism other than displacement shear. One proposition is that this process may involve fluid streaming between the sliding parallel plates formed by the reticular and tectorial membranes.

2.2 TONOTOPIC REPRESENTATION IN THE AUDITORY SYSTEM

Hair cells in the different regions of the cochlea are maximally stimulated by different frequencies. This results in a spatial representation of sound frequency across the basilar membrane where the hair cells are located. The fundamental research by von Békésy in 1970 brought experimental proof that the cochlea performs a spectral analysis of sounds; he demonstrated that a tone of a certain frequency caused the highest vibration amplitude at a certain point along the basilar membrane. This means that each point along the basilar membrane is tuned to a certain frequency and a frequency scale can be identified along the cochlea, with high frequencies located at the base and low frequencies at the apex of the cochlea (Figure 2.1). As a consequence, each hair cell produces responses that, near the threshold of hearing, are tuned to a characteristic frequency. Von Békésy convincingly demonstrated that sounds set up a traveling wave motion along the basilar membrane and this traveling wave motion is the basis for the frequency selectivity. He concluded that the motion of the basilar membrane becomes a traveling wave motion because the stiffness of the basilar membrane decreases from the base of the cochlea to its apex. Rhode (1980) successively showed that the frequency selectivity of the basilar membrane deteriorates after death therefore metabolic energy might be necessary to maintain the high degree of frequency selectivity of the basilar membrane. Besides the frequency selectivity decreased when the intensity of the test sounds was increased above threshold. The reason that the frequency selectivity of single auditory nerve fibers is intensity dependent is the non-linearity of the vibration of the basilar membrane. The explanation of this phenomenon is that the outer hair cells are active elements that make the tuning of the basilar membrane non-linear and sharpens the tuning of the basilar.

The resulting representation is a topographic map of sound frequency, also called a tonotopic representation or tonotopic map, the fundamental principle of organization in the auditory system (Figure 2.1).

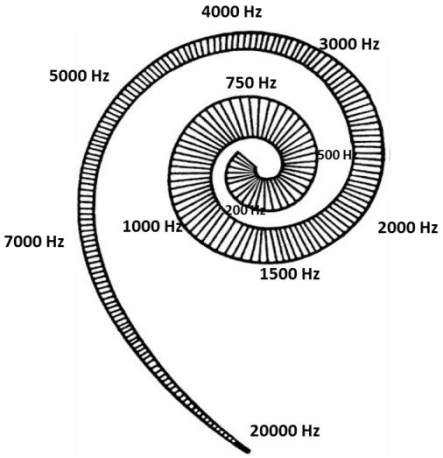

Figure 2.1. The basilar membrane and the tonotopic map of the cochlea.

However, the studies of Von Bekesy were done using pure tone presented in a quiet background, and the frequency threshold tuning curves of single nerve, cells that have been used to establish the tonotopic organization may not reflect the function of the auditory system under normal conditions because frequency threshold tuning curves are obtained by determining the threshold to pure tones at very low sound intensities.

Two hypotheses have been presented to explain the physiologic basis for discrimination of frequency or pitch. One hypothesis, the *place principle* based on the studies of Von Bekesy, claims that frequency discrimination is based on the frequency selectivity of the basilar membrane resulting in frequency being represented by a specific place in the cochlea and subsequently, throughout the auditory nervous system. It is believed that high frequency coding is dominated by this physiological mechanism. The other hypothesis, *the temporal principle*, claims that frequency discrimination is based on coding of the waveform (temporal pattern) of sounds in the discharge pattern of auditory neurons, known as phase locking, this coding strategy seems to be more dominant in conveying pitch for low-frequency signals and this time-based mechanism locks onto the temporal fine structure of the signal and conveys intonation by keeping the auditory nerve fibers' firing rate at the same frequency as the signal.

There is considerable experimental evidence that both the spectrum and the time pattern of a sound are coded in the responses of neurons of the classical ascending auditory nervous system including the auditory cerebral cortices. While there is ample evidence that both these two representations of frequency are coded in the auditory nervous system, it is not known which one of these two principles is used by the auditory system in the discrimination of natural sounds or for the discrimination of unnatural sounds. It may be that the place and the temporal principle of frequency discrimination may be used in parallel by the auditory system for discrimination of sounds of different kinds.

The fact that studies indicate that temporal information plays a greater role than place coding in discrimination of complex sounds such as speech sounds does not mean that spectral analysis (the place principle) cannot provide the basis for speech intelligibility. This observation underlines that the auditory system possesses a considerable redundancy with regard to the role of frequency discrimination as a basis for speech discrimination.

2.3 BINAURAL HEARING PROCESSING OF SIGNAL

Hearing with two ears is the basis for directional hearing, which is an ability to determine the direction to a sound source in the horizontal plane. Binaural hearing provides several benefits over monaural hearing, especially under challenging listening conditions: discrimination of sounds in a noisy background is better with two ears than with one, the "unmasking" from hearing with two ears benefits from both a time (phase) difference between the sounds and also from intensity differences. Studies have shown that the advantage of hearing with two ears is greater if the masking noise in the two ears is different such as shifted by 180°. Two basic effects that involve advantages for binaural hearing are binaural squelch effect and head shadow effect. Binaural squelch effect refers to the capacity of the central auditory system to process the stimuli received from each ear and to reproduce it with a higher signal-to-noise ratio (SNR) by comparing interaural time and intensity differences. On the other hand, head

shadow effect results from the physical placement of the head, which acts as an acoustic barrier and leads to an increase in SNR in the ear far from the noise when signal and noise are spatially separate (Moore 1991). Research in normal hearing subjects indicated a 3 dB improvement in squelch for the binaural speech recognition threshold and an average increase of 3 dB SNR for head shadow effect that is more dominant for attenuation of high frequencies and can cause even 8 to 10 dB of improvement.

If hearing is impaired more in one ear than in the other ear, the advantages of hearing with two ears diminishes. People often become aware that they have an asymmetric hearing loss because they have difficulties in understanding speech where many other people are talking.

In normal hearing people, sound localization abilities in the horizontal plane depend primarily on acoustic cues arising from differences in arrival time and level of stimuli at the two ears. Localization of unmodulated signals up to approximately 1500 Hz is known to depend on the interaural time difference arising from disparities in the fine-structure of the waveform. The prominent cue for localization of high-frequency signals is the interaural level difference cue (Blauert, 1982). However, it has also been well established that, for higher frequency signals, interaural time difference information can be transmitted by imposing a slow modulation, or envelope, on the carrier (Bernstein, 2001). The use of modulated signals with high frequency carriers is particularly relevant to stimulus coding by CI processors that utilize envelope cues and relatively high stimulation rates (Skinner et al., 1994; Vandali et al., 2000; Wilson and Dorman, 2007). Both the differences in the arrival time and the difference in the intensity of the sound at the two ears are determined by the physical shape (acoustic properties) of the head and the outer ears, together with the direction to the sound source. The sound arrives at the same time at the two ears when the head is facing the sound source (azimuth = 0°) and directly away from the sound source (azimuth = 180°). At any other azimuth, sounds reach the two ears with a time differences and the sound intensity at the entrance of the ear canals of the two ears is different. The difference in the sound intensity has a more complex relationship to the azimuth than the interaural time difference.

2.4 SENSORINEURAL DEAFNESS

Deafness may occur before or during birth (prenatal and perinatal, respectively) and in this case is referred to as congenital. It can also occur after birth (postnatal). Congenital deafness may arise from genetic causes, chromosomal abnormalities, or diseases affecting the mother during pregnancy. Postnatal deafness is mostly from disease or injury, but may also be the result of delayed genetic effects. In adults the most common cause of hearing loss is the presbyacusis. Other causes are the exposure to noise or occupational hearing loss, chronic otitis media, exposure to ototoxic agents, sudden sensorineural hearing loss, Menière disease or autoimmune inner ear disease.

2.4.1 Genetic hearing loss

Nonsyndromic

Genetic deafness frequently occurs alone without other abnormalities. In about 80% of children with nonsyndromic deafness, the inheritance is autosomal recessive (Dahl et al, 2001). Using DNA markers, genetic linkage studies have shown over 20 genes for nonsyndromic deafness. A mutation of the connexin 26 gene has been found to account for up to 50% of cases of nonsyndromic deafness in children of European descent (Denoyelle et al 1997). Connexin 26 belongs to a family of proteins that mediate the exchange of molecules between adjacent cells. Connexin is highly expressed in the cells lining the cochlear duct and the stria vascularis. It is thought that it is important for the recycling of K^+ ions from sensory hair cells into the endolymph in the process of transduction of sound to electrical signals.
Cochlear malformations were classified as Michel deformity, common cavity deformity, cochlear aplasia, hypoplastic cochlea, incomplete partition types I (IP-I) and II (IP-II) (Mondini deformity) (Sennaroglu, 2002). Incomplete partition type I (cystic cochleovestibular malformation) is defined as a malformation in which the cochlea lacks the entire modiolus and cribriform area, resulting in a cystic appearance, and there is an accompanying large cystic vestibule. IP-I and cochlea hypoplasia may be the result of a defective vascular supply from the blood vessels of the IAC (Sennaroglu 2016). In IP-II there is a cochlea consisting of 1.5 turns (in which the middle and apical turns coalesce to form a cystic apex) accompanied by a dilated vestibule and enlarged vestibular aqueduct. Good results have been reported both for cochlear implants with connexin 26 gene mutation (Rayess et al. 2015), the IP-I (Berrettini, 2013) and with classic Mondini deformity (Manzoor, 2016).

Some molecules involved in nonsyndromic deafness.

Molecule	**Inheritance**	**Type of Protein**
Connexin 26	Dom+Rec	Channel component
Connexin 31	Dom+Rec	Channel component
Connexin 30	Dom	Channel component
KCNQ4	Dom	Channel component
Pendrin	Rec+Pendred	Ion transporter
Myosin 7A	Dom+Rec+Usher	Motor molecule
Myosin 15	Rec	Motor molecule
Diaphanous	Dom	Cytoskeletal protein
POU3F4	X-linked Rec	Transcription factor
POU4F3	Dom	Transcription factor
α-tectorin	Dom+Rec	Extracellular matrix
Coch	Dom	Extracellular matrix
Otoferlin	Rec	Synapse component

Syndromic

In a number of children deafness is associated with other abnormalities, and hearing loss may be the first symptom. In Waardenburg's syndrome (WS), the features other than deafness are a lateral displacement of the inner canthus of the eye, heterochromia of the iris, and a white

forelock. It is inherited as autosomal dominant. Pathologically there is atrophy of the organ of Corti and stria vascularis, and a reduction in the number of ganglion cells. In albinism, where there is loss of pigmentation resulting in fair skin and poor vision, the deafness is bilateral

and severe. It is inherited as an autosomal-dominant or -recessive or sex-linked trait. With onchodystrophy there is sensorineural deafness and nail dystrophy. Pendred's syndrome may account for 10% of recessive deafness; in this syndrome there is abnormal iodine metabolism, and it is often associated with a Mondini deformity of the cochlea. In Jervell and Lange-Nielsen's syndrome (JLS) there is a bilateral severe hearing loss and cardiac abnormality (prolonged Q-T interval) that can lead to sudden death (Stokes-Adams attacks). It is inherited as autosomal recessive. Usher's disease is a congenital condition in which there is combined sensorineural hearing loss and retinitis pigmentosa. It is inherited as sex linked or autosomal dominant, and there is a recessive form. The branchiootorenal (BOR) syndrome is a genetic condition inherited in an autosomal dominant pattern characterized by hearing loss of early onset, preauricular pits, branchial clefts, and early progressive chronic renal failure. Deafness may also occur due to chromosome abnormalities. Trisomy 13 and trisomy 18 are often associated with other ear or body defects, and very short life expectancy.

Some molecules involved in syndromic deafness

Molecule	**Other Affected Sites**	**Syndrome**	**Type of Protein**
Connexin 32	Peripheral nerves	CMT	Channel component
ATP6B1	Kidney	RTA	Ion pump
Pendrin	Thyroid	Pendred	Ion transporter
KVLQT1	Heart	JLS	Channel component
KCNE1	Heart	JLS	Channel component
Myosin 7A	Retina	Usher 1B	Motor molecule
EYA1	Kidney, jaw	BOR	Transcription factor
PAX3	Pigmentation	WS1	Transcription factor
MITF	Pigmentation	WS2	Transcription factor
SOX10	Pigmentation, gut	WS4	Transcription factor
EDNRB	Pigmentation, gut	WS4	Receptor
EDN3	Pigmentation, gut	WS4	Ligand
FGFR3	Skull	CSS	Receptor
Treacle	Skull and jaw	TCS	Trafficking protein
Norrin	Eye, brain	Norrie	Extracellular matrix
USH2A	Retina	Usher 2A	Extracellular matrix
Collagens 4	Kidney	Alport	Extracellular matrix
Collagen 2	Eye, joints, palate	Stickler	Extracellular matrix
DDP	Muscle	DFN1	Mitochondrial protein

2.4.2 Presbycusis

Presbycusis appears as a gradually sloping hearing loss towards higher frequencies, and is usually associated with degeneration of cochlear hair cells, mainly outer hair cells in the basal portion of the cochlea. Age-related hearing impairment is presumed to be caused by the effect of morphologic changes in cochlear hair cells; these changes are similar to those seen in other injuries to the cochlea such as those from noise exposure. The loss of outer hair cells is more pronounced in the basal portion of the cochlea, thus the changes begin in the basal end of the cochlea (higher frequencies), spreading toward the apex as the condition progresses. The individual variability is important and hereditary factors are critical.
Loss of outer hair cells is the most evident change, and it has received more attention than other changes, but other responsible factors may be also changes in the auditory nerve, such as the variations in fiber diameter of the axons in the auditory nerve, which increases with age. Animal studies showed that aging and acoustic trauma reduced the response strength at both brainstem and cortical levels, and increased the response latencies more at the cortical level than at the brainstem level suggesting that presbycusis involves both peripheral hearing loss and biological aging in the central auditory system (Gourévitch and Edeline, 2011).

2.4.3 Ototoxic agents

Many commonly used medications can cause hearing loss. Antibiotics of the aminoglycoside family can cause permanent hearing loss. Streptomycin (dihydrostreptomycin) was the first of this family of antibiotics found to cause hearing loss, but commonly used antibiotics of the same family such as gentamycin, kanamycin, amikacin and tobramycin have also been found to be ototoxic in a variable degree. Erythromycin and polypeptide antibiotics such as vancomycin have produce hearing loss, but it is mostly reversible once the drugs are terminated. Commonly used agents in cancer therapy (chemotherapy) such as cisplatin and carboplatin are also ototoxic. Most ototoxic drugs induce hearing loss by injuring outer hair cells and thus impairing the function of the cochlear amplifier, in a similar way as occurs in presbycusis and in noise induced hearing loss. Inner hair cells are usually unaffected. However, the effect of toxic substances such as salicylate is different from that of noise in that it affects the cell bodies of the outer hair cells, while noise also causes a decoupling between the outer hair cell stereocilia and the tectorial membrane. Hearing loss caused by ototoxic drugs seldom exceeds 50–60 dB and it usually begins at high frequencies and extends gradually towards lower frequencies as it progresses. Most drugs cause the maximum damage to hair cells in the basal region of the cochlea; hence the greatest hearing loss occurs at high frequencies. High frequency audiometry (determination of the pure tone threshold at frequencies above 8 kHz) may therefore reveal a beginning hearing loss before it reaches frequencies that affect speech discrimination.

2.4.4 Menière disease

Menière's disease is a progressive disorder that is defined by a triad of symptoms: vertigo with nausea, fluctuating hearing loss and tinnitus, sometimes associated with ear fullness. It is believed that the symptoms of Ménière's disease are caused by pressure (or rather volume) imbalance in the fluid compartments of the inner ear (endolymphatic hydrops). The hearing loss in Ménière's disease can be explained by a distension of the basilar membrane causing the largest enlargement where its stiffness is least, i.e., in the apical portion. It is one of a few types of sensorineural hearing loss that involves initially the low frequencies. Typically, hearing loss in the early stages of Ménière's disease affects only low frequencies and it fluctuates and increases during an acute attack. The hearing returns to normal after each attack at the beginning of the disease but as the disease advances, residual hearing loss from each attack accumulates and the hearing loss spreads to higher frequencies. Over time, hearing loss progresses and extends to higher frequencies; but it rarely exceeds 50 dB. Speech discrimination is slightly compromised in the early stages of the disease but may become affected in the advanced, late stage of the disease. The end stage of the disease, reached 10–15 years after its debut, is flat hearing loss of approximately 50 dB and speech discrimination scores of approximately 50%. The symptoms are initially unilateral but many patients experience bilateral symptoms after 10–15 years.

2.3.5 Noise exposure

Exposure to excessive sound is the most common cause of acquired adult sensorineural hearing loss. The effects of noise are pervasive, and many studies of noise-induced trauma had demonstrated that there are mechanical damages of the anatomic and physiologic structures of the organ of Corti impacting the the neural, sensory, supporting, and vascular structures of the inner ear (Henderson and Hamernick 1995). The primary site of lesion induced by noise exposure is the hair cells in the organ of Corti and the primary neural degeneration occurs in synaptic terminals of cochlear nerve fibers and spiral ganglion cells. Moreover mechanical damages induced by noise exposure include also the disruption of Reissner's membrane and basilar membrane, loss of stereocilia bundles, disruption of subcellular organelles, damage of the inner and OHCs, injury of stria vascularis and spiral ganglion cells, and destruction of the lateral walls of the OHCs. There is a rapid and irreversible loss of cochlear nerve peripheral terminals on hair cells and a slow degeneration of spiral ganglion cells after noise exposure. Because the neural loss is not associated with hair cell loss, it can be considered a "primary" neural degeneration rather than occurring secondary to the hair cell degeneration. In addition, noise-induced loss of spiral ganglion cells is delayed by months and can progress for years after noise exposure.

The primary neural degeneration induced by noise exposure has been shown in widespread and severe swelling of the synaptic terminals of cochlear nerve fibers of ears in a variety of mammals such as cat, guinea pig, and mouse. The timing of noise-induced neural

degeneration recoveryd is of clinically fundamental importance to the development of pharmacological treatments for noise-induced hearing loss.

As a result of noise exposure, synaptic degeneration and neural plasticity were found in the central auditory system, especially in the dorsal cochlear nucleus (DCN) (Salvi et al, 2000). Pathological changes induced by noise exposure in the central auditory system have been identified by many studies, and even in the absence of cochlear damage, new findings suggest that environmental noise may progressively degrade hearing through alterations in the way sound is represented in the adult auditory cortex (Gourévitch et al. 2014).This indicates that noise-induced hearing loss may progress as a neurodegenerative disease with the capacity for synaptic reorganization within the cochlear nucleus however, the mechanisms involved in synaptic degeneration and plasticity of the central auditory system induced by noise exposure are not clear.

3 The cochlear implants

The cochlear implant (CI) is an auditory device that acts as a transducer that transform acoustic energy into an electrical signal. It stimulates the spiral ganglion cells of the auditory nerve in the modiolus of the cochlea, thus bypassing the nonfunctional or absent hair cells. The technology takes advantage of the tonotopic arrangement of auditory organ that allows the distribution of several stimulating electrodes along the tympanic ramp of the cochlea. Djourno and Eyries first described direct electrical excitation of the auditory nerve in 1957 opening the way to the research on cochlear implantation. The first implantations in adult patients were performed in the same year in Paris and Los Angeles (Chouard & Mac Leod, 1973, 1976, House & Urban 1973, House et al. 1976) and some year later in Vienna and Melbourne and San Francisco. These groups of investigators before, and successively others, continued during the last three decades to investigate on the development and the improvement of the cochlear implants proposing different coding strategies, new electrodes design, expanding the criteria of the indication for cochlear implantation. The research in cochlear implants allowed, within these decades, an improvement of the hearing results of the implanted patients and led to new objectives in cochlear implantology i.e., improvement the quality of the perceived sound in noisy environment and the music appreciation, and the possibility to rehabilitate partial or unilateral deafness.

There are currently 5 manufacturers of CIs: Med-El GmbH (Innsbruck, Austria), Advanced Bionics Corporation (Valencia, CA, USA), Cochlear Corporation (Lane Cove, Australia), and Oticon Neurelec (Vallauris, France), Zhejiang Nurotron (Hangzhou, China). Despite variations in component design and sound-processing strategies, device performance is generally comparable between all 4 implant manufacturers with current devicedesigns. All of them are composed by an external and an internal part (Fig. 3.1). The external part consists of a behind-the-ear device connected to an external transmission coil which provides a radio-frequency (RF) link to a matching coil in the internal part, the implant. The implant consists of a miniature enclosure containing electronics connected to a number of electrodes. There are one or more reference electrodes on the enclosure or on a separate lead, and there is an array of multiple intracochlear electrodes, between 12 and 22 depending on the manufacturer and array type. The stimulation current flows between selected electrodes to activate the neural structures of the cochlea. As illustrated in figure 3.1, sound or speech is captured in the external device by a microphone system (one or more microphones). Pre-processing is applied to optimize the input dynamic range relative to input signal levels and to adjust the spectrum shape using a pre-emphasis filter. In some systems there is also fixed or adaptive noise-reduction processing that typically exploits the differences between signals obtained from several microphones to enhance desired sounds suppressing competing noise. The stimulation ‘strategy’ refers to the transformation of the input sound signal into a pattern of electrical pulses. Digital specifications of the required stimulation patterns produced by the stimulation strategy are coded in the transcutaneous RF transmission. The RF signal also

provides power to the internal part. The electronics of the implant include one or more current sources to deliver the electrical stimulation pattern to the electrode channels. A channel is defined as a set of two or more electrodes with currents flowing between them. The term "monopolar" stimulation is used to describe current passing between an intracochlear electrode and a remote reference electrode, whereas "bipolar" refers to stimulation current passing between two intracochlear electrodes.

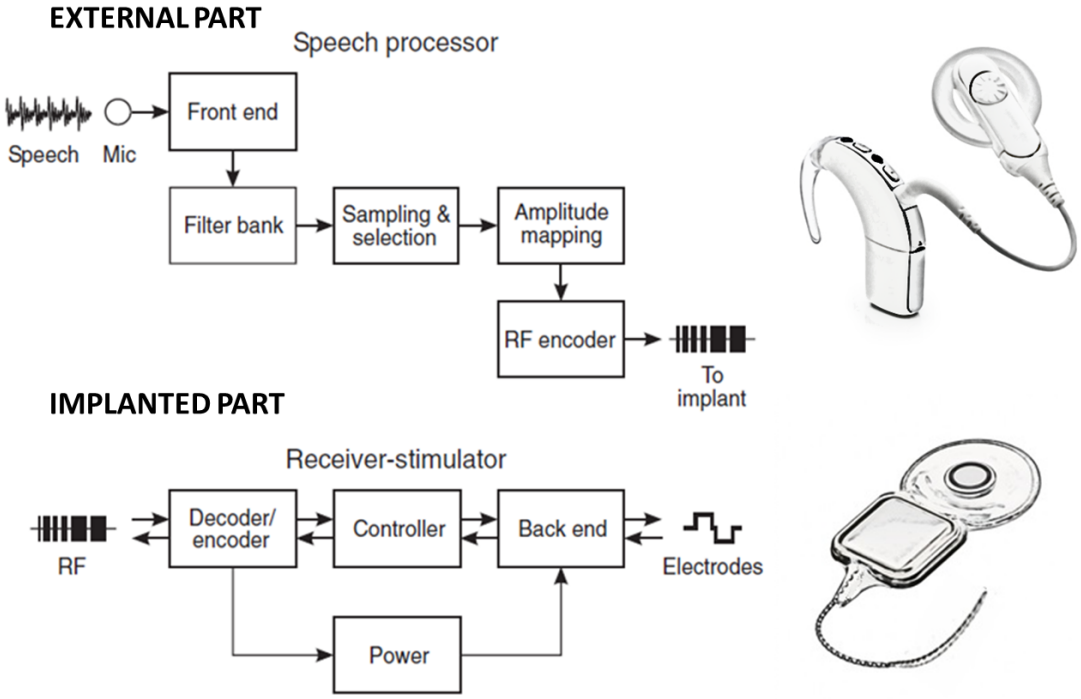

Figure 3.1. Block diagram of complete cochlear implant system. Modified from Clark, 2003.

3.1 PROCESSING OF THE SIGNAL IN COCHLEAR IMPLANTS

Cochlear implants (CIs) bypass the frequency selectivity of the basilar membrane and replace it by a more rough spectral auditory resolution than what the cochlea normally provides. The success of cochlear implants in providing useful hearing may appear surprising because even multichannel cochlear implants cannot replicate the spectral analysis that occurs in the cochlea and in the majority of speech strategies do not include temporal coding of sounds. The spectral information is roughly coded through multi-channel representation following the auditory system's natural tonotopic organization; i.e., acoustic spectral information is normally represented from low to high frequency in a corresponding spatial progression within the cochlea.

The fact that CIs are successful in providing good speech comprehension without the use of any temporal information sets the importance of the temporal code of frequency in question, and confirms that the auditory system could adequately discriminate speech sounds on the

basis of information on power in a few frequency bands. Three main reasons why cochlear implants are successful in providing speech intelligibility may be identified:

1 The redundancy of the natural speech signal.

2 The redundancy of the processing capabilities of the ear and the auditory nervous system.

3 The large ability of the central nervous system to adapt through expression of neural plasticity.

Individuals with normal hearing can either understand speech solely on the basis of temporal information or on spectral (place) information as well. This means that frequency discrimination can rely both on the place and the temporal hypothesis. The finding that good speech comprehension can be achieved on the basis of only the spectral distribution of sounds seems to contradict the results of animal studies of coding of the frequency of sounds in the auditory nerve (Sachs and Young, 1976; Young and Sachs, 1979). Such studies have shown that temporal coding of sounds in the auditory system is more robust than spectral coding. On these grounds it has been concluded that temporal coding is important for frequency discrimination (see Chapter 2). These and other studies have provided evidence that the place principle of coding of frequency is not preserved over a large range of sound intensities and that it is not robust (Moller, 1977). On the basis of these findings it was concluded that the place principle is of less importance for frequency discrimination than temporal information. It was always assumed that frequency discrimination according to the place principle would require narrow filters and many filters covering the audible frequency range but studies in connection with development of channel vocoders, and more recently in connection with cochlear implants, showed clearly that speech comprehension could be achieved using much broader and much fewer filters. One of the strongest arguments against the place coding hypothesis has been the non-linearity of the basilar membrane frequency tuning. Indeed, the frequency to which a certain point on the basilar membrane shifts at high intensity of stimulation (see chapter 2). This lack of robustness of cochlear spectral analysis has been regarded an obstacle to the place hypothesis for frequency discrimination. Since the band pass filters in cochlear implants do not change with sound intensity, the cochlear implants may actually have an advantage over the cochlea as a "place" frequency analyzer. The spectral acuity of the cochlea also changes with sound intensity, which is not the case for the filters used in cochlear implants.

3.2 CODING STRATEGIES OF THE SIGNAL

Since the introduction of the first stimulation strategies in multi-channel CIs over 30 years ago, a number of diverse sound-processing strategies have been developed and evaluated. These strategies focus on better spectral representation, better distribution of stimulation across channels, and better temporal representation of the input signal. Three different main processing strategies have been developed and used since now: the n-of-m approach (SPEAK, ACE, APS) in which the speech signal is filtered into m bandpass channels and the n highest envelope signals are selected for each cycle of stimulation. The CIS strategy filters the speech

signal into a fixed number of bands, obtains the speech envelope, and then compresses the signal for each channel. On each cycle of stimulation, a series of interleaved digital pulses rapidly stimulates consecutive electrodes in the array. The CIS strategy is designed to preserve fine temporal details in the speech signal by using high-rate, pulsatile stimuli. The Simultaneous Analog Stimulation (SAS) filters and then compresses the incoming speech signal for simultaneous presentation to the corresponding enhanced bipolar electrodes. The relative amplitudes of information in each channel and the temporal details of the waveforms in each channel convey speech information. All the coding strategies that have been in use in CIs during the last 15–20 years rely mainly on envelope information (Muller et al 2012). In general, users of these coding strategies show good to very good speech perception in quiet, moderate speech perception in noise and poor to moderate music appreciation. The 4 most commonly used in the present day are: ACE (Advanced Combination Encoder) with channel selection based on spectral features, MP3000 with channel selection and stimulation based on spectral masking, FSP (Fine Structure Processing) based on enhancement of temporal features, and HiRes120 (High Resolution) with temporal feature enhancement and current steering to improve the spatial precision of stimulus delivery (Fig. 3.2).

Pitch perception with CIs is extremely poor. This is due both to limitations at the interface with electrical stimulation (spread of excitation) and to imprecise coding of temporal cues. The large spread of excitation in the cochlea and the small number of channels to code the low frequencies with electrical stimulation reduces the spectral resolution and therefore the precision of spectral pitch. Another limitation with electrical stimulation is the inability of CI users to perceive the temporal fine structure. Therefore the only remaining mechanism is periodicity pitch perception, which is much weaker than temporal fine structure's pitch and limited by the maximum frequency at which pitch changes are perceived, around 300 Hz. Furthermore, temporal envelope fluctuations are not always accurately coded by current sound-processing strategies. Specifically, the transmission of tonal speech information, such as prosodic contour or speaker gender, tonal languages (e.g. Mandarin Chinese) as well as music perception and appreciation is poor in CI users compared to normal-hearing listeners. To improve the transmittance of fine structure information, the fine structure processing (FSP) coding strategy was developed by MED-EL (Innsbruck, Austria). FSP is intended to better enable users to perceive pitch variations and timing details of sound. The aim of this coding strategy is to represent temporal fine structure information present in the lowest frequencies of the input sound signals by delivering bursts of stimulus pulses on one or several of the corresponding CI electrodes.

These bursts contain information about the temporal fine structure in the lower frequency bands that is not available in the envelope of those signals, potentially leading to improved perception for CI users. The FSP, FS4, and FS4-p are the 3 temporal fine structures coding strategies currently available (Riss et al. 2014). Results indicate that FSP performs better than CIS+ in vowel and monosyllabic word understanding. Subjective evaluation demonstrated strong user preferences for FSP when listening to speech and music (Muller et al 2012). Other authors demonstrate that there was no difference in speech perception with FSP compared to CIS at an extended frequency spectrum; the extended frequency spectrum in the low frequencies might explain a benefit of FSP observed in other studies (Riss et al 2014).

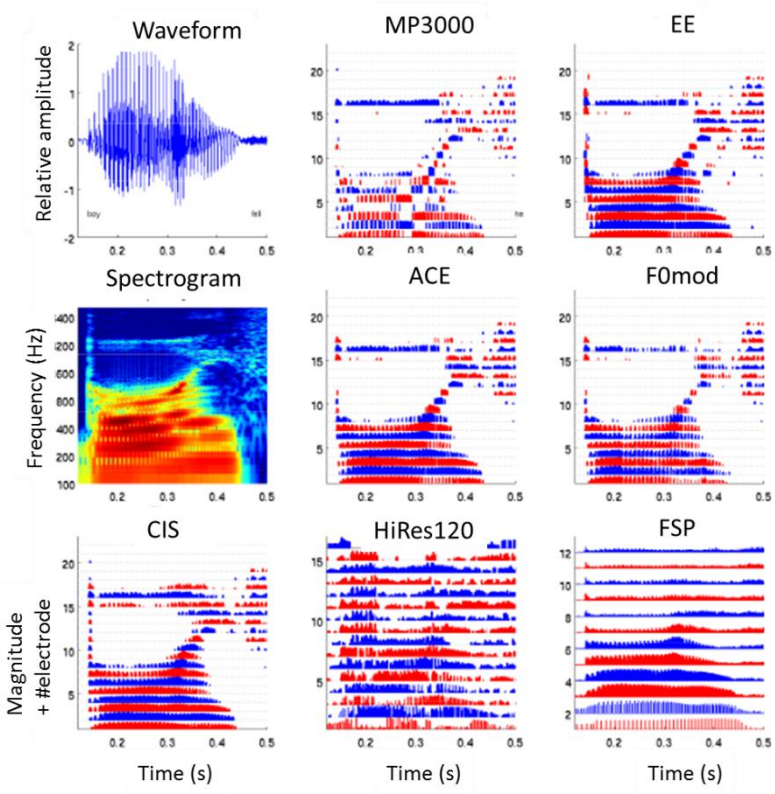

Figure 3.2. Waveform, spectrogram and electrodograms of the word "boy". The signal was presented at an average RMS level of 60 dB SPL. For the electrodograms, the vertical axis indicates the channel, and the height of each vertical line represents the magnitude of the pulse. The magnitude is expressed in different units for different strategies. The red and blue colors visually distinguish adjacent channels. Modified from Wouters et al. 2015.

3.3 INDICATIONS FOR COCHLEAR IMPLANTATIONS

The indications for the cochlear implantation gradually changed over the years maintaining the evident objective to never have patients that perform more poorly with their cochlear implant than they previously performed with hearing aids alone (Waltzman & Roland, 2006). In earlier times, unilateral implantation was the standard treatment for hearing rehabilitation for adults and children presenting with bilateral profound hearing loss (National Institutes of Health Consensus Conference 1995), and the use of the contralateral hearing aid was not recommended or in general not accepted. On the contrary now the indications are extended to the deafness with residual hearing in the low frequencies and the minimal traumatic surgery with the attempt to preserve the residual hearing is the gold standard. The use of contralateral (Bimodal) or ipsilateral (Hybrid) acoustic stimulation of the ear is recommended to improve speech comprehension and spatial localization performance. Moreover when the benefit of the contralateral hearing aid ceases to be useful a bilateral implantation is advised. In some selected cases the indication of cochlear implantation is performed in single sided deafness (i.e., unilateral untreatable tinnitus associated to hearing loss, experimental study protocols, selected countries, etc).

There is not a worldwide consensus or guidelines for the audiological indication for cochlear implantation, but in general less than 50% of speech discrimination of disyllabic words or phrases in the best aided condition at 60-70 dB SPL is well recognized as a good indication for implantation.

In France the indications for the cochlear implantation in adult patients are:
No limitation for the age; in elderly people a psycho-cognitive test is required
In general, there is no indication for prelingual deafness in adults
Speech discrimination of disyllabic words inferior or equal to 50% in free field in the best hearing aided condition
In case of hearing fluctuation, cochlear implantation may be indicated if a major impact in the communication exists
The bilateral implantation is indicated in case of bacterial meningitis, bilateral temporal bone fracture or other causes that could lead in short time to bilateral cochlear ossification; or among unilateral implanted patients in case of loss of hearing benefit of the contralateral hearing aid, or in case of loss of autonomy in elderly unilateral implanted patients
In Italy the indication for cochlear implantation in adults are similar to those reported above and has been published by the Italian society of Otolaryngology in 2009 (http://www.actaitalica.it/issues/2009/Argomenti/Argomenti%201_2009.pdf). During the last years several centers in Italy began the cochlear implantation in case of unilateral sensorineural hearing loss or as therapy for intractable tinnitus following the new trends in cochlear implantation (Cabral et al. 2016, Friedman et al. 2016, Mertens et al. 2016), at the time of the redaction of this manuscript four adults patients presenting single sided deafness have been implanted at the cochlear implant center in Policlinico Umberto I, Sapienza University of Rome (unpublished data). In France a multicenter study is ongoing aimed to test the efficacy of cochlear implant in single sided deafness. The patients tried the bi-CROS system and bone conductive band before choosing to keep one of the two devices or move toward a cochlear implantation. Eight patients have been implanted so far in the cochlear implant center of the Pitie-Salpetriere Hospital, and the hearing results are under analysisOther important factors to take in account for the cochlear implantation are the radiological parameters. Cochlear malformations in general are not contraindication for a cochlear implantation, while an intracochlear fibrosis or ossification may represent a relative or absolute contraindication. The absolute contraindication is represented by the cochlear nerve aplasia. As we will see in the next chapters the preoperative study of the radiologic parameters of the cochlea may lead to the choice of the type of the electrode to be implanted or to the choice of the side to be implanted.

The surgery for the cochlear implantation is a well standardized procedure including a simple mastoidectomy and a posterior tympanotomy to reach the the round window region through the mastoid cavity; finally the electrodes array is inserted in the scala tympani of the cochlea through a cochleostomy or by opening the round window membrane. Other different techniques have been proposed such as the suprameatal approach that permits to reach the cochlea performing an epitympanotomy with theoretically less surgical risk for the facial nerve (Kronenberg et al. 2001).
Three weeks to one month after implantation and at regular intervals thereafter, stimulation levels are adjusted ("fitted") to the individual patient. In each fitting session a patient-specific 'map' is set up containing all stimulation parameters. For each channel, minimal levels of stimulation (min) and levels of maximal comfortable loudness (max) are determined. In some cases also the shape of the growth function between min and max that converts the input

acoustic levels to electric stimulation levels is determined. During a fitting session impedances of the stimulation channels can be measured and some electrodes can be deactivated if impedances are high, non-acoustic stimulation are obtained or basal electrodes migrated outside the cochlea, and parameters of the pre-processing stage can be adjusted.

3.4 HEARING PRESERVATION IN COCHLEAR IMPLANTS

Von Ilberg et al. (1999) first discussed the possibility to use electric and acoustic stimulation simultaneously in patients with functional residual hearing in the low frequencies. These patients do not benefit from conventional hearing aids that are not efficient for severe hearing loss in the high-frequency range (>1 kHz). However, traditionally cochlear implantation was not considered as a treatment for these patients with a considerable amount of residual hearing either.

During the last years the "soft surgery" for cochlear implantation began to be applied to all cochlear implantation regardless the presence of residual hearing in order to preserve the functional acoustic hearing when present with the possibility to acoustically stimulate these frequencies and to reduce the inner ear mechanical traumatism and the inflammatory insult (i.e., fibrosis and ossification) determined by the intracochlear array insertion. Another important opportunity to prevent hearing loss after cochlear implantation with preservation of residual hearing may be in intracochlear drug treatment to protect the organ of Corti against apoptotic physiopathological pathways.

Several studies have been performed until now to investigate on the possibility to preserve the residual hearing using both a short (Gantz et al. 2006), standard length (Skarzinsky et al. 2014, Mick et al. 2014, Tamir et al. 2012) or precurved (Hunter et al. 2016) electrodes array.

Useful residual hearing was conserved in 88% of subjects at 1-year postopoperative in a multicenter European study comprising 66 adults implanted with the Nucleus hybrid System. Sixty-five percent of subjects had significant gain in speech recognition in quiet, and 73% in noise. Speech perception was significantly improved over preoperative hearing aids, as was sound quality and quality of life (Lenarz et al. 2013). The same electroacoustic system was tested in a multicenter study in USA (88 adult patients) and was demonstrated to provide significant improvements in speech intelligibility in quiet and noise for individuals with severe high-frequency loss and some low-frequency hearing. The authors concluded that this device expands indications to hearing-impaired individuals who perform poorly with amplification due to bilateral high-frequency hearing loss and who previously were not implant candidates (Roland et al 2016).

3.5 VARIABILITY OF HEARING RESULTS IN COCHLEAR IMPLANTED PATIENTS

Several studies and metanalysis report that speech perception and quality of life improve with unilateral and bilateral implantation, especially in noisy conditions (Gaylor et al. 2013). A large number and difference of speech and hearing tests across studies exists and it creates difficulty in comparing their findings. However, significant improvements in speech outcomes pervade the identified literature. Compared with unilateral implantation, bilateral

cochlear implantation provided added improvements in speech perception in noise and localization of the sound source. Nevertheless, despite the overall good to very good results reported in literature after cochlear implantation both in children and in adult patients a wide heterogeneity of the hearing outcomes emerges in the single studies, and patients with poor results both in unilateral and bilateral cochlear implantation were reported (Holden et al. 2013; Mosnier et al. 2009). Poor performers have been defined in different studies on the basis of the percentile division of the speech score results (Lenarz et al. 2012, Holden et al. 2013), the percentage of speech score improvement after cochlear implantation (Bodmer et al. 2007) or arbitrarily divided from good performers as patient having < 60% of speech recognition scores (Mosnier et. al 2009). In these studies, patients with low speech perception score at 1-year after cochlear implantation were reported to vary from 10% to 25%.

Several patients' specific factors have been identified as affecting speech score, including duration of deafness and duration of cochlear implantation, residual preoperative speech recognition, pre/postlingual status, different speech coding strategy. In multicenter study involving more than 2000 implanted patients and fifteen cochlear implant centers, 15 pre-, per- and postoperative factor have been studied. The pure tone average threshold of the better ear, the brand of device, the percentage of active electrodes, the use of hearing aids during the period of profound HL, and the duration of moderate HL were significant factors able to explain the 22% of the variance of the results (Lazard et al. 2012). The other 78% of the variance remains unexplained. Cognitive reorganization may be involved as well as other variables not considered in the study. Other studies investigated the variability in intracochlear array positioning in terms of distance to the spiral ganglion cells, depth of insertion and scalar translocation as factor affecting speech performance has also been investigated by several authors (Finley et al. 2008).

During the last years new imaging techniques such as the cone beam CT scan have been used in cochlear implant studies to correct identify the electrode position into the cochlea in order to ameliorate the spatial resolution of the multislice CT scan and reduce the metallic artifact of the electrode that impede the correct identification of the intracochlear structures.

In this thesis the anatomy of the cochlea and the position of the electrode array, in implanted patients have been studied with the attempt to identify affecting factors that contribute to the variability of the inter- and intra-individual speech discrimination score. A group of bilateral simultaneous implanted patients accurately selected in order to reduce the variability of other factors have been enrolled to study the role of the depth of insertion, the distance of the electrodes to the modiolus and the number of active electrodes in the short and 5-years follow up. The role of scalar translocation of the array on hearing outcomes and subjective quality of hearing has been studied in another group of patients that underwent postoperative cone beam CT scan. The methodology for the assessment of intraochlear positioning of the electrode in cone beam CT scan images has been validated in a radio-histological study in temporal bones. Finally, the study of the insertion forces in a temporal bone model has been performed in order to to estimate the maximal value of the force that should be applied to ensure an atraumatic insertion and preserve the integrity of the inner ear structures.

OBJECTIVES OF THE THESIS

The objective of this thesis was to study parameters of cochlear implants insertion with the aims of reducing the inter- and intra-individual variability in the outcomes of surgical hearing restoration.

Three aspects have been investigated:

1) The reliability of cone beam CT scan to identify the correct position of the electrode array within the cochlea

2) The role of the position in the cochlear lumen of the electrodes array on speech scores performance and its influence over time

3) The insertion forces during the implantation and their relation with inner ear structures trauma

4 Cone beam CT for identification of scalar positioning of the electrodes

The correct intracochlear positioning in cochlear implants is of paramount importance for the stimulation of spiral ganglion cells and the correct hearing rehabilitation, thus the verification of the localization of the electrodes array is extremely important in cochlear implant surgery. Several imaging techniques are available for the assessment of the intracochlear location of the electrodes in implanted patients (Fig. 4.1) and in temporal bone specimens (Fig. 4.2).
The first interest of radiological electrode localization is to confirm the intracochlear position immediately after the implantation. The intraoperative or early postoperative imaging for the assessment of the position of the cochlear implant is routinely performed in cochlear implant centers worldwide, allowing a prompt reinsertion in case of a misplaced electrode (i.e., superior semicircular canal). Some authors advice to perform both the intra-operative cochlear response telemetry that give measurement of impedances and can evaluate the integrity of implant electrodes and the status of the electrode cochlea interface, and the intraoperative imaging to confirm correct positioning of the array (Viccaro et al. 2009). For a long time, intra-operative plain X-rays were considered the method of choice for confirmation of the correct position of the cochlear implant both intraoperatively than after the surgery. Plain radiography is simple, inexpensive and reliable. C-arm fluoroscopy has replaced conventional portable radiography fotr intraoperative imaging in most institutions. Rotational C-arm fluoroscopy can provide 3D radiographs during operation after insertion of the electrodes, thus providing increased certainty of correct positioning and enabling repositioning with low dose and little increase in operation time. Conventional multi-detector CT scanners were also recently used for intra-operative guidance of CI insertion in difficult cases providing high-quality imaging information to the surgeon for cochleovestibular anomalies and an abnormal course of the facial nerve (Yuan et al. 2012).

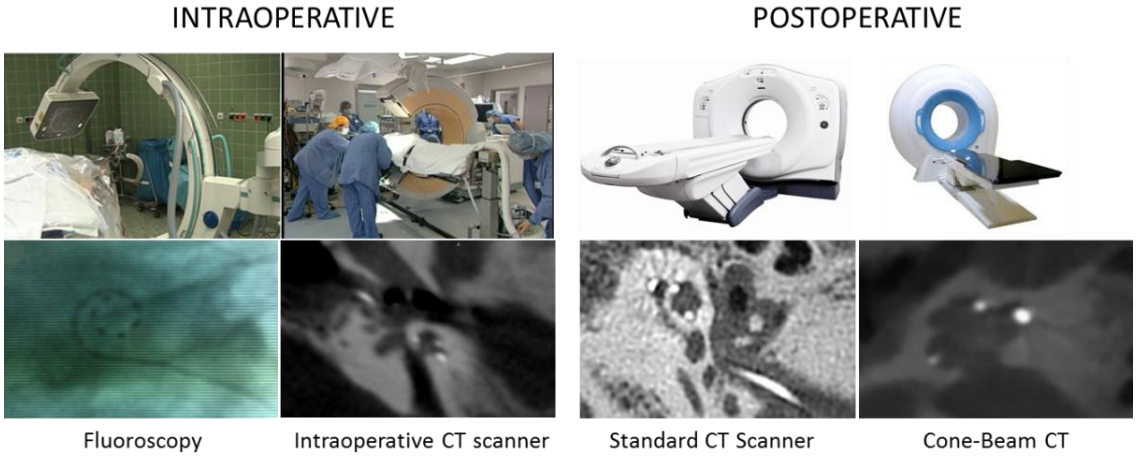

Figure 4.1. Different imaging modalities available for the evaluation of the intracochlear position of the electrodes array. Post-operative techniques offer the best image resolution.

Multislice helical CT scan represents nowadays the standard technique for postoperative evaluation of the electrodes position before the discharge of the patients from the hospital. The cone beam CT scan is beginning to replace the MSCT in some center, due to its low radiation dose, low cost and compact size compared to conventional CT scanners. In the next paragraph the differences between these two radiological techniques will be presented.

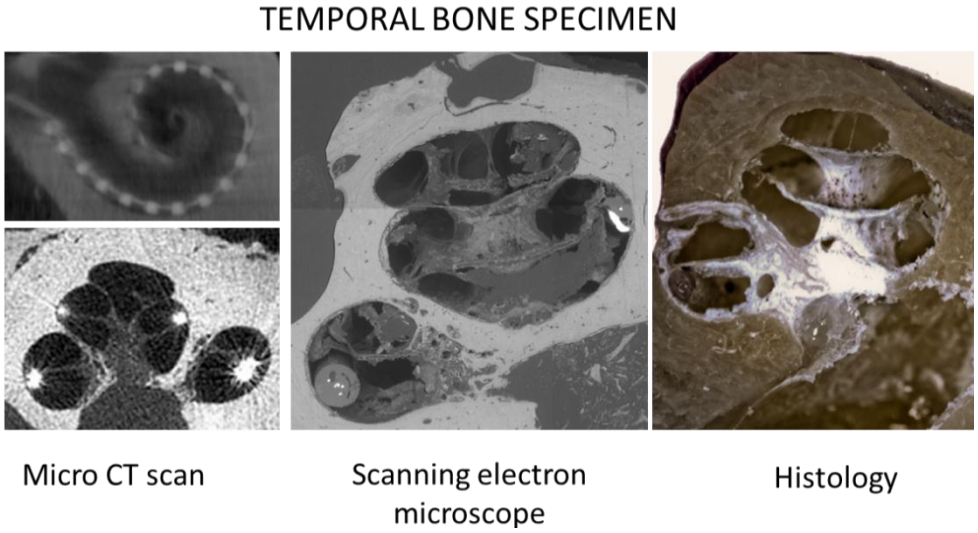

Figure 4.2. Ex vivo modalities for the assessment of the cochlear implant positioning. The micro CT allows to correct evaluate the electrodes array without sectioning the specimen, but two long and low dose expositions, one for the electrode and another for the biologic structures and a fusion of the acquired images are necessary to limit the metallic artifact of the electrode.

4.1 CONE BEAM COMPUTED TOMOGRAPHY (CBCT)

During the last years with the diffusion of the mini invasive, hearing preservation surgery an increasing interest was developed in the assessment of the scalar localization of the cochlear array. The need for a reliable, more precise and alternative to the multislice helical CT scan (MSCT) led to focus the interest on the CBCT.

The first CBCT scanner became commercially available for dental and maxillo-facial imaging in 2001 (NewTom QR DVT 9000; Quantitative Radiology, Verona, Italy), and the first trial on cochlear implanted temporal bones were soon published (Hussted et al. 2002, Aschendorff et al. 2003). Comparatively low dosing requirements and a relatively compact design have also led to intense interest in surgical planning and intraoperative CBCT applications, particularly in the head and neck but also in spinal, thoracic, abdominal, and orthopedic procedures.

In CBCT systems, the x-ray beam forms a conical shape between the source and the detector in contrast to conventional fan-beam geometry (Fig. 4.3), in which the collimator restricts the x-ray beam to approximately 2D triangular shape.

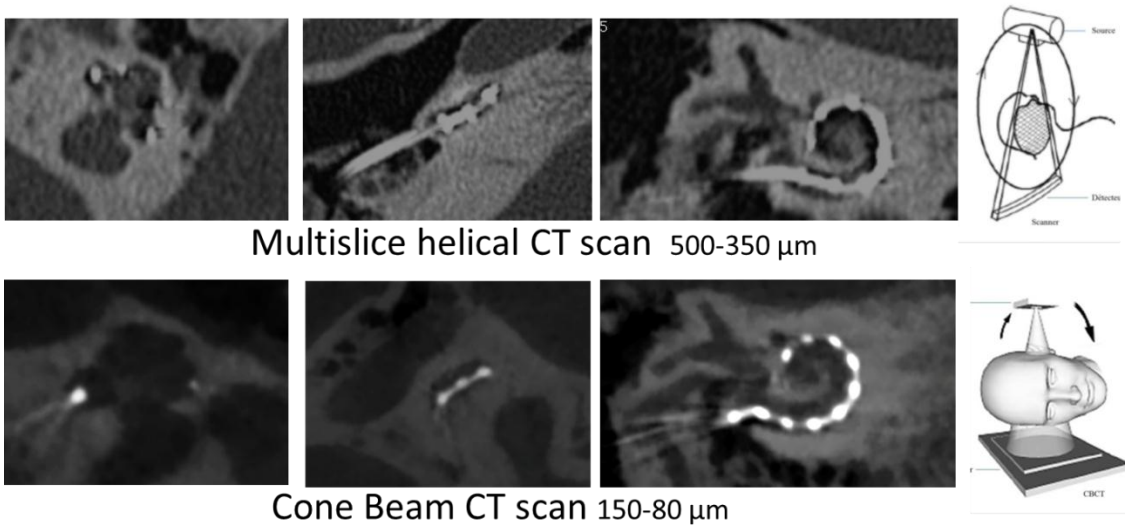

Figure 4.3. An example of visualization of the same electrode (Medel flex 28) in the same cuts in multislice helical CT (MSCT) and in cone beam CT (CBCT) images. The metallic artifacts are more visible in MSCT scan. In the right part the schematization of the flat triangular shape of the beam in MSCT scan and the conical shape in the CBCT scan.

In fan-beam single-detector arc geometry, data acquisition requires both rotation and z-direction translation of the gantry to successively construct an image set composed of multiple axial sections. In CBCT systems using a 2D flat panel detector, however, an entire volumetric dataset can be acquired with a single rotation of the gantry. A primary difference between CBCT and MSCT is the isotropic nature of acquisition and reconstruction in cone beam systems. In a CBCT a reconstruction of the acquisition produces a volumetric dataset with isometric voxels as small as 80 x 80 µm. This ensures identical spatial resolution whatever the slice orientation within the volume. MSCT, on the contrary, reconstructs volume by superimposition of slices, and the constituent voxels are rarely cubic in shape. The volume is said to be "anisotropic"; spatial resolution varies according to slice orientation (Hodez et al. 2011). Compared with MSCT, in which 500 x 500 μm^2 in-plane and 500- to 1000- µm z-axis resolutions are expected, CBCT theoretically reduces the effect of partial volume averaging and can improve the spatial resolution of high-contrast structures in any chosen viewing plane.

The radiation-dose parameter in CT imaging is mainly related to patient safety, but it is also associated with image quality. In a simplistic model of MSCT, radiation dose increases proportionally with increased voltage and tube current (mA) and can be decreased if the pixel size, section thickness, or pitch is increased. With other parameters held constant, increased radiation dose generally decreases quantum noise and affords improved contrast resolution. Cone-beam imaging's key feature is its radiation intensity, which is notably lower than in CT, whether for sinus or ear exploration. For example, the Computed Tomographic Dose Index of a CT scan of the middle ear is around 170 mGy, compared to 15–30 mGy for cone beam imaging.

Several physical descriptors and parameters are commonly enlisted to characterize the quality of an image. In characterizing CT systems, quantum noise, spatial resolution, contrast resolution, and detector quantum efficiency are of particular interest. Quantum noise is

fundamentally related to image quality and is a function of dose, tissue transmissivity, and voxel size. Noise is, in turn, a principal determinant of contrast resolution and, to a lesser extent, spatial resolution, which, along with artifacts, constitute the major observable determinants of overall image quality. CBCT imaging with FPD technology typically achieves excellent spatial resolution with a relatively low patient dose. Contrast resolution suffers, however, due to increased x-ray scatter and the reduced temporal resolution and dynamic range of the FPDs.

In conclusion the increased spatial resolution of CBCT as compared to MSCT scan (Dahmani-Causse et al. 2011) provides reliable morphologic assessment of the temporal bone (fig. 4) with significantly reduced radiation doses. Morphologically it is an improvement on MSCT to which it is fully comparable for purposes of ear pathology exploration in patients. As we will see in the next chapters the use of CBCT permitted to better identify the correct intracochlear position of the electrodes and to better investigate on the relationship between inner ear structures preservation and hearing performance after cochlear implantation.

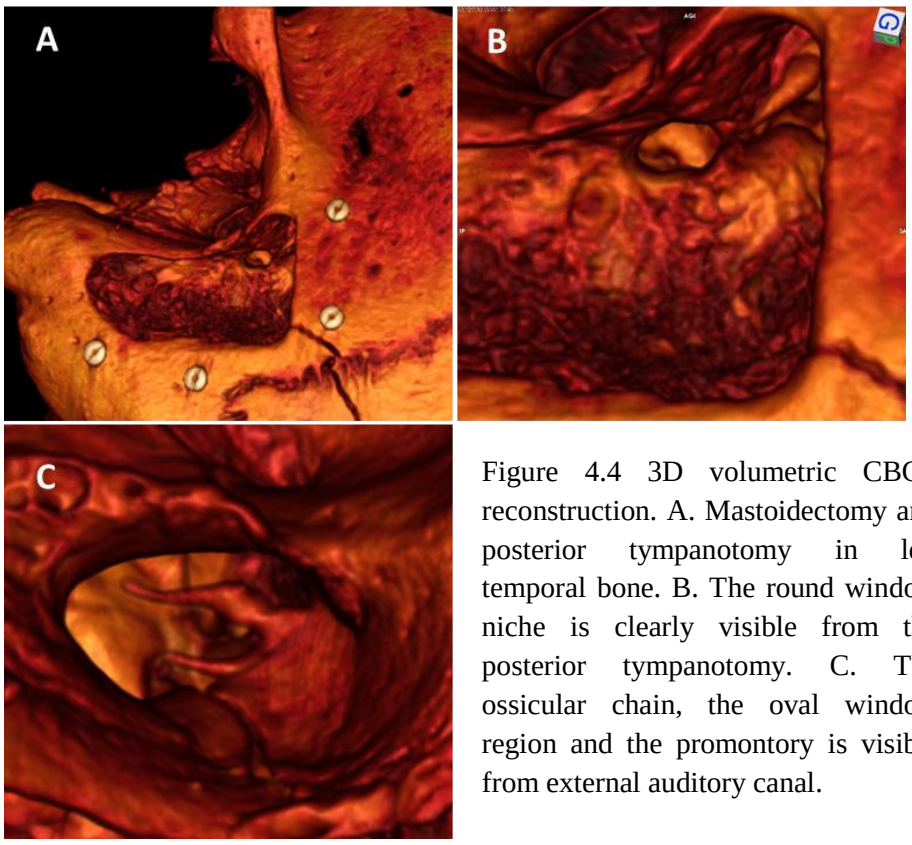

Figure 4.4 3D volumetric CBCT reconstruction. A. Mastoidectomy and posterior tympanotomy in left temporal bone. B. The round window niche is clearly visible from the posterior tympanotomy. C. The ossicular chain, the oval window region and the promontory is visible from external auditory canal.

4.2 CONE BEAM CT SCAN FOR ELECTRODE POSITION ASSESSMENT IN TEMPORAL BONE AND IN IMPLANTED PATIENTS

Objective: To determine if the position of a long and flexible electrodes array within the cochlear scalae could be reliably assessed with Cone Beam CT (CBCT) images in implanted patients and temporal bones.

Study Design: A retrospective review of post-op CBCT of 8 adult patients underwent cochlear implantation with straight flexible electrodes array were compared with CBCT images of 15 fresh temporal bones implanted with the same electrodes array. The insertions were made using an extended round window approach for all the cases. An expert oto-radiologist and two otologists examined the images and assessed the electrodes position. The temporal bone specimens underwent histological analysis for confirm the exact position.

Setting: Tertiary referral center.

Main outcome measures: The position of the electrodes was rated by three evaluators between Scala Tympani (ST), Scala Vestibuli or intermediate position for the electrodes at 180°, 360° and for the apical electrode in implanted patients and in temporal bones.

Results: In the patients group for the electrodes at 180° all observers agreed for ST position except for 1 evaluation, while a discrepancy in three patients both for the 360° and for the apical electrode assessment were found: 3 evaluations over 24 possible for the two electrodes were not in accordance In five temporal bones the evaluations were in discrepancy for the 180-degrees electrode, while at 360-degrees a disagreement between raters on the scalar positioning was in six temporal bones. A higher discrepancy between was found in assessment of the scalar position of the apical electrode (average pairwise agreement 45.4%, Fleiss k = 0.13). A good concordance was found between the histological results and the consensus between raters for the electrodes in the basal turn, while low agreement (Cohen's k=0.31, pairwise agreement 50%) was found in the identification of the apical electrode position confirming the difficulty to correct identify the electrode position in the second cochlear turn in temporal bones.

Conclusion: The CBCT is an excellent radiologic exam for correctly evaluate the position of a lateral wall flexible array in implanted patients in the basal turn while some artifacts impede to exactly evaluate the position of the apical electrode. The CBCT was hence considered a reliable imaging technique for the identification of the electrode array position in cochlear implanted patients; in temporal bone studies other radiological techniques should be preferred.

Manuscript prepared for submission: De Seta D, Mancini P, Russo FY, Torres R, Mosnier I, Bensimon JL, Ferrary E, De Seta E, Heymann D, Sterkers O, Bernardeschi D, Nguyen Y. 3D curved multiplanar reconstruction of cone beam CT images for intracochlear position assessment of straight electrodes array. A temporal bone and patients study. Acta Otorhinolaryngol Italica.

4.2.1 Introduction

The indications for cochlear implantation during the last decades have extended including not only the severe-profound bilateral deafness but also the sensorineural hearing loss involving only medium-high frequencies or single sided deafness. The so-called soft or minimally invasive surgery and its principles are regularly applied to the standard procedures in cochlear implantation not only in hearing preservation surgeries. In this context the pre- and post-operative imaging gained importance both for the planning of the surgery and the choice of the kind and length of the electrode array to be implanted, and for the correct evaluation of the position of the implanted array. The use of Cone Beam CT (CBCT) in otology increased during the last years being a lower dose cross-sectional technique for visualizing bony structures in the ear (Miracle and Mukherji, 2009) providing a better resolution than multislice helical CT for the bone structure with strong density contrast (Dahmani-Causse et al., 2011). Several studies reported the reliability to assess the scalar position of electrodes array using CBCT in isolated temporal bones (Kurzweg et al., 2010; Cushing et al., 2012; Guldner et al,. 2012; Marx et al., 2013; Saeed et al., 2014) or whole cadaveric heads (Diogo et al., 2014), but the possibility to apply these results on real clinical situation on cochlear implanted patients has not been studied in detail. The scalar position of the electrodes in implanted patients was analyzed in a study including precurved and straight arrays implanted in 61 ears (Boyer et al. 2015) but the reliability of the radiological exam was not reported. Moreover the results might change in function of the different implanted arrays (i.e perimodiolar or straight array). Studies in cochlear implanted temporal bones reported excellent reliability in scalar localization of precurved perimodiolar array (Kurzweg et al., 2010; Marx et al., 2014; Saeed et al., 2014), while for slim straight electrodes the position assessment still remain difficult in some cases (Guldner et al., 2012; Saeed et al., 2014). Diogo et al. (2014) reported a lower degree of cochlear implant (CI) metal artifacts in the images of the whole head in comparison with the same isolated temporal bones that present reduced soft-tissue absorption of radiation, but still difficult to evaluate the precise location in the more apical regions of the cochlea. Another issue to take in account is the artifact due to the movement of the patient, totally absent in studies on cadaveric specimens, considering the duration of the CBCT exam longer than other radiological imaging techniques of the ear. Aim of the study is to validate the 3 dimensional curved multiplanar reconstruction in CBCT images as a method for the assessment of long straight cochlear implant electrodes array scalar position in implanted adult patients and compare the results with a temporal bone radio-histologic study using the same electrode array and surgical technique.

4.2.2 Materials and methods

The scalar position of two electrodes located in the basal turn of the cochlea and a third one located in the second turn in temporal bones and in adult implanted patients was assessed by

an expert otoradiologist and two otologists by reviewing the CBCT reconstruction images. The scalar position and the ratings of the temporal specimens were successively confirmed by histological analysis. Each step is described in details below.

Temporal bones

Fourteen fresh temporal bone (seven left and seven right from the same subjects) were prepared with a simple mastoidectomy and posterior tympanotomy. The MedEl flex 28 arrays (Innsbruck, Austria) were provided by the manufacturer and used for this study. The temporal bone was fixed to an in-house made temporal bone holder and the electrodes arrays were inserted through an extended round window approach using an in-house made motorized insertion tool (Nguyen et al 2014). This tool comprised a rotary actuator (RE10CLL, MDP, Miribel, France) connected to a threaded screw that pushed a blunt pin into an insertion tube loading the array. The tool was held steady by a flexible arm. The actuator speed was controlled via laboratory power supply and set at 0.8 mm/s. The round window was irrigated with saline serum and sodium hyaluronate (Healon, Abbott Medical Optics, Abbott Park, Illinois, USA) was applied before the CI insertion. A cone beam CT (CBCT) scan (NewTom 5G, QR s.r.l. Verona, Italy) was performed on the temporal bone specimens after the CI insertion.

Patients

Eight adult patients (nine ears) cochlear implanted with MedEl flex 28 arrays in the cochlear implant program at a tertiary referral center where prospectively enrolled in study and accepted to receive a CBCT postoperatively. All the patients were operated by the same experienced CI surgeon (EDS) via standard retroauricular approach followed by mastoidectomy and posterior tympanotomy, and extended round window insertion of the array. The patients were discharged at day 1 postsurgery and received a CBCT scan one month postimplantation; the activation of the CI was performed between 3 and 4 weeks postoperative. The patients signed a written informed consent, the study was approved by the local IRB.

Imaging

The NewTom 5G CBCT scanner (NewTom, Verona, Italy) was used both for patients and temporal bones using the same setting. The system setup used a 200 x 25 mm flat panel detector at 650 mm from the radiation source. One 360-degree rotation of the x-ray tube took 36 seconds. The tube voltage was 110 kV, with a 19-mA charge at the terminals. Total filtrations were 2 mm, with a pitch of 125 Km; this corresponded to a field view of 12 x 7.5 cm diameter. The images were isometric voxel rendered from the 125-Km sections.

Scalar position assessment

Two otologists and an expert otoradiologist reviewed the CBCT images and assessed the position of the electrode array within the cochlea. The DICOM (Digital Imaging and Communications in Medicine) data were analysed by Osirix program (Osirix v 4.0 64-bit;

Pixmeo Sarl, Bernex, Switzerland). This program allowed the realization of multiplanar reconstructions for the evaluation of the scalar position of the arrays was used for the measurements of the cochlear sizes. The largest cochlear diameter (distance A) going from the center of the round window membrane to the opposite lateral wall (Escude et al.2006) as well as the angular depth of insertion, were calculated on a plane perpendicular to the modiolus axis and coplanar to the basal turn as already reported (De Seta et al. 2016). The round window was considered as the 0-degrees reference angle in accordance with the consensus of cochlear coordinates (Verbist et al., 2010).The reconstruction plane for the evaluation of the electrodes position was the midmodiolar plane obtained with the curved multiplanar reconstruction (3D curved MPR viewer in Osirix ®). This plane was defined as a 3D Bezier path along the electrodes array. Once the path is defined by means of the selection of all the single electrodes the array is straightened and visible in the curved MPR viewer window. In this window the cochlear lumen and the electrodes array can be easily visualized in a dynamic series of midmodiolar section of the cochlea (Fig. 4.5). The raters assigned the localization scala tympani, scala vestibuli or intermediate position for each of the electrodes positioned at 180-, 360-degrees and for the apical electrode both for the temporal bone implanted specimens and for the implanted patients. For more information on the 3D curved MPR see: (http://www.osirix-viewer.com/pixmeo/documents/OsiriX-3DCurvedMPR.pdf).

Histological procedures

Immediately after its insertion in temporal bones the electrode array was fixed with cyanoacrylate glue to the round window region in order to avoid any displacement during the successive steps. Cochlea was removed from the temporal bone and was fixed in 10% buffered formalin. The specimen was successively dehydrated in graded alcohol and casted in methyl methacrylate resin (10% Polyiethylene Glycol 400, 20% Technovit 7200 VLC, Heraeus Kultzer Gmbh, Germany; 70% Methylmethacrylate). The specimen was sawed (Leica SP 1660 Saw Microtome, Nussloch GmbH Germany, sawing speed 3) perpendicularly to the basal turn passing through the round window and the images under white light microscope were obtained for the two parts. The half cochlea was successively grinded in order to visualize the apical electrode if the first cut did not allow the visualization.

Statistical Analysis

Results are reported as means ± SD. Inter-rater reliability has been calculated using the Fleiss' kappa for three raters and the Cohen's kappa for two raters as appropriated. The averaged pairwise percent agreement among raters for each of the 3 examined electrodes was calculated. "R" statistical software (http://www.r-project.org) was used for the statistical analysis.

4.2.2 Results

In table 4.1 are reported the pre- and postoperative cochlear measurement in patients and temporal bones. The mean distances A were 9 ± 0.1mm 9 ± 0.07 mm in patients and temporal bones respectively. Among the patients, the full insertion of the array was achieved in six ears (angular depth of insertion 498 ± 17 degrees), in three ears a partial insertion was founded. In temporal bones 8 arrays were fully inserted (angular depth of insertion 464 ± 20 degrees).

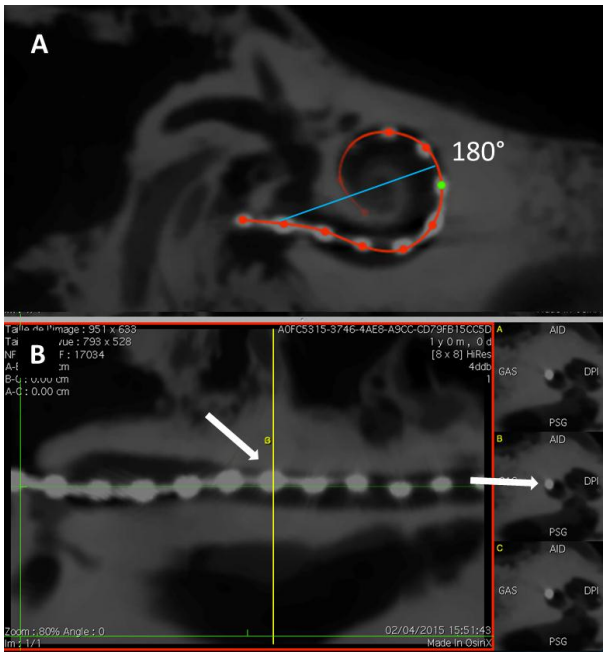

Figure 4.5. 3D curved multiplanar reconstruction (MPR) of the electrode array in a temporal bone. A. The electrodes were first selected with the 3D MPR tool in a Bezier path (red line).
B. This function permitted to straightened electrode array and follow it along its trajectory in the cochlear lumen in a dinamic way accross a continuos series of midmodiolar reconstruction of the cochlea (MPR views on the right down panels). The interelectrode part of the array has a very limited metallic artifact thus the assessment of the electrode position results easier in this part of the array.

Electrodes position in implanted patients

There was an overall high agreement within raters for the assessment of the electrodes position within the cochlea (Fig 4.6). The intracochlear position for the electrode at 180-degrees in the implanted patients showed a great concordance among rater with only 1 evaluation in disagreement, one evaluator rated as inferior an electrode rated as intermediate for the other two evaluators (average pairwise agreement 92.5%, Fleiss k = 0.46). For the electrode at 360-degrees three evaluations were not in agreement between raters (average pairwise agreement 88.8%, Fleiss k = 0.38). For the position of the apical electrode the raters were more discordant with 4 evaluations in disagreement (average pairwise agreement 70.3%, Fleiss k = 0.35). A consensus on the position of the electrodes from the three raters was obtained after rereading the images and two arrays resulted translocated, both in the second turn (Fig 4.6 B-C).

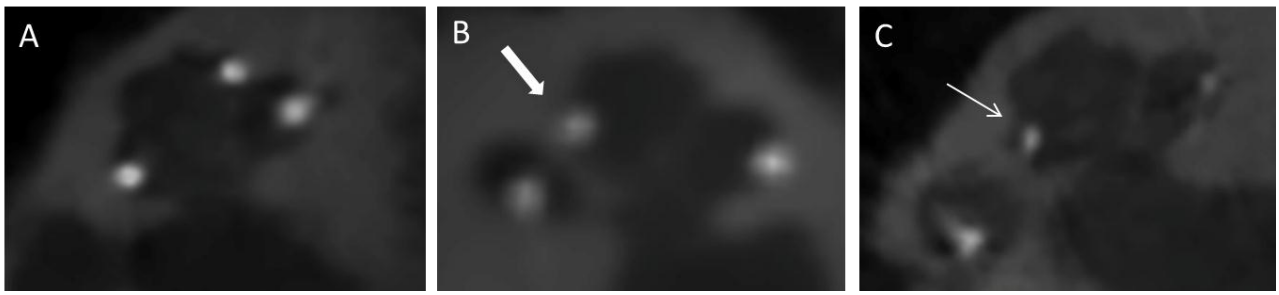

Figure 4.6. Cone beam CT in cochlear implanted patients. In A, all raters indicated the three electrodes in scala tympani position. The apical electrode in B (thick arrow) was indicated by all raters as translocated. In C the apical electrode (thin arrow) was considered in intermediate position by two raters and translocated by one, and finally considered as a traumatic insertion after consensus.

Electrodes position in temporal bones

In temporal bones the rate of agreement was similar to what founded in implanted patients for the electrode at 180-degrees (average pairwise agreement 71.5%, Fleiss k = 0.48) and for the electrode at 360-degrees (average pairwise agreement 61.9%, Fleiss k = 0.35) (Fig 4.7). In five temporal bones the evaluations were in discrepancy for the 180-degrees electrode, while at 360-degrees a disagreement on the rating of the scalar positioning was in six temporal bones. A higher discrepancy between rater was found in assessment of the scalar position of the apical electrode (average pairwise agreement 45.4%, Fleiss k = 0.13). In one temporal bone the raters were in totally disagreement with the same apical electrode assessed either as SV, ST or intermediate position (Fig 4.8). A collective statement on the position of the electrodes from the three raters was obtained after rereading the images; this statement was compared to the histological results.

The histological analysis confirmed the localization of the electrodes and showed a translocation between scala tympani and scala vestibuli in 6 temporal bones (42 %). All the translocation occurred between 150- and 180-degrees. A good concordance was found between the histological results and the consensus between raters for the electrodes at 180-degrees (Cohen's k=0.54, pairwise agreement 78.7%) and 360-degrees (Cohen's k=0.71, pairwise agreement 85.7%). The identification of the apical electrode position after the consensus between the raters was poor (Cohen's k=0.31, pairwise agreement 50%), highlighting the difficulty to correct identify the electrode position in the second cochlear turn in temporal bones.

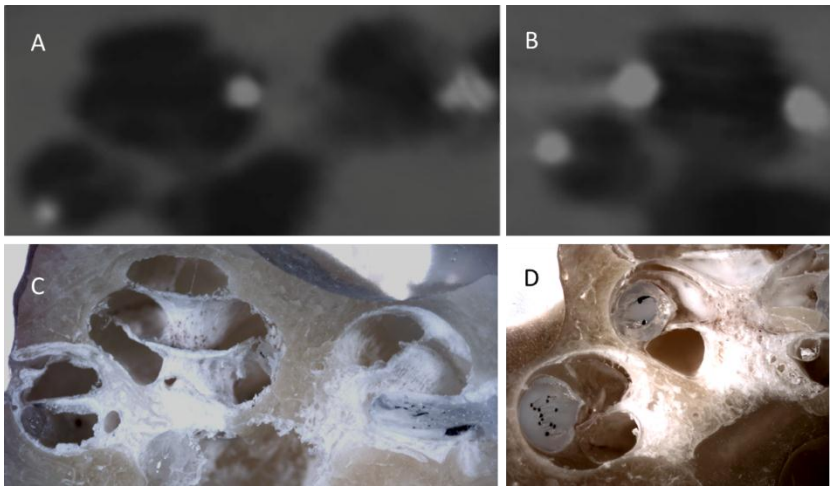

Figure 4.7. Electrodes array in the scala tympani position (left) and in scala vestibuli (right) in temporal bone specimen. In these examples a full concordance on the electrodes localization on CBCT images (A, B) was obtained among the three raters and after the histological analysis that confirmed the electrodes position (C, D).

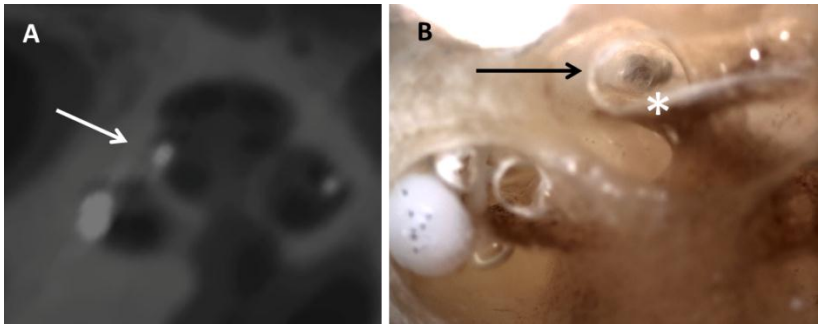

Figure 4.8. Difficulty in the assessment of the apical electrode. A, In this specimen the raters assessed the electrode (white arrow) either as scala vestibuli, scala tympani or intermediate position. B, the histology confirmed the translocation (black arrow). * Osseous spiral lamina.

Table I Preoperative and postoperative measurements in temporal bones and patients

Patient	Distance A (mm)	Angular depth of insertion	Inserted electrodes
1	9,77	480	12
2	9,16	533	12
3	8,93	512	12
4R	8,82	422	12
4L	8,62	507	12
5	9,35	407	10
6	8,91	403	11
7	8,92	461	11
8	9,1	535	12
Temporal bones			
1R	9,07	440	12
1L	9,49	400	12
2R	8,67	270	8
2L	8,85	369	10
3R	9,52	365	11
3L	9,46	387	11
4R	9,22	412	12
4L	8,77	520	12
5R	9,13	472	12
5R	9,02	514	12
6R	8,45	404	11
6L	8,42	529	11
7R	9,48	522	12
7L	9,52	434	12

Table II inter raters agreement for electrodes positioning assessment in patients and temporal bones

	electrode		
	180-degrees	360-degrees	apical
	Patients		
Mean pairwise agreement	92.5 %	88.8 %	70.3 %
Fleiss' kappa	0.46	0.38	0.35
	temporal bones		
Mean pairwise agreement	71.5%	61.9%	45.4%
Fleiss' kappa	0.48	0.35	0.13

4.2.3 Discussion

In this study the cone beam CT scan was confirmed to be a reliable radiological technique for the assessment of intracochlear location of straight and flexible electrodes array in adults implanted patients. In temporal bones the assessment of the more apical electrodes resulted more difficult than in patients. The 3-dimensional curved multiplanar reconstruction as a method to evaluate the electrode position helped to standardize the methodological technique among the raters and was a reliable, rapid and easy tool for intracochlear identification of electrodes position.

Several studies investigated the reliability of the cone beam CT on the scalar position assessment of cochlear implants. For precurved arrays Marx et al. (2013) reported a high sensitivity (100 %) and specificity (90 %) in scalar assessment localization of the array), in another study the exact position was reviewed correctly by means of CBCT in 11 of 13 cases (85%) (Kurzweg et al. 2010). The position of precurved electrodes array was reported to be correctly assessed in the oblique sagittal plane (Lane et al. 2007) or using midmodiolar reconstruction also in multislice CT, with a radioanatomic correlation at 0.94 (0.89-0.98) after the consensus of two raters (Lecerf et al. 2011).

The identification of electrode position could be different using different kind of electrodes array and could result easier for precurved electrodes. Indeed, the perimodiolar position of the electrode array is more consistent than that of straight electrodes (Saeed et al. 2014). The presence of osseous spiral lamina clearly divide the medial portion of the cochlear lumen in two compartment and the electrode is firmly held by this bony structure either in a lower or higher position i.e., tympanic or vestibular ramp. In contrast the lateral wall of the cochlear lumen has a rounded shape and the spiral ligament being less resistant is deformed or bended by the cochlear array that can assume an intermediate position close to the midline of the cochlear lumen even without damaging the basilar membrane or the spiral ligament, thus assuming a position that sometimes is difficult to be identified. For this reason we adopted a third "intermediate" position for array location assessment that was never used in other studies. This third position increased the number of possible choices for the raters making more difficult a high percentage of inter-observer agreement.

Inter-observer agreement for the imaging characteristics (scala implanted, number of contacts inserted into the cochlea and presence of kinking within the electrode array) was 100% among three reviewers in a temporal bone study where a straight electrode was implanted (Cushing et al 2012). In this study the authors only evaluated the presence or not of the translocation of the array and did not evaluated the location of 3 electrodes with three possible positions like we performed in our study, moreover the implant used was different and this might also explain the different findings. Boyer et al. (2015) found a very low translocation rate (3%) and high agreement between raters for the correct intracochlear localization of the MEDEL flex electrodes; also in this study the methodology for the evaluation of the position of the electrode was different to that used in our study and the results are not completely comparable.

In studies performed in temporal bones that evaluated the same electrodes array used in the present study reported a reliable postoperative control of the intracochlear position in the basal turn but difficulties in the evaluation of the localization in the medial and apical turns (Guldner et al., 2012). Diogo et al. (2014) found a higher metallic artifact of the electrodes in temporal bone in comparison to the whole head, probably due to the lower absorption of radiation by soft tissue determining greater surface radiation of the metal, and thus a greater artifact. The amount of the metallic artifact was not considered in this study, but the different results in the identification of the apical electrodes between temporal bones and patients may be caused by the different intensity of the artifact. Indeed, the CBCT is an artifact lean but not an artifact free method (Guldner et al., 2012).

A possible drawback of the CBCT for analysis of submillimetrical structures could be represented by the longer duration of the exam (18-36 seconds) in comparison with MSCT (4-6 seconds) that may result in possible artifacts due to the head movement of the patient (Schulze et al., 2011). Moreover, the higher the spatial resolution, the smaller the movement necessary to move the patient structures out of the ‘‘correct’’ position. Nevertheless, in the eight CBCT images obtained from the patients we did not observed any artifact. The cone beam machine used in this study allowed the lying down position and the use of head holder helped to avoid the artifacts.

In conclusion the CBCT is confirmed to be a reliable imaging technique for the identification of the intracochlear electrodes position also for straight and flexible array in adult implanted patients. In temporal bones probably due to higher metallic artifacts the position of the electrodes in the apical region of the cochlea were difficultly assessed. For this reason we advise the use of histologic analysis for the confirmation of the electrodes position in temporal bones studies.

With this study we validated a technique to identify the intracochlear position of straight electrodes array in the cone beam CT images using the 3D multiplanar reconstruction method (MPR). The Osirix® program and 3D MPR have been used in the next studies of this thesis for the preoperative cochlear anatomical measurement and for the postoperative measurement of the implant positioning both in Cone Beam CT and Mulihelical Spiral CT images.

5 Relationship between hearing outcomes and the position of the electrodes array

The continuous evolution and development in speech processing, electrode array design and surgical techniques led to an improvement of hearing outcomes in cochlear implanted patients over the last decades with similar average speech-reception abilities across different devices. However, within the same device a wide variability in speech reception is seen across individuals suggesting that significant patient dependent factors could influence the speech reception at the individual level. Several recipient specific factors have been identified as affecting hearing outcomes, including duration of deafness and duration of cochlear implant (CI) use, residual preoperative speech score, onset of the hearing impairement (pre- peri or post-lingual), sound processing strategy, and method and quality of fitting. Green et al. (2007) reported duration of deafness to be an independent predictor of performance, accounting for 9% of the variability in a retrospective study examining 117 postlingually deaf patients implanted between 1988 and 2002. Neither preimplant residual hearing nor age at implantation was a significant predictor of CI outcomes. Leung et al. (2005) examined a large group of CI recipients 14 to 91 years of age enrolled in different centers. The recipients were divided into a younger group (<65 years of age, n = 491) and an older group (≥65 years of age, n = 258). No correlation between age at implantation and postimplant monosyllabic word scores was seen. Other factors, known to vary across subjects include mediolateral placement of electrodes within scala tympani, depth of insertion or scalar displacement have been studied but the results across the different studies are controversial.

All these studies indicate that different factors may potentially influence the individual hearing performance with a CI; nevertheless, apart from duration of deafness, there was no agreement among studies on which factors have the greatest role on speech recognition. As studies done by Shepherd et al. (1993) reported that the scala tympani is the ideal place for electrode placement, a number of recent studies have proposed that electrode traslocation from the scala tympani to the scala vestibuli may be an important determinant of audiological outcome. Skinner et al. (2007) and Finley et al. (2008) used rigid registration methods, which are based on aligning structures from postoperative to preoperative computed tomographic scans and use of a high-resolution cochlear atlas to overcome the inability to positively identify the basilar membrane on clinically applicable temporal bone computed tomographic scans.

In the following sections of this chapter the influence of electrode position on postimplant speech scores will be evaluated in a bilaterally and unilaterally implanted patients in two studies with the use of multislice spiral CT scan and Cone Beam CT images respectively.

5.1 DEPTH OF INSERTION AND PROXIMITY TO THE MODIOLUS: SHORT AND LONG TERM INFLUENCE IN BILATERAL COCHLEAR IMPLANTED PATIENTS

Objective: To evaluate the influence of the electrode placement and to analyze the change of hearing performance and sound localization between 1 year and 5 years measurement intervals in adult patients bilaterally and simultaneously implanted patients.

Design: In this prospective, longitudinal, multicenter study, twenty-six patients were evaluated at 1-year and 5-years after bilateral and simultaneous implantation using long straight electrode arrays (MED-EL Combi 40+, Standard Electrode array 31 mm). Speech perception was measured using disyllabic words lists in quiet and noise, with the speech coming from the front and a cocktail-party background noise coming from 5 loudspeakers. Speech localization measurements were performed in noise in the same test conditions. In 19 patients, the size of the cochlea was evaluated using the largest cochlear diameter and the cochlear height on postoperative high-resolution CT scan. The electrode-to-modiolus distance (EMD) for the electrodes positioned at 180- and 360-degrees and the angle of insertion of the array were also measured.

Results: At 5-years postimplantation, speech perception scores in quiet were stable for each ear alone, and in bilateral condition. Compared to 1-year, in noise, speech perception scores of the poorer ear improved, whereas no significant change was observed for the better ear, and in bilateral condition. The speech perception scores of the 7 patients with 'poor performance' (<60% of correct responses for the better ear in quiet at 1-year) improved for each ear alone in quiet and dramatically in noise. Speech localization remained stable over time. In patients with a full electrode insertion, no correlation was found between the angle of insertion and hearing performance both at 1- and 5-years postimplantation, whereas the EMD distance at 180-degrees was correlated with the speech perception scores in quiet and in noise, but only at 1-year postimplantation.

Conclusion: In adult patients simultaneously and bilaterally implanted, the poorest ear speech perception scores still improved after one year of cochlear implant experience. Using MedEl 31 mm straight array, the full electrodes array insertion and the proximity to the modiolus might be determining factors to obtain the best speech performance at 1-year, without influence on the speech perception scores after long-term use.

Published as:

5-Years Outcomes in Bilateral Simultaneously Cochlear Implanted Adult Patients. Daniele De Seta, Yann Nguyen, Antoine Vanier, Evelyne Ferrary, Jean-Pierre Bebear, Benoit Godey, Alain Robier, Michel Mondain, Olivier Deguine, Olivier Sterkers and Isabelle Mosnier. *Audiol Neurotol under revision*

The Role of Electrode Placement in Bilateral Simultaneously Cochlear Implanted Adult Patients. Daniele De Seta, Yann Nguyen, Damian Bonnard, Evelyne Ferrary, Benoit Godey, David Bakhos, Michel Mondain, Olivier Deguine, Olivier Sterkers, Daniele Bernardeschi and Isabelle Mosnier. *Otolaryngol Head and Neck Surg. Accepted for publication April 1 2016*

5.1.1 Introduction

The bilateral cochlear implantation is now well accepted worldwide to rehabilitate the hearing in severe to profound bilateral deafened adults. The efficacy of bilateral cochlear implantation is acknowledged both in children and in post lingual adults. Several studies demonstrated the effectiveness of bilateral simultaneous or sequential implantation in relatively large study groups (Müller et al. 2002; De Seta et al. 2005; Ricketts et al. 2006; Litovsky et al.2006; Peters et al. 2007; Dunn et al. 2008; Mosnier et al. 2009; Sparreboom et al.2010; Dunn et al. 2012), although systematic reviews (van Schoonhoven 2011) underline the need for more studies with higher level of evidence. Bilateral cochlear implantation effectiveness is proved when the advantages of binaural hearing listeners can be found in bilateral CI users. Until the last years, health care professionals have recommended unilateral, rather than bilateral cochlear implantation for several reasons, including: cost/reimbursement issues, preservation of one ear for future technologies, additional risk of two, or extended, surgeries, and lack of evidence documenting bilateral cochlear implant benefit. The substantial benefits of binaural hearing are two: better discrimination in noisy environment and spatial sound localization. The first component is related to the physical "head shadow effect" and two other central mechanisms, the "squelch effect" and the "binaural summation". The ability to localize the sound source derives primarily from acoustic cues arising from differences in arrival time (for lower pitches) and level (for higher pitches) of stimuli at the two ears. The bilateral benefit is mainly observed in noise in studies using two separate speech and noise sources (Litovski et al. 2006) as in studies evaluating speech perception in more complex and realistic environments using multiple noise sources (Ricketts et al. 2006; Dunn et al. 2008; Mosnier et al. 2009). The more robust bilateral advantage is seen when the subjects are able to take advantage of the head shadow effect. The contribution of the binaural summation and of the squelch effect is weaker in these studies at 1-year postimplantation (Litovski et al. 2006). In quiet, the advantage of the bilateral condition in comparison with the better of the two unilateral conditions has been found at very early stage (1-month post activation) (Litovski et al. 2006; Buss et al. 2008); this bilateral benefit continued to improve during the first 12 months (Litovski et al. 2006; Buss et al. 2008; Mosnier et al. 2009). Moreover, all studies demonstrated that bilateral implantation provide a marked improvement in sound localization in quiet and noise compared to unilateral implantation (Tyler et al. 2007; Grantham et al. 2007; Mosnier et al. 2009; Litovsky et al. 2009; Kerber & Seeber, 2012).

Despite this clear benefit of bilateral implantation, substantial inter but also intraindividuals variability in speech perception scores exists among bilaterally cochlear implanted recipients (Litovsky et al. 2006, Mosnier et al. 2009). Indeed, in a prospective multicenter study, asymmetrical performance between the two ears was reported in 42% of simultaneously implanted patients at 1-year postimplantation (Mosnier et al. 2009). The etiology, the durations of hearing deprivation, of hearing loss, of hearing aid use, and the number of activated electrodes were similar between the two ears, and the reasons of this asymmetry remain to be understood. An explanation to account to this asymmetrical performance could be differences in electrode position within the cochlea between the two ears (Esquia Medina et al. 2013; Holden et al. 2013; Buchman et al. 2014).

Moreover, the evolution of asymmetrical performance over time is unknown. Although several studies report the long term hearing outcome of unilateral cochlear implanted patients (Lenarz et al. 2012), only few studies assess the effect of experience on unilateral and bilateral speech perception scores, and on localization tasks in simultaneously bilateral implanted adults (Eapen et al. 2009; Chang et al. 2010) and the results remains ambiguous. Chang et al. (2010), in a group of 48 patients with a follow-up of 6 years, observed no major improvement of the speech performance in quiet and in bilateral condition after 2 years and of the sound localization after 1 year. In contrast, Eapen et al. (2009) showed an improvement of the speech perception scores in a group of 9 patients between 1-year and 4-years postimplantation. In noise, an increase was found for the squelch effect after 1 year, but the binaural benefit of the head shadow and of the summation effects remains stable between 1 year and 4 years.

The objective of this study was to analyze the influence of electrode placement within the cochlear lumen, on speech performance at 1-year and 5-years follow-up in 26 adult patients bilaterally and simultaneously implanted, and to assess changes between 1-year and 5-years measurement intervals in speech perception and sound localization in this population.

5.1.2 Materials and methods

Selection criteria and subjects

Subjects enrolled in this study were adult patients with a post-lingual bilateral profound or total hearing loss. To be implanted, they were required to have a maximum of 10% open set disyllabic word recognition in quiet environment at 60 dB SPL in the best-aided condition, a duration of severe to profound hearing loss of less than 20 years, a difference in duration of profound hearing loss between the 2 ears of less than 5 years, fluency in the French language, and no malformations of the cochlea. All patients underwent bilateral implantation in a simultaneous surgical procedure with the same device (MED-EL Combi 40+, Standard Electrode Array, 31 mm length; Innsbruck, Austria). Cochlear implants were simultaneously activated using the same speech coding strategy CIS (Continuous Interleaved Sampling) in both ears, although each ear underwent independent mapping. The speech coding strategy and the sound processors remained the same for all the patients for the 5 years of follow-up. The number of the active electrodes remained stable over time (1- / 5-years). All the patients signed a written informed consent; the study was approved by the local ethical committee (Saint-Louis, Paris, No. 61D0/22/A).

Twenty-seven adult patients were enrolled before implantation in six tertiary referral centers. Results of 26 patients were included in the data analysis; one patient in pregnancy did not complete the tests at the 5-years follow-up interval. Demographic data for the patients are summarized in Table 5.1. The duration of deafness, of hearing deprivation, of hearing aid use and the etiologies were similar between the 2 ears.

Radiological analysis

A multi-slice spiral CT scan (500 µm slice thickness) was performed in 19 patients 5-years after implantation. The DICOM (Digital Imaging and Communications in Medicine) data were analyzed by Osirix program (Osirix v 4.0 64-bit; Pixmeo Sarl, Bernex, Switzerland). This program allowed the multiplanar reconstructions for the measurement of the cochlear anatomy and the position of the arrays within the cochlea. All the images, acquired by different CT scanner in the different centers, were reconstructed with 0.1 mm increments in order to standardize the measurement technique and reduce the error of measurement. To examine the cochlear dimensions and their relationship with the insertion depth, a three-dimensional coordinate system was used, in accordance with the consensus of cochlear coordinates (Verbist et al. 2012), with the exception of the cochlear height that was measured in a reformatted coronal view. The largest cochlear diameter (distance A) going from the center of the round window membrane to the opposite lateral wall, as described by Escude et al. (2006) was calculated in the cut, perpendicular to the modiolus axis and coplanar to the basal turn, named 'cochlear view' by Xu et al. (2000) (Fig. 5.1A). The cochlear height was measured from the mid-point of the basal turn to the mid-point of the apical turn on a coronal section (Purcell et al. 2003; Mori et al. 2012) (Fig. 5.1B). The electrode-to-modiolus distances (EMD) for the electrodes positioned at 180- and 360-degrees were measured in the plane of modiolus axis crossing the mid of the round window (Fig. 5.1C). The angle of insertion of the array was measured in the 'cochlear view' (thick cut of 5 mm) considering the 0° the mid-point of the round window (Fig. 5.1D). To minimize the error, all the measurements were performed blindly by an otologist, each measurement was repeated three times in nonconsecutive days, and the mean value was then considered.

Table 5.1 : Patient Demographics (n= 26)

Age at implantation (yrs)	45 ± 2.4 [24-68]
Sex, Male/Female	7/19
Duration of hearing loss (yrs)	
Right ear	25 ± 2.5 [1-51]
Left ear	25 ± 2.7 [1-51]
Duration of profound hearing loss (yrs)	
Right ear	3 ± 0.5 [1-9]
Left ear	2.7 ± 0.5 [0-9]
Use of hearing aids before implantation (yrs)	
Bilateral	17
Unilateral	1
None[a]	8
Duration of hearing aid use (yrs)	
Right ear	14 ± 2.8 [1-41]
Left ear	15 ± 2.9 [1-41]
Etiology[b]	
Unknown	6
Sudden hearing loss	8
Genetic/Familial	9
Traumatism	1
Otosclerosis	1
Meningitis	1

Values are expressed as mean ± SEM [range] or only number of patients

a These patients never tried hearing aid because of sudden total bilateral hearing loss. b. Same etiology for both ears.

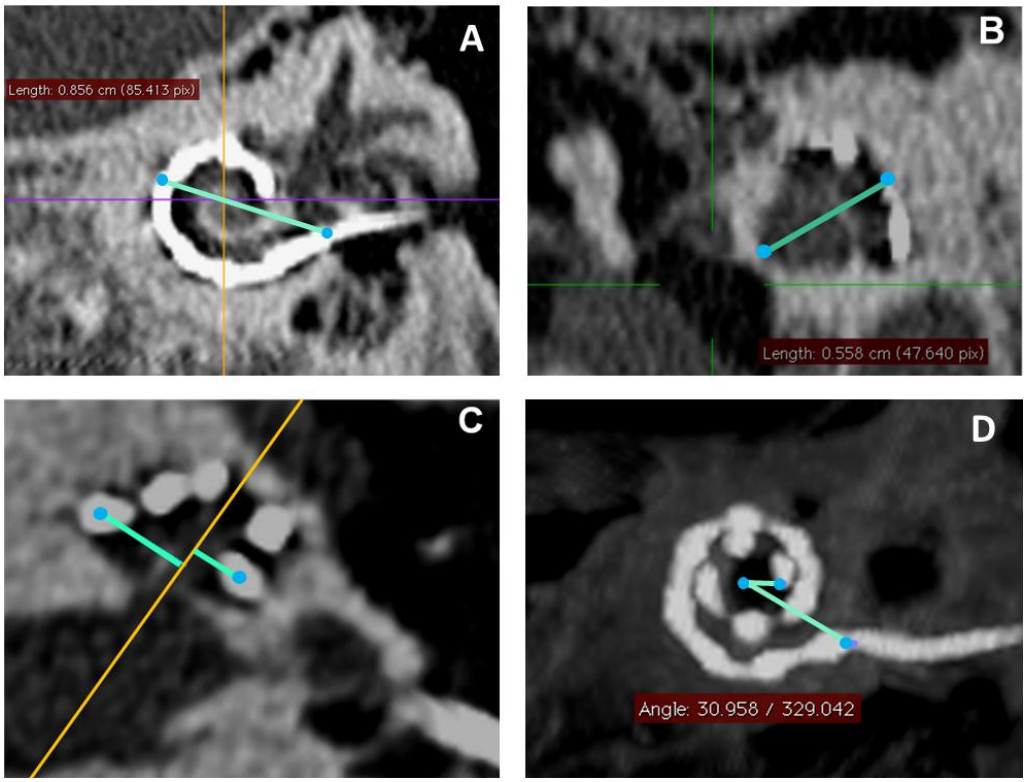

Figure 5.1: Radiological analysis (CT scan). A. The greatest cochlear diameter (Distance A) was measured from the round window to the opposite lateral wall of the cochlea in a cut perpendicular to the modiolar axis passing through the round window, the superior semicircular canal and the lateral semicircular canal. B. The cochlear height was measured in the coronal reconstruction. C. The electrode-to-modiolus distance (EMD) was measured from the middle of the electrodes positioned at 180-degrees and 360-degrees to the modiolar axis. D. The angle of insertion was measured in the same plane of A with a thickness of 5 mm.

Speech perception measures

Speech perception tests were performed before implantation, 3, 6, 12 months, and 5 years after activation. Study design and mean speech perception during the first year of follow-up were previously reported in Mosnier et al. (2009). Measurements were performed in a sound-treated room using five loudspeakers (Monacor MKS-40, frequency response: 80–18000 Hz) positioned at 45° intervals in the frontal hemi-field, ranging from –90-degrees to +90-degrees. Test materials consisted of 50 lists of 10 disyllabic words (Fournier word lists) recorded in quiet and in noise. Speech was always presented at 70 dB SPL from a loudspeaker placed at 0-degrees. Tests in noise were administrated at a signal-to-noise ratio (SNR) of +15 dB, +10 and +5 dB, with the speech stimuli coming from the front and a cocktail party background noise coming from the 5 loudspeakers, including the central one that presented the speech target. Tests at 0 dB were also performed at 5-years follow-up. Randomization of test lists presented for each patient was carried out independently at each test site. Responses were scored as the percentage of words correctly identified.

Sound localization

Sound localization measurements in noise were performed at 1- and 5-years. The test stimuli, dissyllabic words, were presented in a random sequence from each of the 5 loudspeaker locations for a total of three times, at an intensity level varying from 60 to 80 dB SPL. The competing sound material was a cocktail party background noise coming from the 5 loudspeakers. In order to test only the localization, without interference from the hearing performance, the SNR was adapted for each subject and each listening conditions (monaural right, monaural left, and binaural condition) in order to obtain a 50% correct speech recognition score for disyllabic words coming from the central loudspeaker. After each stimulus presentation, subjects reported the loudspeaker number corresponding to the perceived sound location. For each loudspeaker, the number of correct responses was noted, and results were expressed as the mean percentage of correct responses per loudspeaker.

Statistical analysis

Values are expressed as means ± standard error of the mean (SEM).

The better ear was defined as the ear with the better speech score in quiet. In case of equality of speech scores between the two ears in quiet, the score of the better ear in noise at SNR + 15 dB was considered. Speech performance score was modeled using a linear mixed model with 3 fixed effects (1. Time: 1-year or 5-years after implantation; 2. Ear: Better, Poorer or Bilateral; 3. Noise: Quiet, SNR +15 dB, SNR +10 dB or SNR +5 dB) and 1 random effect (random intercept for each patient). To select the most parsimonious model including only relevant effects of interest, a first model was fitted with the 3 fixed effects and including all the possible second and third order interaction terms between the fixed effects. Then, a backward selection procedure was applied in order to remove interaction terms that did not contribute to explain speech performance score. The final selected model was the one with the lowest Bayesian Information Criterion (BIC) value. Based on the final model estimates, post-hoc two-by-two comparisons were performed using relevant contrasts with p-values adjusted for multiple comparisons according to Holm-Bonferroni step down procedure (Holm, 1979).

Spearman correlation coefficients (r) were estimated between the difference in speech performance score from 1-year to 5-years after implantation and the corresponding speech performance score at year 1-after implantation. These analyses of correlations were only performed for conditions where an evolution over time was found to be significant according to the previous analyses. The estimated correlation coefficients were tested against the null hypothesis of an absence of correlation with an a priori Type I Error level fixed at 5%.

Evolution of sound localization between 1 year and 5 years after implantation

The number of correct responses (as a percentage) was modeled using a linear mixed model with 3 fixed effects (1. Time: 1 year or 5 years after implantation; 2. Ear: Unilateral right, Unilateral left or Bilateral condition; 3. Loudspeaker: LS1 to LS5) and 1 random effect (random intercept for each patient). Model selection and post-hoc two-by-two comparisons were performed according to the aforementioned procedure used for the evolution of speech performance.

For correlations between cochlear anatomy and cochlear array localization and its relation with speech perception scores, Pearson’s correlation coefficient ® was calculated and the

ANOVA was used to test the slope of the linear regression line. Student's t-test was used for comparisons between groups (male/female, right/left cochleae, full/partial insertions). One-way ANOVA was used for calculate the influence of the number of activated electrodes on speech performance. Two-ways ANOVA was used to analyze the influence of cochlear anatomy on speech perception score between the two ears in patients with asymmetric results. For all comparisons, $p < 0.05$ was considered as significant.
All statistical analyzes were performed using IBM SPSS for Windows (v 22.0, SPSS Inc., Chicago, Illinois, USA).

5.1.3 Results

Cochlear anatomy and electrode position
The cochlear anatomical parameters are presented in Table II. The distance A was positively correlated with the cochlear height measure ($r = 0.52$, $p < 0.001$, data not shown). Surprisingly, the distance A and the cochlear height were different between the two ears (difference of mean distance A: 0.22 ± 0.05 mm, $p < 0.05$; difference of mean cochlear height: 0.3 ± 0.06 mm, $p < 0.001$, paired *t* test); no right or left ear predominance was observed. The distance A and the cochlear height were also different between male and female ears, having males a diameter and a cochlear height greater than females ($p < 0.001$, Student's *t* test).
A full insertion of the electrode array was achieved in 26 ears, and a partial insertion in 12 ears (3 patients with a bilateral partial insertion, and 6 patients with a unilateral partial insertion). In ears with an incomplete insertion, the mean number of extracochlear electrodes was 2.4 (range 1 to 4). The size of the cochlea (i.e. distance A and cochlear height) was similar between ears with a full insertion and ears with a partial insertion (Table III).

Table 5.2: Cochlea measurement and electrode array placement on CT scan
(19 patients, 38 ears)

Distance A (mm), n = 38	9.4 ± 0.08 [8.8 – 10.6]
Male (n = 10)	9.9 ± 0.12 [9.65-10.59]
Female (n = 28)	9.3 ± 0.07 [8.8-10.2] **
Ears with full insertion of electrode array (n = 26)	9.4 ± 0.09 [8.8-10.59]
Ears with partial insertion of electrode array (n = 12)	9.6 ± 0.16 [8.9-10.2]
Cochlear height (mm), n = 38	5.5 ± 0.09 [4.2 - 6.4]
Male (n = 10)	6 ± 0.09 [5.5 - 6.4]
Female (n = 28)	5.5 ± 0.09 [4.2 - 6.6] **
Ears with full insertion of electrode array (n = 26)	5.4 ± 0.12 [4.2 - 6.6]
Ears with partial insertion of electrode array (n = 12)	5.5 ± 0.13 [4.9 - 6.4]
Insertion angle (degrees)	
Ears with full insertion (n = 26)	643 ± 93 [510 - 880]
Ears with partial insertion (n = 12)	403 ± 82 [318 - 590]
Total (n = 38)	567 ± 23 [318 - 880]
EMD 180-degrees (mm), n = 26	0.29 ± 0.004 [0.25 - 0.36]
EMD 360-degrees (mm), n = 26	0.22 ± 0.004 [0.18 - 0.32]

Values are expressed as mean ± SEM [range]. A full electrode array insertion was achieved in 26 ears and a partial electrode array insertion in 12 ears. Comparison of distance A and cochlear height between males and females,

** $p < 0.001$, Student's *t* test . EMD electrode-to-modiolus distance

In the 26 ears with a full electrode insertion, the angle of array insertion within the cochlea varied widely [510-880-degrees] (Fig 5.2), was negatively correlated with the distance A (r = -0.55, $p < 0.005$) (Fig. 5.3A), no correlation was found with cochlear height (Fig 5.3B). The EMD was positively correlated with distance A at both 180- (r = 0.47, $p < 0.05$) and 360-degrees (r = 0.66, $p < 0.001$, Fig. 5.3C) and with cochlear height at 360-degrees (r = 0.6, p= 0.001, Fig.5. 3D). These results indicate that in large cochleae (distance A), the electrode array was less deeply inserted (angle of insertion) and more distant from the modiolus at the basal turn (EMD at 180-degrees and 360-degrees). In the present study, the distance A

resulted to be sufficient to define the cochlear size and reliable for the prediction of the position of the implant within the cochlea.

Table 5.3: number of inserted electrodes, cochlear measurements and speech perception score at 1 year

Inserted Electrodes (n) No. of ears	Distance A (mm)	Cochlear height (mm)	Speech score at 1yr	
			Silence	SNR +15 dB
Full insertion (12), 26 ears	9.4± 0.08 [8.8 - 10.6]	5.4± 0.12 [4.2 - 6.6]	64±6	54±7
Partial insertion (11) 3 ears	9.5± 0.14 [9.2 - 9.6]	5.2± 0.12 [5.3 - 4.9]	63±27	46±13
(10) 4 ears	9.7± 0.32 [8.8 - 10.2]	5.9 0±.19 [5.6 – 6.4]	52±18	30±4
(9) 2 ears	9.8± 0.13 [10.1 - 9.6]	5.7 0.25 [5.6 – 5.9]	60±40	15±15
(8) 3 ears	8.8± 0.09 [8.7 – 8.9]	5.3 0.17 [5.1 – 5.5]	43±18	10±10 *

Values are expressed as mean ± SEM [range]. The mean number of electrodes outside the cochlea was 2.4 (range: 1-4). * One-way ANOVA, post hoc Dunnett's t test $p < 0.05$

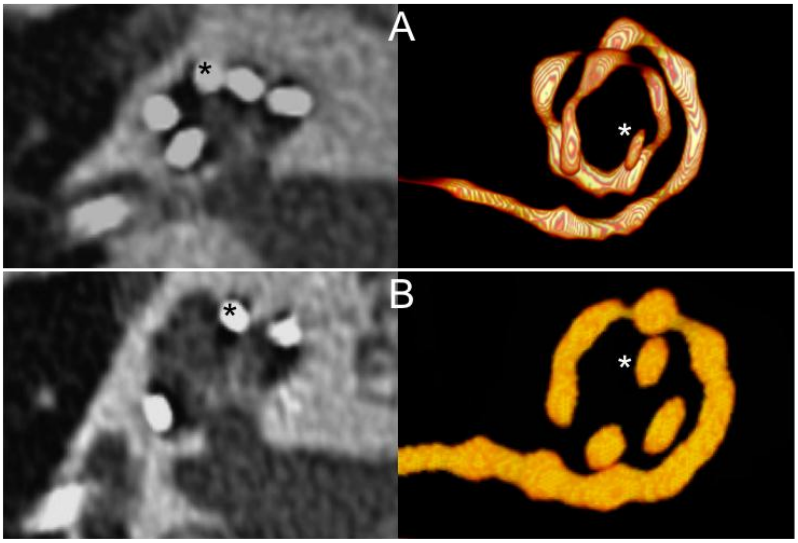

A. 880-degrees insertion.

B. 550-degrees insertion. The asterisks (*) represent the apical electrode.

Figure 5.2: Variability of the angular depth of insertion among cochleae with complete array insertion in mid-modiolar cuts and 3D volumetric reconstruction of the array

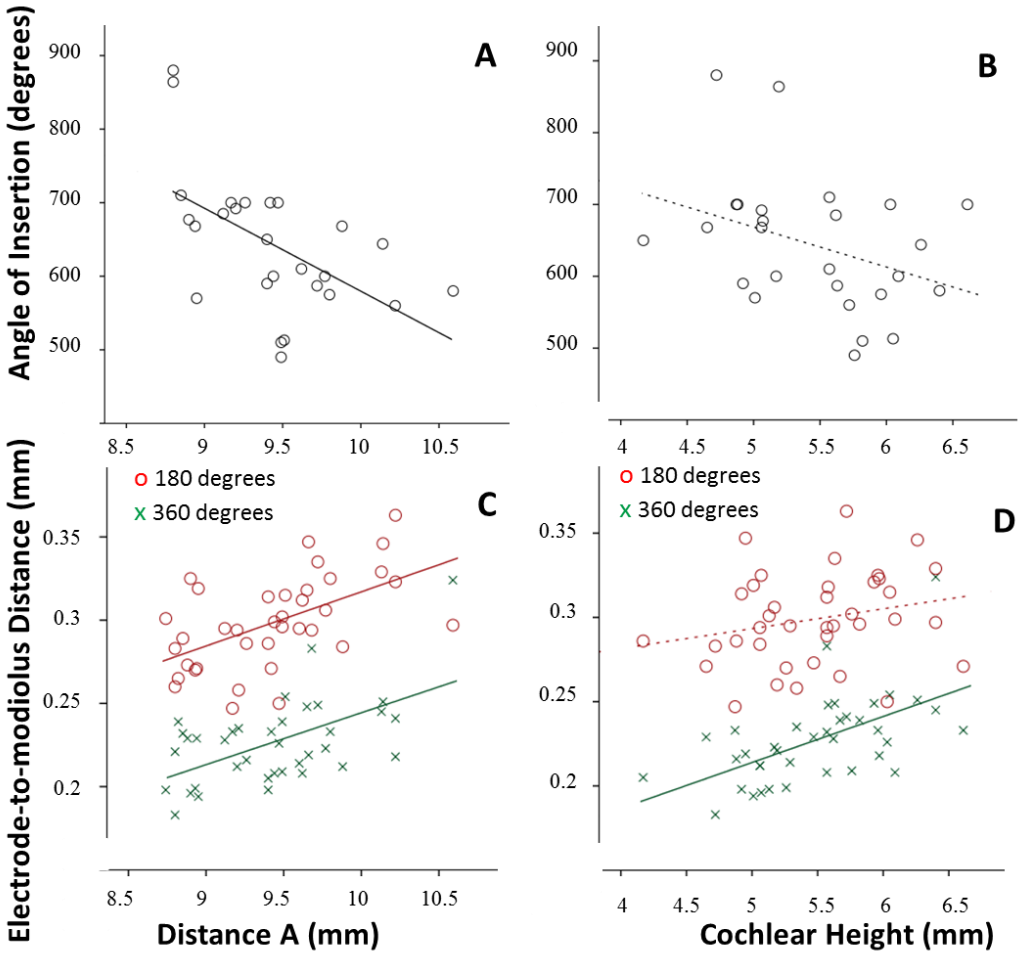

Figure 5.3. Correlation between the size of the cochlea (largest cochlear diameter and cochlear height) and the position of electrode array. The CT scan was available for 19 patients (38 ears). In the 26 ears with a full insertion of the electrode array, the distance A was negatively correlated with the angle of the insertion of the array (r = -0.55, $p < 0.005$) (A) and positively correlated with the electrode-to-modiolus distance at 180 degrees and 360-degrees (r = 0.47, $p < 0.05$; r = 0.66, $p < 0.001$ respectively (C). The cochlear height was not correlated with the angle of insertion (B), but positively correlated with the electrode-to-modiolus distance at 360-degrees (D). The solid lines represent the significant linear regression line. The dotted lines represent the not significant linear regression line where the slope was equal to zero (ANOVA, $p > 0.05$). r, Spearmann correlation coefficient.

Correlation between electrode position and speech perception

At 1-year after cochlear implantation (38 implanted ears), speech perception scores were negatively correlated with EMD at 180-degreess both in quiet (r=-0.34, p=0.02) and in noise (SNR +15 dB: r=-0.44, p=0.006; SNR +10 dB: r=-0.63, p=0.0005; SNR+5 dB: r = -0.52, p=0.01, Fig. 5.4). The greater the EMD was, the poorer was the performance. No correlation was observed at 360-degrees. The number of inserted electrodes was correlated with speech perception in noise at SNR +15 dB and SNR +10 dB (ANOVA, p=0.02). The speech perception scores in noise gradually decreased as a function of the number of inserted electrodes (post hoc Dunnett's t test p=0.02) (Table 5.3). Considering the obvious

interdependence between the number of intracochlear electrodes and the depth of insertion, we analyzed the influence of electrode position on hearing outcomes among the 26 ears with a full insertion of the electrode array. No correlation was found between the speech perception scores and the angular depth of insertion, both in quiet and in noise, whereas the speech perception scores were negatively correlated with EMD at 180-degreess both in quiet (r=-0.38, *p*=0.048) and in noise (SNR +15 dB: r=-0.4, *p*=0.049; SNR +10 dB: r=-0.62, *p*=0.006; SNR+5 dB: r=-0.51, *p*=0.032, data not shown).

The asymmetry in speech perception scores (difference ≥20%) between the better and the poorer ear, observed at 1-year in nine patients, was not explained by difference in anatomical variation (distance A, cochlear height) between the two cochleae (not significant, two-ways ANOVA). Furthermore, in these patients, an incomplete insertion of the array was found in 4 poorer ears and 2 better ears (not significant, Fischer's exact test).

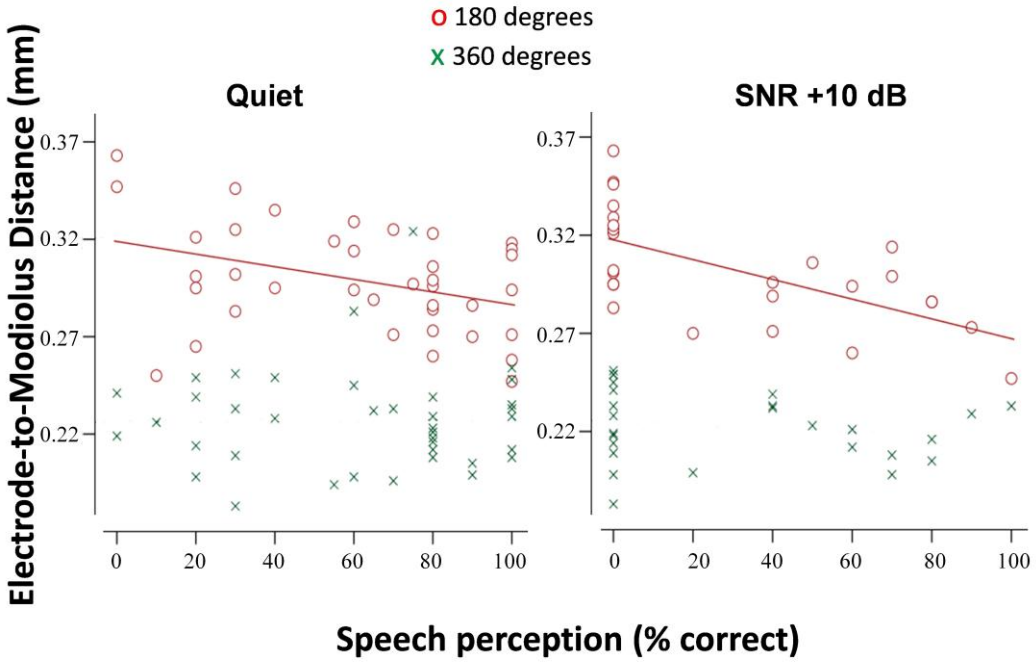

Figure 5.4: Correlations between electrode array position and speech perception scores in quiet and at SNR +10 dB at 1-year. The speech perception scores in quiet were negatively correlated with the distance of the electrode to the modiolus at 180-degrees (solid line). A correlation was also found at SNR +15 dB and +5 dB (data not shown). No correlation was found between speech perception scores and electrode-to-modiolus distance at 360-degrees (dotted line).

Hearing performance after 5 years of bilateral cochlear implantation

Figure 5.5 displays the mean values of speech performance score observed in each studied conditions at 1- and 5-years postimplantation.

The most parsimonious linear mixed model that was retained for analyses included a significant interaction term between time and ear effect (global $p < 0.001$) as well as a significant noise effect (global $p < 0.001$) (Table 4). After post-hoc two-by-two comparisons with adjustment of p-values for multiple comparisons the difference of speech performance score between 1- and 5-years after implantation was found significant between each possible pair of comparisons for noise effect, regardless of time and ear (Table 4).
An improvement of speech performance score between 1- and 5-years after implantation was found to be significant in the subgroup of the poorer ear (+12.1 ± 2.6%, $p < 0.001$), regardless of noise. The evolution of speech perception score between 1- and 5-years was not found to be statistically significant in other subgroups of ears (bilateral or better) (Table 2).
At 1-year after implantation, the difference of speech performance score was found significant between each possible pair of comparisons for ear effect, regardless of noise (Bilateral - Better: +8.5 ± 2.7%, $p = 0.01$; Better - Poorer: +16.9 ± 2.7, $p < 0.001$, Table 1). These differences of speech performance scores between ear conditions were not found to be statistically significant at 5-years after implantation (Table 5.4). The most difficult noisy condition, SNR 0 dB, was only tested at 5-year, therefore was not considered in the mixed model analysis. The speech perception scores in this condition of noise were for the poorer, better and bilateral conditions: 12 ± 3.1%, 18 ± 4.3% and 30 ± 4.6% respectively (Figure 5.5).

Correlations between the evolution of speech performance scores and speech performance score at 1-year

Table 5.5 shows the estimated correlations between the evolution of speech performance score between 1- and 5-years after cochlear implantation and the corresponding speech performance score at 1-year for each noise conditions. The correlations were calculated only for the poorer ear (as it was the only ear for which the evolution between 1- and 5-years after cochlear implantation was found to be significant). For Quiet and SNR +15 dB, a significant negative correlation was found between the evolution of speech performance over time and the corresponding speech performance score at 1-year (Quiet: $r = -0.62$, $p = 0.001$; SNR +15 dB: $r = -0.58$, $p = 0.002$). The two corresponding scatterplot (Figure 5.6) show the correlation between the scores at 1-year and the evolution of the scores over time. Overall, the poorer ears with the lower speech perception seemed more likely to have improved over time (with a greater improvement associated with a lower score at 1-year), while poorer ears with the highest scores at 1-year seemed more likely to have been stable or to have decreased over time.

Table 5.4. Time, Noise and Ear effect explaining the variability of speech performance score

Linear Mixel Model tests of effects			
Global fixed effects			**p (global)**
Time			0.33
Noise			< 0.001
Ear			< 0.001
*Time*Ear (interaction term)*			< 0.001
Post-hoc two-by-two comparisons			
Comparison	**Estimate**	**SEM**	**Adjusted p**
Noise Effect			
Quiet – SNR +5 dB	29.6	2.1	< 0.001
SNR +15 dB – SNR +5 dB	22.7	2.1	< 0.001
SNR +10 dB – SNR +5 dB	15.9	2.2	< 0.001
Quiet – SNR +15 dB	6.9	2.0	0.006
Quiet – SNR +10 dB	13.7	2.1	< 0.001
SNR +15 dB – SNR +10 dB	6.8	2.1	0.01
*Time*Ear Effect*			
5 Year*Bilateral – 1 years*Bilateral	-2.2	2.6	0.79
5 Year*Better – 1 years*Better	0.8	2.6	0.79
5 Year*Poorer – 1 years*Poorer	12.1	2.6	< 0.001
1 year*Bilateral – 1 year*Better	8.5	2.7	0.01
1 year*Better – 1 year*Poorer	16.9	2.7	< 0.001
1 year*Bilateral – 1 year*Poorer	25.4	2.7	< 0.001
5 year*Bilateral – 5 year*Better	5.5	2.5	0.13
5 year*Better – 5 year*Poorer	5.6	2.5	0.13
5 year*Bilateral – 5 year*Poorer	5.6	2.5	0.13

Table 5.5. Estimated Spearman correlation coefficients between the difference of speech performance score over time and the corresponding score at 1-year

Conditions	**r (Spearman)**	**p**
Quiet, Poorer ear	-0.62	0.001
SNR +15 dB, Poorer ear	-0.58	0.002
SNR +10 dB, Poorer ear	-0.27	0.29
SNR +5 dB, Poorer ear	-0.45	0.06

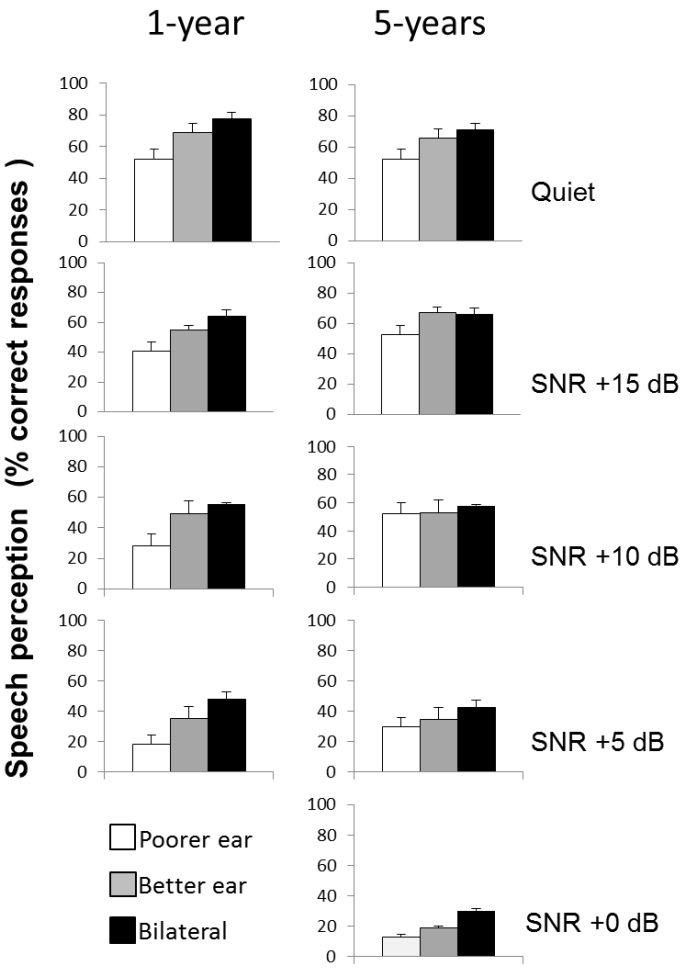

Figure 5.5: Speech perception scores (disyllabic words, 70 dB SPL) at 1- and 5-years after simultaneous bilateral implantation in the whole study group (n=26). Results are expressed as means ± SEM.

Evolution of sound localization between 1-year and 5-years postimplantation

Figure 5.7 displays the mean values of sound localization score observed for each loudspeaker. The most parsimonious linear mixed model that was retained for analyses included only the main fixed effects (no interaction terms). The loudspeaker and ear effects were significant (global $p < 0.001$ for both effects). A change in sound localization performance over time was not evidenced by the analyses (Table 5.6). After post-hoc two-by-two comparisons with adjustment of p-values for multiple comparisons an improvement in sound localization was found to be significant between the bilateral condition and the unilateral right or unilateral left condition, regardless of time and ear (Bilateral - Right: +31.8% ± 2.6%, $p < 0.001$; Bilateral - Left: +29.9% ± 2.6%; $p < 0.001$). No difference was found between the two sides (Table 5.6). A difference of sound localization was found to be significant between the most peripheral loudspeakers and the central ones, on the left side (LS1 - LS4: +13.9% ± 3.4%, $p < 0.001$; LS1 – LS3: +13.0% ± 3.4%, $p < 0.001$; LS1 - LS2: +17.1% ± 3.4%, $p < 0.001$), as well as on the right side (LS5 – LS2: +10.9% ± 3.4%, $p = 0.009$) (Table 3).

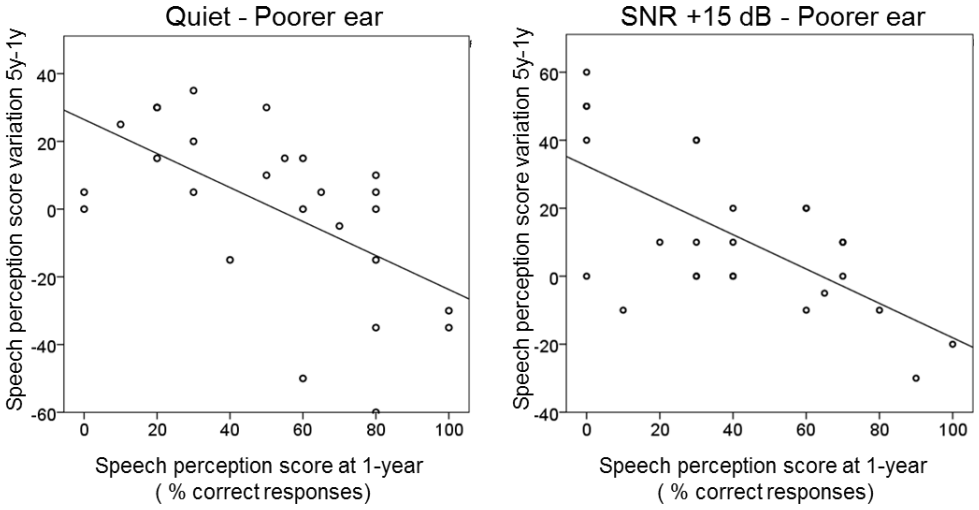

Figure 5.6: Correlation between speech perception score of the poorer ear at 1-year and its variation at 5-years in Quiet ($r = -0.62$) and at SNR +15 dB ($r = -0.58$). The lower was the speech perception score at 1-year, the higher was the improvement found at 5-years.

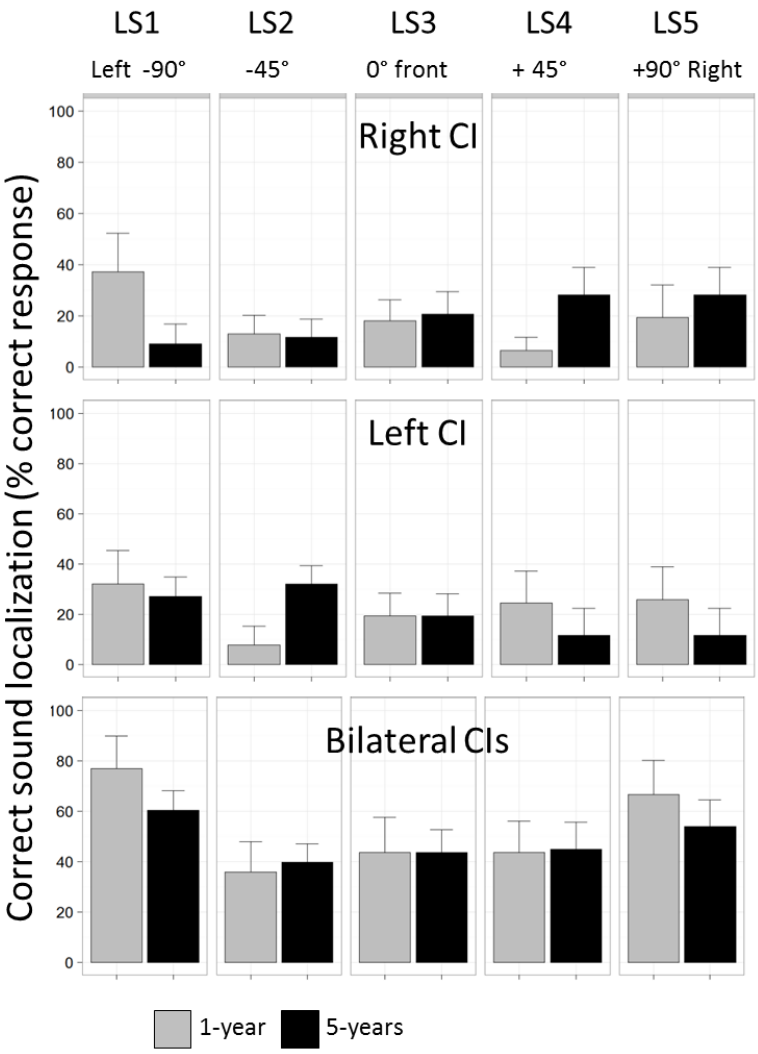

Figure 5.7: Sound localization in noise in bilateral and unilateral conditions at 1-year and 5-years after simultaneous bilateral implantation (26 patients). The mean correct localization of the speech stimuli was improved with bilateral implantation compared to either implant alone for each loudspeaker ($p < 0.001$) both at 1- and 5-years postimplantation. The results were stable between 1- and 5-years postimplantation.

Table 5.6. Time, Loudspeaker and Ear effect explaining the variability of sound localization performance

Linear Mixel Model tests of effects			
Global fixed effects			**p (global)**
Time			0.38
Loudspeaker			< 0.001
Ear			< 0.001
Post-hoc two-by-two comparisons			
Comparison	**Estimate**	**SEM**	**Adjusted p**
Ear Effect			
Bilateral - Monaural Right	31.8	2.6	< 0.001
Bilateral - Monaural Left	29.9	2.6	< 0.001

Monaural Right - Monaural Left	-1.9	2.6	1
Loudspeaker Effect			
LS1 - LS5	6.2	3.4	0.33
LS1 – LS4	13.9	3.4	< 0.001
LS1 – LS3	13.0	3.4	< 0.001
LS1 – LS2	17.1	3.4	< 0.001
LS2 - LS5	-10.9	3.4	0.009
LS2 – LS4	-3.2	3.4	1
LS2 – LS3	-4.1	3.4	0.91
LS3 - LS5	-6.8	3.4	0.25
LS3 – LS4	0.8	3.4	1
LS4 - LS5	-7.7	3.4	0.15

Studying the relationship between the electrode insertion parameters and the hearing outcomes, no correlation was found at 5-years postimplantation between speech perception scores and the angular depth of insertion, both in the entire sample and in the group with full insertion of the electrode array. In contrast to what observed at 1-year postimplantation, the EMD was not correlated with speech perception scores, both at 180-degrees and 360-degrees (data not shown).

5.1.4 Discussion

This prospective study demonstrate that both the distance between electrode array and modiolus at 180-degrees, and the number of inserted electrodes, are important variables that influence the early achievement of the best speech perception scores, whereas the angular depth of insertion of the array did not influence cochlear implant outcomes. Furthermore, in adult simultaneously implanted patients, the speech performance varied between 1-year and 5-years postimplantation. Patients with poor speech perception on both ears at 1-year improved their scores both in quiet and noise within the 5-years of cochlear implant experience. In contrast, a worsening of the scores of the better ear and of the bilateral condition was observed in patients with good performance at 5-years postimplantation.

The variability in cochlear anatomy influences electrode array position

A variation in human cochlear anatomy is well known and intersubject variability is described in several studies (Erixon et al. 2009, Rask-Andersen et al. 2012, Martinez-Monedero et al. 2011). The variations in cochlear anatomy include do not only the diameters and heights but also the shape, the coiling pattern, the width of various turns and the number of turns, to such a point that these individual design and proportion have been described as a "fingerprint" (Erixon et al. 2009).

In this study the cochlear size was assessed using the greatest cochlear diameter of the basal turn (distance A) that is assumed to be a good predictor of the length of the two first turns of the cochlea (Erixon & Rask-Andersen 2013; Singla et al. 2014) and using the cochlear height. These two measures are clearly correlated to each other meaning that a larger diameter of the basal turn is related to a higher cochlea. Both distance A and cochlear height vary with sex, males having bigger cochlea compared to females (present study, Escude et al, 2006; Mori & Chang, 2012, van der Marel et al. 2014). Furthermore, we observed an asymmetry between the two ears in distance A (0.22 mm) that is in accordance with the results of Escude et al. (2006), and in cochlear height (0.3 mm). No ear predominance was found as previously reported (Mori & Chang, 2012; Singla et al. 2014; Pelliccia et al. 2014; van der Marel et al. 2014).

The large variation of the gross anatomy of the cochlea leads to similar variations in the internal dimensions of the cochlear scalae and angles between turns. Different studies investigated the relations between cochlear anatomy and electrodes array position within the cochlea (Franke-Trieger et al. 2014, van der Marel et al. 2014, Esquia-Medina et al. 2013, Verbist et al. 2009 and Kawano et al. 1996). Important variations with unusual narrowing or constriction were reported in the first segment of the scala tympani. Kennedy (1987) reported that the most frequently damaged structures during CI insertion are the spiral ligament at the junction of the first and second half of the first turn, basilar membrane, and osseous spiral lamina. The basal end of the cochlea is of great interest in cochlear implant surgery; it curves in three dimensions, resembling a ''fish hook'' and its anatomical variation makes, in some cases, difficult for the surgeon to optimally chose the cochleostomy site and reach the scala tympani without destroying any inner ear structures (Rask-Andersen et al. 2012); even a round-window insertion, in some cases, would probably damage the spiral lamina. Martinez–Monedero et al. (2013) reported how underdeveloped cochleae may show great differences in the angle between the first and second turns and a smaller length of the base of the cochlea making more difficult the insertion of a cochlear implant.

This study demonstrated a strong correlation between the distance A and the angular depth of insertion in ears with a full insertion of the electrode array (Pearson's coefficient of -0.6) that corroborates results of studies using similar arrays as in our study (Franke-Trieger et al. 2014) or perimodiolar arrays (Escude et al. 2006). A correlation was also found between the distance A and the EMD and as a result, between the insertion angle and EMD, and between EMD and cochlear height. To summarize, in patients implanted with long and straight electrode arrays, which have a lateral position in the cochlear lumen, the smaller the cochlea was, the closer laid the electrode array to the modiolus at the basal turn, and the deeper was the array insertion.

In our study, radiological analysis showed an incomplete insertion of the electrode array in 12/38 ears (32 %). There was no significant difference of the size of the cochlea between ears with incomplete and complete insertions. Nevertheless the 3 cochleae with 4 electrodes out had smaller distance A than rest of the ears, but the sample was probably too small to provide significative difference. Indeed, the ideal cochlea able to be implanted with a 31 mm length array would have a distance A at least of 9.2 mm as reported by Alexiades et al. (2014), and that was not the case of the 3 ears. Some variations in cochlea anatomy such as a narrowing of the cochlear duct or a sharp bend of cochlear coiling between the first and the second turn has been reported to influence electrode array insertion, especially when using longer electrodes, that could explain these incomplete insertions (Rask-Andersen et al. 2012). A crucial point in the choice of the array is to measure the distance A and tailor as consequence the length of the electrode array to be implanted. The mean insertion angle was 643-degrees (ranging from 510- to 880-degrees) in ears with full insertion of the electrode array, similar to previously reported results using the same electrode (Boyd, 2011; Franke-Trieger et al. 2013; Buchman et al. 2014). In studies reporting lower correlation coefficient between cochlear size and insertion depth, or no relationship, electrode arrays of various length and ears with incomplete insertion have been included in the analysis explaining the lower angle of insertion and the discrepancies in the results (468-degrees for Esquia-Medina et al. 2013; 480-degrees for Van de Marel et al. 2014). No significant difference in the size of the cochlea between ears with incomplete and complete insertions was found in our study, nevertheless it should be noticed that the three cochleae with 4 electrodes outside, had a smaller distance A than the other ears (see Table 3). On the base of the cochlear length equation based on distance A value (Alexiades et al. 2015), we can assume that a 31 mm length array was too long to be totally inserted in these three ears. At the present, different lengths of cochlear arrays are available, and it is crucial to measure the distance A before implantation in order to adapt the type (and length) of the electrode array to be implanted.

Influence of electrode position on cochlear implant outcome

In the present study, despite a large variation of the insertion angle, no correlation was found between the angular depth of insertion angle and the hearing outcome at 1-year and 5-years in ears with a full insertion of the electrode array. This observation is consistent with a histological analysis over a series of 27 temporal bone specimens of subjects with cochlear implant (Lee at al. 2010). Van der Marel et al. (2015) analyzed six position-related variables including the angular and linear insertion depth of the array and did not find any correlation with speech outcomes at 2-years postoperative. In a prospective randomized study including 13 patients (Buchmann et al. 2014), no difference was found in speech perception scores between MedEl standard array (mean angular depth of insertion 657-degrees) and medium array (mean angular depth of insertion 423-degrees), a better performance was found in the standard array group when 6 more patients were included retrospectively. On the contrary, other studies reported poorer performance in case of deeper insertions (Skinner et al 2007), explained by the increased number of electrodes in the scala vestibuli, reduced pitch discrimination, decreased basal stimulation (Finley et al 2008), and pitch confusion at apical contacts (Gani et al. 2007). The negative correlation between the electrode angular depth of

insertion and hearing outcomes found by Yukawa et al. (2004) may be explained by the presence of confounding factors, such as the lower number of activated electrodes in case of partial insertion. Indeed, in the present study, in case of incomplete insertion, the speech perception scores in noise at 1-year decreased as a function of the number of inserted electrodes (see Table 3).

Considering the distance between the electrode array and the modiolus, it has been shown that a closer position to the spiral ganglion cells was associated with better speech perception (Finley et al 2008). This effect may be related to the minimization of channel interaction, which leads to reduction of electrical thresholds and/or improvement of the spatial selectivity. Our findings are in accordance with Esquia-Medina et al.(2014) who reported a correlation between speech perception scores and average EMD of the 6 most basal electrodes of MED-EL devices (corresponding approximately to the region from 0- to 180-degrees) at 6 months, whereas no correlation was found at 12 months. In this study, as well as the present one, such relationship was not present for the electrode at 360-degrees, possibly due to the narrowing of the scala tympani from base to apex35 that reduces the variability of the array position. This relationship between the EMD and the hearing performance could point out a preferential use of perimodiolar electrode array in order to obtain a rapid hearing rehabilitation. Nevertheless, Doshi et al. (2015) reported no differences between speech perception outcomes at 3- and 9-months in patients implanted with either straight or perimodiolar electrodes array. A reason could be the more frequent dislocation from scala tympani to scala vestibuli in case of perimodiolar electrodes (Boyer et al 2015). Although such scalar dislocation is difficult to assess in standard CT scan, it might negatively influence the cochlear implant outcome (Aschendorff et al. 2007, Gani et al. 2007, Wanna et al. 2014). An aspect that has not been explored in this study is the surgeon's gesture. A recent study described a high intra- and inter-individual variability of the insertion axis of the array into the cochlea; yet, this variability was reduced among expert surgeons (Torres et al. 2015). Since all the participants to the present study were senior otologists, we estimate that this doesn't represent a great factor of bias of the study. Furthermore, how the insertion axis influences the trajectory of insertion or the final position of the array has not yet been described or reported. An additional limitation of this study could be represented by the migration of the array possibly occurring between 1- and 5-years. Nevertheless, in all patients, the most basal electrodes remained activated, providing auditory responses, and with stable impedance values, thus an extrusion of the electrodes in our cohort should be unlikely (Johnston et al. 2016).

Evolution of speech performance

In this study, five years after simultaneous bilateral implantation, the performance of the poorer ear improved in comparison to 1 year postimplantation. In a study prospectively analysing 9 adult patients simultaneous and bilaterally implanted (MED-EL Combi 40+) with poor speech perception scores at 1-year postimplantation (unilateral scores < 50% for Consonant-Nucleus-Consonant (CNC) words in quiet), Eapen et al. (2009) reported a gradual improvement of the unilateral and bilateral scores over a 4 years follow-up period, and a growth of the squelch effect, whereas the benefit from head shadow and summation effects

remained stable. Chang et al. (2010) also observed better speech performance in bilateral condition for CNC words in quiet at 4-years postimplantation, compared to 1-year performance, in a group of 17 adults simultaneously implanted. Our results corroborate these two studies, but the missing speech perception assessment between the 1-year and 5-years measurement intervals did not allow us to evaluate if the poorest speech perception scores improved gradually or not over the 4-years of follow-up period. The improvement of the poorer ear observed in the present study was possibly related to an enhanced cortical representation of the voice when using bilateral cochlear implant. The improvement after the 1 year of follow up of the poorer ear that was observed in the present study has not been reported in patients unilaterally implanted, even in studies with long-term follow-up (Lenarz et al., 2012; Holden et al. 2013). A link between the score improvement and more frequent follow up cannot be ruled out. Indeed, indeed patients having poor performance had a more intense training in terms of frequency of cochlear implant fittings, and of speech training sessions, as compared to patients who rapidly obtain good performance, and consequently are less prone to continue the speech rehabilitation exercises. Another factor not analyzed in the present study was the time of daily use of the cochlear implants. These parameters have not been studied in our study group, and have to be analyzed in a future report.

In the present study, the advantage of the bilateral condition over the better unilateral ear in speech perception scores that was present at 1-year was not found five years after the implantation. Nevertheless, the most difficult condition in noise i.e., SNR 0, was only tested at 5-years and was not considered in the evolution of the scores and in the mixed model analysis. It appears from the results (see Figure 5) that the difference between bilateral and better ear at SNR 0 (+11±3.6 %) was higher than the other significant differences between bilateral and better ear observed at 1-year both in quiet and in noise. That might indicate that the bilateral cochlear implantation could still provide benefit in complex and difficult noisy environment five years after the implantation compared to unilateral implantation.

Sound localization in noise

The sound localization on the horizontal plane provided by the bilateral implant was better than the unilateral one and remained stable from the results observed at 1-year. This result is consistent with several studies evaluating sound localization in quiet, reporting that major improvement occurred in the first 6 months after cochlear implantation (Basura et al. 2009; Chang et al. 2010). It appears from the results, as expected, that the localization of the sound source results easier in the most peripherals loudspeakers where the interaural time and level differences are higher than the more central loudspeakers. Moreover, it seems that 5 years after bilateral implantation the best results in localization with unilateral CI is more consistent when the stimulus was presented ipsilateral to the tested ear, i.e., -90 and -45 or +90 and +45 for the left and right ear respectively. This tendency was not evident at 1-year postimplantation and may represent an evolution of the sound localization for the individual ears related to the overall improvement of the poorer ear that had not side prevalence.

Our short-term results suggest that the number of activated electrode seems more relevant than the depth of insertion, and that perimodiolar electrodes should be preferred to straight electrodes in large cochleae. However, this influence of the electrode positioning on cochlear implant outcome does not persist with a longer term use, presumably because of the improvement of the poorest speech perception scores, moreover perimodiolar electrodes array seems to dislocate more frequently toward the scala vestibuli. A positron emission tomography study reported that bilateral auditory stimulation in quiet in bilateral simultaneous implanted patients 3 years after implantation improves brain processing of voice stimuli on the right temporal region compared to monaural stimulation, and activate the right fronto-parietal cortical network implicated in attention (Coez et al. 2014). These results suggest that the improvement of poorer speech perception scores is possibly related to an enhanced cortical representation of the voice when using bilateral cochlear implant. In the present study the speech perception test failed to detect, in quiet, an advantage of bilateral implantation over the unilateral stimulation at 5-year postimplantation. Further investigations are needed to investigate the long-term effect of brain processing after reactivation of bilateral auditory pathways.

In conclusion, whereas our 1-year results suggest that the number of activated electrodes and the distance electrode-to-modiolus were related to good performance, these parameters did not influence the speech scores after long term use, presumably due to the delayed improvement of the poorest speech perception scores. The bilateral auditory stimulation improves the poorest performance after 1 year representing an additional reason to recommend bilateral implantation. In order to obtain a rapid hearing rehabilitation, the preoperative measurement of the cochlear diameter (distance A) would help in the choice of the electrodes array length to achieve a complete insertion. A smaller distance A would reduce the EMD and could address the choice of the side to be implanted. In case of poor performance in bilateral implanted patients, our results should encourage these patients to continue to follow the speech training sessions after one year postimplantation, and continuing to daily wear their cochlear implants because the speech scores would improve over time.

5.2 INFLUENCE OF SCALAR TRANSLOCATION ON THE AUDITORY PERFORMANCE

Abstract

Objective: To analyze the influence of the intracochlear position of the electrodes array (CI422) on speech perception score and quality of life assessed with a questionnaire assessing hearing impairement impact on everyday life at 6 months and 1 year in a group of adult implanted patients using postoperative cone beam CT for electrode positioning assessment.

Design: Twenty-seven patients, mean age 56 years [range 28-81] were included (29 ears). Auditory speech scores in quiet (monosyllabic words) were tested at 6 and 12 months after activation. The Abbreviated Profile of Hearing Aid Benefit inventory (APHAB) was also evaluated at 6 and 12 months after the activation. The patients were successively evaluated in noise (adaptive test SRT 50%). Electrode-modiolus distance for the electrodes at 180° and 360°, the angle of insertion and the electrode array scalar translocation were studied in post-operative cone beam CT scan reconstructions.

Results: The speech perception scores in quiet at 1 year were correlated to the SRT 5o% and the APHAB. All the electrodes array were fully inserted (mean angle 404° +- 38) except in one patient. A translocation from the scala tympani to scala vestibuli was observed in 6 ears (20%). The distance between the electrode at 180-degrees and the modiolus was correlated to speech scores in quiet at 6 months (Spearman r = -0,704, $p<0.01$). No correlation was found between the depth of insertion and auditory performance. The electrode-modiolus distance at 180-degrees was correlated with auditory performance at 6 months (Spearman r = -0.69, $p < 0.01$), at 1 year no correlation was found. No difference in speech perception score in quiet was found between scala tympani or scala vestibuli positioning of the electrode in quiet, and in noise (NS Mann-Whitney test). Considering the APHAB score the patients presenting a translocation of the array had lower score both at 6 months and at 1 year for the global score at 6 months and also in two subgroup score at 1-year (Mann-Whitney test) indicating a minor impact in everyday life problems associated with the cochlear implant.

Conclusion: The translocation of the electrode from the scala tympani to scala vestibule influenced the APHAB inventory scores indicating better results for patients having all the electrodes in the scala tympani. This result is not confirmed by the speech perception scores in quiet and in noise; nevertheless a tendency on the results is present. Further studies with more homogeneous study group and multifactorial analysis of the results are necessary to demonstrate a relationship between scalar translocation and postoperative auditory performance.

This work was presented by Daniele De Seta as:

Podium presentation at the Congress of the French Society of Otolaryngology October 10-12 2015, Paris

Poster at 14th International Conference on Cochlear Implants. May 11-14, 2016, Toronto, Canada

5.2.1 Introduction

The preservation of the inner ear structures during the insertion of cochlear implant, together with the identification of the ideal site of stimulation in the cochlea, should allow the best hearing performance. As a consequence, the quality of insertion of the cochlear implants has been extensively studied during the last decades. In this context, three parameters have been more accurately investigated: the depth of insertion of the electrode array, the proximity of the electrodes to the spiral ganglion cells and the translocation of the array with the subsequent basilar membrane rupture. All the currently available electrode arrays have their own specific length, diameter, shape, and physical properties that influence the trajectory during the insertion and determine the final position in the cochlear lumen. As demonstrated in the previous chapter the proximity of the electrodes to the modiolus using a straight and long electrodes array influenced the speech perception scores in a group of bilateral implanted patients, on the contrary the depth of insertion considering only completed inserted array was not correlated to speech scores. Another factor that may account for postoperative hearing performance could be represented by the scalar positioning and translocation of the electrodes array. The scalar translocation as factor influencing the hearing outcomes has been studied by several authors and the results reported are controversial. The intracochlear electrode position with regard to speech performance results demonstrated advantages of scala tympani insertions for precurved perimodiolar electrodes (Aschendorff et al. 2007) and for straight electrodes (Finley et al. 2008), whereas Wanna et al. (2011) reported that he presence of the electrodes solely in the scala tympani was not predictive of hearing outcome after cochlear implantation.

In this study we investigate on the influence of scalar translocation a group of adult implanted patients by means of a quality of life questionnaire the Abbreviated Profile of Hearing Aid Benefit (APHAB) inventory used to quantify everyday life problems associated with hearing impairment and an adaptive speech perception test in noise. The patients underwent postoperative CBCT scan for scalar positioning assessment of the electrodes array.

5.2.2 Material and methods

Twenty-seven adult patients, mean age 56+-16 ys [range 28-81], were enrolled in the study. The patients were implanted with the electrode CI422 (Cochlear, Melbourne Australia); 2 patients were bilaterally implanted, one simultaneous and one sequential implantation.

Speech perception measures

All the patients underwent PTA and speech audiometry in quiet at 6- and 12-months after cochlear implant activation. Measurements were performed in a soundproof cabin using four loudspeakers (Monacor MKS-40, frequency response: 80–18000 Hz) positioned at 90° intervals. Test materials consisted of 50 lists of 20 monosyllabic words (Lafon word and

phoneme lists) recorded in quiet. Randomization of test lists presented for each patient was carried out independently at each test site. Responses were scored as the percentage of words correctly identified.For tests in quiet only the frontal speaker was used. Speech was always presented at 65 dB SPL from a loudspeaker placed at 0-degrees. The French Matrix (HörTech gGmbH, Holdenburg, Germany) adaptive speech perception test in noise was administrated with the speech stimuli coming from the front and a background noise coming from the 4 loudspeakers, including the central one that presented the speech target. After a two 20-item-session lists of training (in silence the first one and in adaptive noise condition the second one), two lists were presented to the patient with the noise level kept constant at 65 dB SPL (Fig. 5.8). The first sentence is presented with a signal to noise ratio (SNR) 0 dB, for the following presentations the level varied in an adaptive procedure aiming for the 50% threshold of speech intelligibility in noise (SRT). Results are expressed in dB as SNR.
The Abbreviated Profile of Hearing Aid Benefit inventory (APHAB) was evaluated at 6, 12, and 18 months after the activation. The ABHAB questionnaire is used to quantify everyday life problems associated with hearing impairment. The questionnaire comprises 24 items that are scored in four subscales. Each item contributes to only one subscale, and there are six items for each subscale, distributed randomly within the inventory. The subscales are: 1, Ease of Communication: the stress of communicating under relatively favorable conditions. 2, Background Noise: communication in settings with high background noise levels. 3, Reverberation: communication in reverberant rooms such as classrooms.4, Aversiveness: the unpleasantness of environmental sounds.

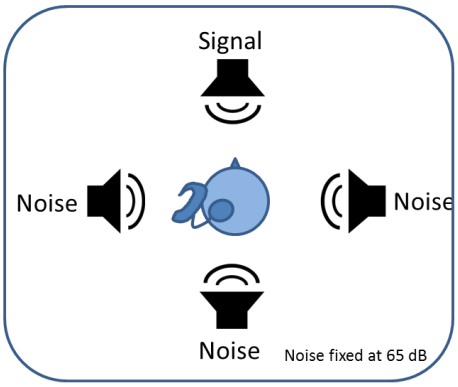

Fig 5.8 Loudspeakers setting in the soundproof cabin. The fixed noise (white noise) is set at 65 dB

Fig 5.9 Selection mask for close response set of the French Matrix test. In the present study the test was performed in open set, i.e., the patients did not have access to the list.

Radiological analysis

A high-resolution CT scan was performed before implantation. After the implantation the patients underwent Cone Beam CT using the 5G NewTom machine (NewTom, Verona, Italy). The system setup used a 200 x 25 mm flat panel detector at 650 mm from the radiation source. One 360-degree rotation of the x-ray tube took 36 seconds. The tube voltage was 110

kV, with a 19-mA charge at the terminals. Total filtrations were 2 mm, with a pitch of 125 Km; this corresponded to a field view of 12 x 7.5 cm diameter. The images were isometric voxel rendered from the 125-Km sections.
The DICOM (Digital Imaging and Communications in Medicine) data were analysed by Osirix program (Osirix v 4.0 64-bit; Pixmeo Sarl, Bernex, Switzerland). This program allowed the multiplanar reconstructions for the measurement of the cochlear anatomy and the position of the arrays within the cochlea. The largest cochlear diameter (distance A), the cochlear height, the electrode-to-modiolus distances (EMD) for the electrodes positioned at 180- and 360-degrees and the the angle of insertion of the array were measured. The measurement planes have been already described and previously reported (De Seta et al.2016). The round window was considered as the 0° reference angle. The position of the electrodes with respect to the basilar membrane was evaluated with the aid of the function the 3D curved MPR of Osirix, the electrode array was straightened and followed along the cochlear lumen (Nguyen et al. 2012) (see chapter 4). A 3D rendering reconstruction of the electrode array was also evaluated to identify changes in the coiling shape of the electrodes array (Fig 5.10). An expert otoradiologist and an otologist independently reviewed the images and assessed the localization as scala tympani, scala vestibuli or intermediate position for each electrode. All the mismatches in the assessment of the electrodes position were reviewed and analyzed until a consensus was obtained.
The study was approved by the local IRB informed consent was obtained from all individual participants included in the study.

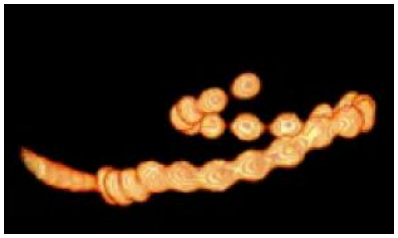

Fig 5.10. Volumetric rendering of electrodes array

Statistical analysis
Results are presented as means ± standard error of the mean (SEM). Individual speech perception scores were compared using paired t test. For correlations between electrode-modiolus distance and speech perception scores, Pearson's correlation coefficient (r) was calculated and the ANOVA was used to test the slope of the linear regression line. A two-way ANOVA was used for calculate the influence of scalar position and time over speech perception score and APHAB score. Mann-Whitney U test was used to compare the difference between APHAB score in patients with or without electrodes array translocation. For all comparisons, $p < 0.05$ was considered as significant. All statistical analyses were performed using IBM SPSS for Windows (v 22.0, SPSS Inc., Chicago, Illinois, USA).

5.2.3 Results

Twenty-eight patients (30 ears) completed the speech test in quiet at 6 and 12 months and the APHAB test. Among these patients stable results were observed in speech perception score (words) between 6 and 12 months postoperatively, whereas the phoneme identification improved (+9.9 ± 5.4%, $p<0.05$, paired t–test) (Fig 5.11). The APHAB score decreased (i.e. decrease of the impact of hearing impairment on the quality of life) between 6 and 12 months postoperatively (reverberation: -3±3, global score: -1.1±2.4; $p<0.05$, paired t test) (Fig 5.11). The SRT 50% test was performed on 19 patients (between 12 and 18 months postoperative). The Speech perception scores at 1 year were correlated to the SRT 5o% and the APHAB (Fig 5.12). No correlation was found between the SRT 5o% and the APHAB. Twenty seven patients performed the postoperative CBCT scan.

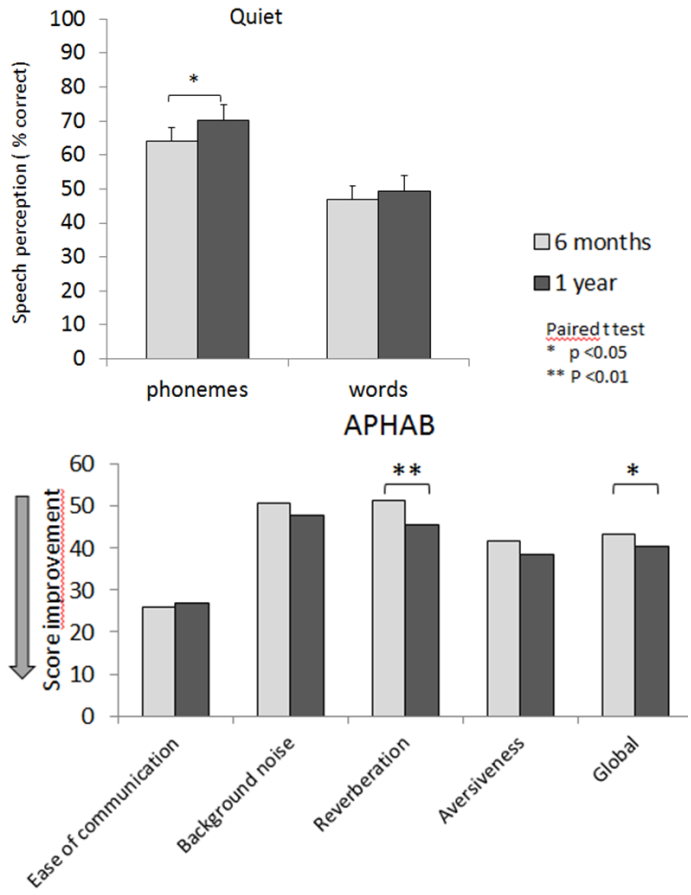

Figure 5.11 Speech perception scores (dysillabic words and phonemes) in silence and APHAB score at 6 and 12 months. (n=28) for the APHAB test only unilateral implanted patients were considered (n=26)

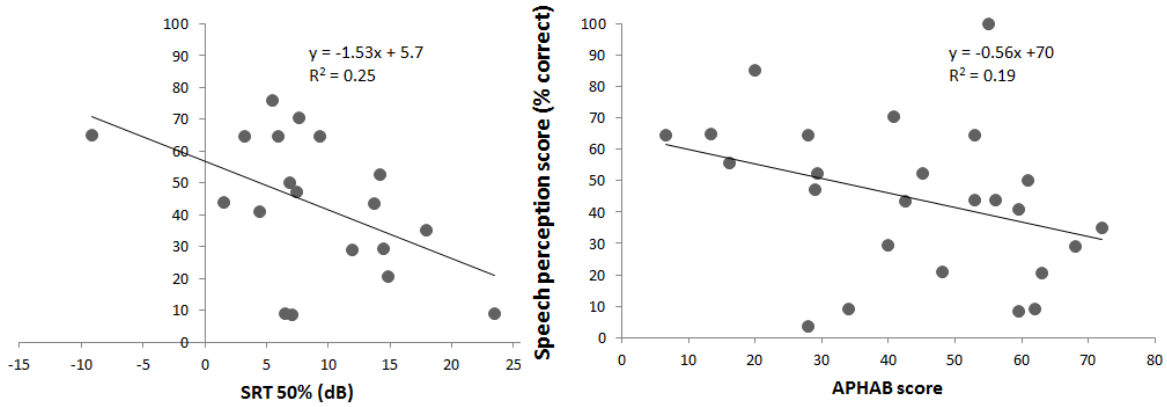

Figure 5.12 Scatterplots and significant negative correlations between speech perception score and SRT 50% score (r = -0.5) and speech perception scores and APHAB score (r = - 0.43). The higher were the hearing scores the lower were the SRT 50% and the APHAB score.

Electrode position assessment

The analysis of the postoperative cone beam CT showed a complete insertion of 28/29 electrodes arrays (mean angle 404 ± 38-degrees). In two patients the scalar position assessment of the electrodes was not possible due to artifact of movement. Twenty-one electrodes arrays were entirely positioned in the scala tympani, and 6 partially or totally inserted in the scala vestibuli. One patient, simultaneously bilateral implanted, had an ossification of the tympanic basal turn, thus the vestibular scala was implanted via cochleostomy. A second patient was affected by intracochlear vestibular schwannoma; in this case the array translocation occurred in the region corresponding to the localization of the tumor (Fig 5.13). Four arrays translocated from the tympanic to the vestibular ramp without any known reason. For one patient was not possible to precisely analyze the postoperative imaging and determinate the electrodes position due to excessive artifact of movement.

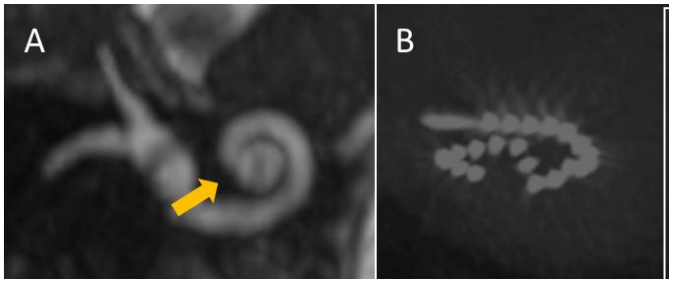

Fig 5.13 Intracochlear Vestibular Schwannoma. A., absence of intracochlear signal is visible in T2 weighted image (arrow) indicating the localization of the tumor. B, the electrode array is translocated in the end of the basal turn corresponding to the localization of the

Electrode position and auditory performance

No correlation was found between the depth of insertion and auditory performance. The electrode-modiolus distance at 180-degrees was correlated with auditory performance at 6 months (Spearman r = -0.69, $p < 0.01$), at 1 year no correlation was found. No difference in speech perception score in quietwas found between scala tympani or scala vestibule positioning of the electrode in quiet both at

6- and at 12 months, and in noise (SRT 50%) at 12-18 months (NS Mann-Whitney test) (Fig. 5.14). Considering the APHAB score the patients presenting a translocation of the array had lower score both at 6 months and at 1 year for the global score at 6 months and also in two subgroup score at 1-year (Mann-Whitney test) (Fig 5.15).

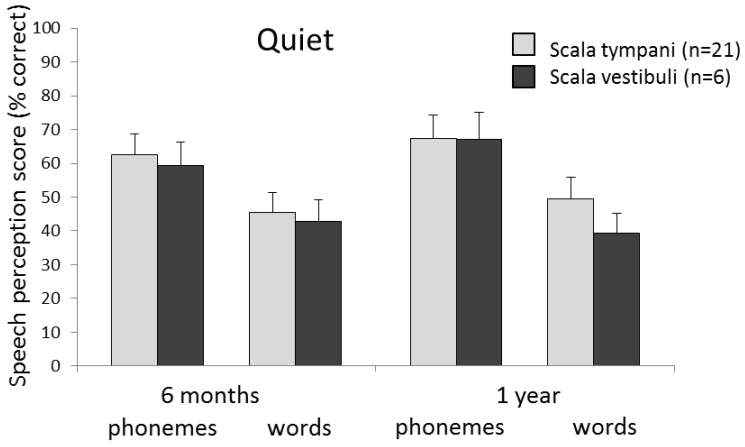

Figure 5.14. Speech perception score in quiet according to the scalar translocation of the electrode. No difference was found between the two groups (not significant , Mann-Whitney test)

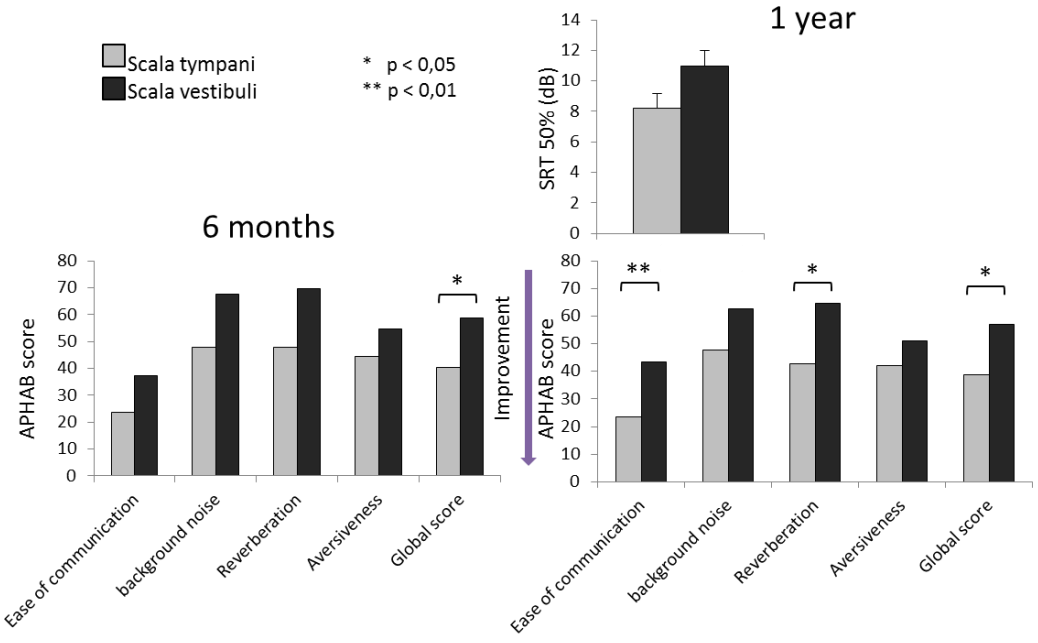

Figure 5.15. APHAB and SRT 50% score according to the scalar translocation of the electrode. Patients having the electrodes array completely inserted in scala tympani had better score in APHAB questionnaire, indicating a better subjective quality of sound in noisy environment. (Mann-Whitney test)The SRT 50% test was performed on 19 patients (15 scala tympani and 4 scala vestibuli position), no difference was found between the two groups.

5.2.4 Discussion and conclusion

This preliminary study show that the translocation of the electrode could impact of the quality of sound in cochlear implanted patients. The low number of translocation probably determined that the two groups of patients were too different to reach a statistically power to demonstrate a difference. Unfortunately the adaptive test in noise was only available for 4 patients presenting a translocation of the electrodes array. Nevertheless, a difference was found in the quality of life questionnaire indicating that the quality of the perceived sound was better for those patients having the electrodes array completely inserted in the scala tympani. The correlation between APHAB score and speech perception was demonstrated, in accordance with other studies (Cox et al 2003), supporting our tendency in favor of the negative influence of the scalar translocation over the hearing outcomes. The adaptive test in noise (Matrix ®) that we used for the first time in our department has been a reliable tool for accurate speech intelligibility measurements in noise. A further study with more participants and a multivariate analysis of the results is necessary and is ongoing in our department, in order to better analyze the influence of the electrode array translocation on the hearing outcomes in cochlear implanted patients.

5.3 DISCUSSION

In this chapter we demonstrated the correlation between the position of the electrodes and hearing performance in two groups of cochlear implanted patients. The site of stimulation of the cochlear implant is not the only factor that influences the hearing performance as we discussed in the chapter 3 since many other factors could influence the speech perception scores (Lazard et al. 2012). Nevertheless, in the first study an homogeneous group of bilaterally implanted patients that we enrolled with relatively strict inclusion criteria and minimal difference between the two ears allowed us to demonstrated a correlation in the short term (1 year) between the distance of the electrodes in the basal turn to the modiolus and the hearing performance both in quiet and in noise. This has been already proposed and discussed by several authors as reported in the discussion of the study. An important factor that we analyzed in this report is the speech perception score evolution over time. In fact, the relationship of electrode positioning and the evolution of speech performance in bilateral implanted patients was never been reported before. Our finding is probably related to the effect of the brain plasticity in bilateral implanted patients. Indeed, Reiss et al. (2014) showed a progressive pitch matching shift over time, emphasizing the role of central auditory pathways in adaptive mechanisms in bilateral implanted patients with different lengths of implanted electrodes. In our study we did not investigate on the pitch matching of our patients having different angular depths of insertion between the two sides, nevertheless, if the mismatch adaptation between the two sides occur for the pitch in bilateral implanted patients we can speculate that a similar mechanism occur for reduce the impact on speech score of the electrode to modiolus distance over time.

Several studies investigated on the correlation between the depth of insertion and hearing performance finding different and contrasting results that have been already discussed in the section 5.1.4. The reason could be related to several factors. First of all, the stimulation of the apical region with coding strategy that do not accounts with the temporal fine structure. Indeed, the coding of the pitch for the low frequencies in the cochlea is based on phase locking signals, and this time based mechanism locks onto the temporal fine structure of the signal and conveys intonation by keeping the auditory nerve fibers' firing rate at the same frequency as the signal. As a consequence, researchers and implant manufacturers started to take efforts in providing fine structure information to cochlear implanted patients. MED-EL launched the first commercially available fine structure coding strategy, the fine structure processing (FSP), in 2006. Nevertheless, several studies (Magnusson et al 2011, Riss et al 2011) found no significant difference in performance between CIS and FSP. Recently new coding strategies, the FS4 and FS4-p, were introduced offering new and further options to transmit temporal fine structure information to the implanted cochlea (Riss et al. 2014, Dincer et al. 2015). In our group of patients the coding strategy was the CIS and remained unchanged for the whole period. Further studies are necessary to demonstrate the efficacy of the stimulation of the apical region of the cochlea with these strategies that rely on temporal fine structure. Another important factor is represented by the preservation of the residual hearing or inner ear structures in the apex of the cochlea. In our study no one of the implanted patients

presented preoperative residual hearing, and the translocation of the electrode array was not studied due to the unavailability of sufficiently high resolution images, i.e. cone beam CT. The last reason could be related to the reliability of the test. For this reason an adaptive test based on the speech reception threshold of 50% was used in the second study presented on this chapter for better differentiate the patients' speech performance in noise and overcome some bias of the commonly used test for speech audiometry (in particular the ceiling effect).

In the second study with the aid of the cone beam images and the scalar assessment methodology that we validated in temporal bones (chapter 4) we evaluated the scalar position of the array in a group of patients and we looked for a correlation between the insertion related inner ear traumatism (defined as the radiological translocation of the electrodes array) and speech perception score in quiet, noise, and in a quality of life questionnaire. As we reported in the previous section, a tendency in the results seemed to indicate a negative impact of scalar translocation on speech perception score in our group of patients. These results are in accordance with Holden et al. (2013) that reported that the CNC final scores were higher when more electrodes were located in scala tymapni compared with scala vestibuli. The relationship between a quality of life questionnaire that quantify everyday life problems associated with hearing impairment and the scalar position of the electrodes in our knowledge has never been reported before. Further studies are necessary to determine the real impact of scalar translocation on hearing performance. It was reported that to test this difference and achieve 90% statistical power would require 1850 patients per group or 1455 for a statistical power of 80% (Wanna et al. 2011). Nevertheless, the same author reported that the scalar translocation is a predictive factor for loss of residual hearing after cochlear implantation (Wanna et al. 2015). Aschenrdorff et al. (2007) reported the differences in results may be explained by a combination of electrode position and differences in trauma associated with the insertion and electrode position. Our findings suggest that a minimal traumatic insertion for cochlear implantation even for those patients who do not have residual hearing should be always attempted. In the next chapter we will see how the reduction of the forces during the array insertion into the cochlea can limit the inner ear structures traumatism in a temporal bone study.

6 Insertion forces and array translocation: A temporal bone study

Hearing auditory performance of implanted patients depends on multiple factors. Some are related to the patient's medical history such as the etiology and the duration of hearing loss, the age of onset, and the sociocultural profile. Anatomic and surgical factors also seem to be determinant in hearing performances. Variations in the inter- and intra-individual morphology of the cochlea have been described to be determinant in the positioning of the electrodes array in the cochlear lumen. Moreover the smaller was the cochlear diameter the closer the straight electrodes array laid to the modiolus and this influenced the hearing outcomes at short term postimplantation (De Seta et al. 2016, Chapter 4). The surgical gesture results obviously determinant on hearing preservation and several authors demonstrated that a minimally invasive or "soft" surgery in cochlear implantation increased the probability to preserve the residual hearing respecting the inner ear structure (i.e. spiral ligament, basilar membrane, lamina spiralis ossea). Indeed, the cochleostomy and the insertion of the electrodes array are potentially related to a direct mechanical inner ear traumatism. The cochlear anatomy and the physical characteristics of the electrodes array could influence the friction forces applied to the cochlea during the electrode array insertion and thus the insertion related traumatism to the inner ear structures

The interest in insertion related trauma in cochlear implantation began early, parallel to the widespread use of the cochlear implants. Kennedy (1987) carefully described the mechanism of damage of the spiral ligament in the basal turn of the cochlea in round windows inserted electrodes (Fig 6.1), and reported the importance to stop the insertion at the point of first resistance. Wardrop et al. (1995 a, b) in an extensive study compared different kind of electrodes array insertion in temporal bones, reporting the histological traumatism for each kind of tested electrode (Spiral Clarion, HiFocus II, Nucleus banded and Nucleus Contour). In their study the authors concluded that partial insertion of the array was less traumatic that the full one and that the reducing of the diameter of the electrodes array should reduce the insertion related trauma. No difference in terms of traumatism was reported between straight or precurved array. Obviously with the use of the positioner, not used anymore, a closer position to the modiolus was obtained but more traumatism was determined during the insertion.

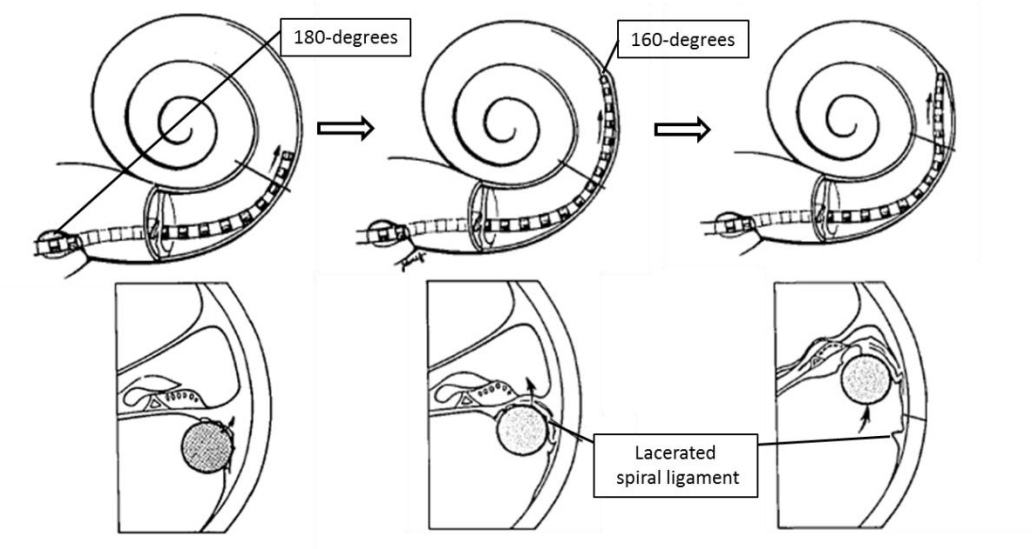

Figure 6.1. Diagrammatic representation of spiral ligament and basilar partition injury during the round window insertion of straight electrode. The region of 160-degrees is at risk for insertion related damage in lateral wall electrodes insertion. Modified from Kennedy, 1987.

The evolution of the electrode design led in the recent years to a significant reduction of the diameters of the arrays, and a more flexibility in order to minimize the insertion trauma and thus permit a better preservation of the inner ear structures. In order to better study the mechanism of insertion trauma, the forces applied during the progression of the array, have been studied in the last years both in plastic models of cochlea and in temporal bones. The work of Roland (1995) described the vectors of the forces applied to the lateral wall of the cochlea by the tip of the electrodes array (Fig 6.2) showing the numerous forces that are applied on the cochlear structure during the insertion.

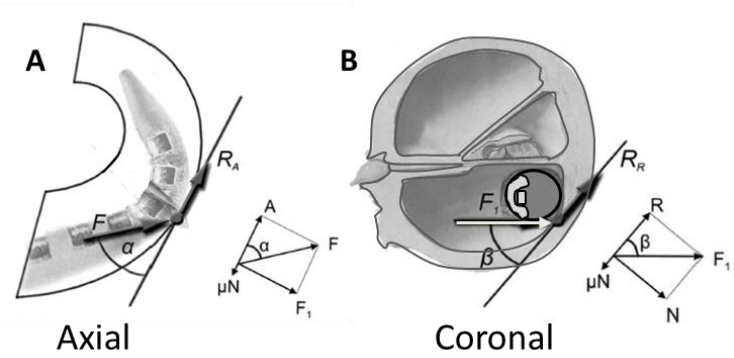

Figure 6.2. Force vector diagram where electrode first contacts the outer wall in the axial (A) and in the coronal plane (B) of the basal turn. The directional insertion force F determines components in the plane of the basal turn, F_1 and A (A). A is the component advancing the array forward, whereas F_1 is the force exerted onto the scala tympani outer wall. Because the outer wall is also angled in the radial plane, the normal force F_1 in the basal plane also determines components in the radial plane, N and R (B). Directional insertion force F generates a significant component advancing the array forward along the scala tympani outer wall, R_A. The rising floor of the scala tympani, in the radial plane, in turn generates a rising component, R_R. This rising force can lift the electrode array toward the basilar membrane. Modified from Roland, 1995.

The insertion forces depend by the electrodes array physical and mechanical characteristics, and by the cochlear model used for the insertion. An automated insertion technique the permit to perform and compare repeated insertion. Moreover, the metrics of insertion forces need to be defined. The preliminary studies performed in our laboratory that allowed us to define and measure the insertion forces components during the cochlear implantation of different electrodes array in different cochlear models are reported in the next chapter.

6.1 MEASURING THE INSERTION FORCES IN COCHLEAR IMPLANTATION

In order to evaluate the intracochlear electrode insertion dynamics, insertion related trauma, and the electrode position two kind of cochlear models have been used. Electrodes insertions in plastic cochlear models have been performed for the evaluation of the electrodes array physical characteristics (Madjani et al. 2010, Annex 1). The advantage of these plastic/resin models is the possibility to test different arrays and to test different insertion parameters (speed, insertion axe, use of lubricant) in the same shape of scala tympani. Furthermore, its transparency permits to study the progression and the behavior of the array during the insertion. The drawback of these cochlear models is represented by the fact that the shape of the scala tympani is round and not ovoidal as in the real cochleae, and the friction force coefficient between the silicone of the array and the resin has not been measured and is probably different by the coefiicient between the silicone and the cochlear endosteum. On the contrary, fresh temporal bone cadaveric specimen represents the more reliable model if the intracochlear traumatism wants to be studied, but the scala tympany is hidden in the bony otic capsule. The standard approach reported to measure array friction forces is to place the sensor below the cochlea model or temporal bone to avoid measurements of frictions forces inside the insertion tool (Roland, 2005).
In order to analyze the electrodes array physical and mechanical characteristics, an automated insertion technique is necessary, it allow to maximize repeatability and minimize inter trial variability. A motorized insertion tool was developed (Miroir et al. 2012), and successively improved (Nguyen et al 2014) in our laboratory. The recording of the insertion force with the use of this tool permitted to study the mechanics of the electrodes insertion, and investigate over the use of lubricant or different insertion speed over the forces in plastic transparent cochlear models (Fig. 6.3).

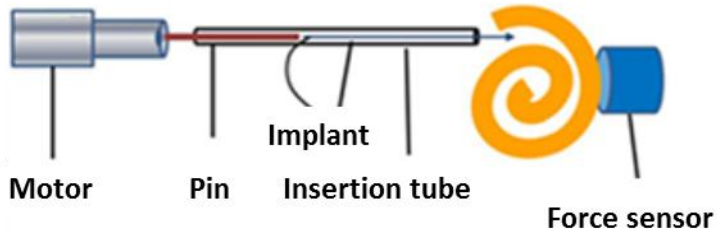

Figure 6.3. Schematic diagram of the system used to measure intracochlear insertion forces in our laboratory.

In a preliminary study the metrics related to the insertion forces during the cochlear implantation have been defined (Nguyen et al. 2014, see Annex 2) using three insertion techniques: manual one with forceps, and using a tool with a manual or motorized insertion temporal bone specimens. In this study the cochlea of twenty fresh temporal bones was extracted and the membranous labyrinth largely exposed (Fig. 6.4 A) in order to visualize the basilar membrane and thus to follow the electrodes array progression and immediately visualize any trauma on the basilar membrane. Five metrics were thus defined and permitted to differentiate the force profile characteristics according to the insertion method. The defined metrics are: The peak of force, the total change in momentum, the number of times where

forces were increased by 50% within a small time step (sudden rise), the number of occurrence where the applied forces were over an arbitrary threshold, fixed at 0.1 N, and the smoothness of the curve, studied as "jerk" variation (expressed as N•s−1).
The need to drill the superior wall of the cochlear lumen for preparation of this model might have modified the resistance of lateral wall and the spiral ligament. For this reason in the next studies we abandoned this model for a more clinical cochlear implantation trough a posterior tympanotomy to better simulate an implantation in patients with the real insertion axes and visualization and avoiding any risk of modify the physical characteristics of the inner ear structures (6.4B).

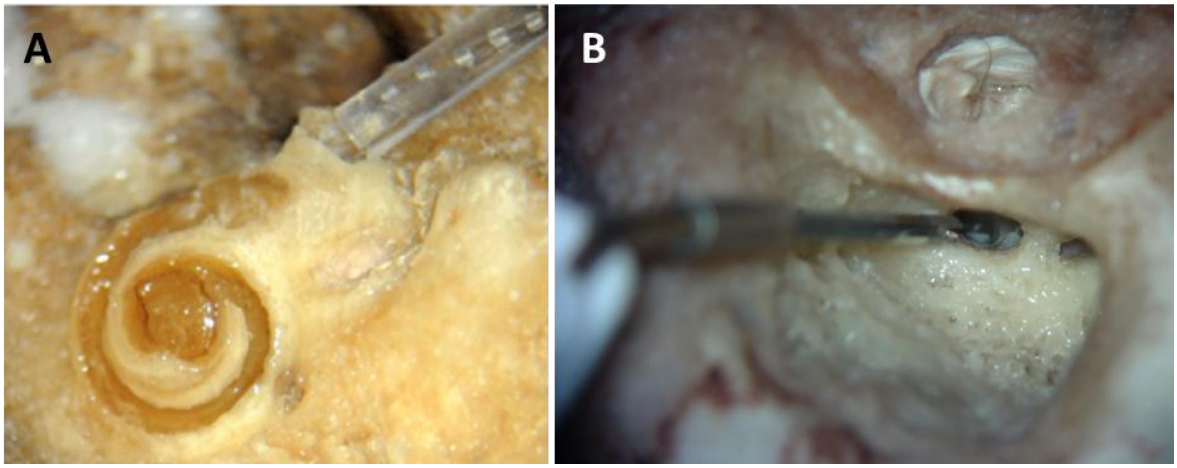

Figure 6.4. A. Microdissected right cochlea for the insertion forces measurement. B. Cochlear insertion through posterior tympanotomy. The insertion tool was aligned with the scala tympani midline adjacent to the cochleostomy but without any contact with the temporal bone to prevent interferences in forces measurements and avoid artifact recording.

Different force sensors have been used in the literature to record the insertion forces in cochlear implantation. In our experience both 1-axis force sensor (range, 0-0.4 N; resolution, 4 mN, millinewton force sensor; EPFL, Lausanne, Switzerland) and a 6-axis force sensor (ATI Nano 17, calibration type SI-12-0.12, resolution: 3 mN, Apex, NC, USA) were used. The six axes where the force is measured are the x, y, and z axes and their rotation moment. The norm of the force vector in the x, y, and z direction of the 6-axis force sensor were considered to calculate the overall friction forces in all our studies. The 3 other axes representing the rotation moment over the x, y and z axes (Rx, Ry, and Rz) were not taken into account in our studies. The theoretical advantage of the 6- (or 3) axes force sensor is to collect all forces generated during the insertion. It should be therefore more appropriate to use a multiple axis force sensor rather than a 1-axis load cell that can ignore other components of the resulting insertion vector. Nevertheless, the difference between the estimated force from the 1-axis sensor and the data from the 6-axis sensor was below 0.01 N at all times during the insertion in a study performed on epoxy scala tympani model and temporal bones (Miroir et al 2011).

The defined metrics have been used to study the relationship between insertion forces and inner ear trauma in a fresh frozen cadaveric cochlear model and the results are presented in the next section.

6.2 IS THE INSERTION FORCE RELATED TO TRAUMATISM?

Abstract

Introduction: The cochlear implant insertion should be the less traumatic as possible in order to reduce the cochlear sensory structures trauma and to preserve the residual hearing. The force applied to the cochlea during the electrode array insertion should be therefore controlled and reduced to limit the insertion related damages; nevertheless the relationship between insertion forces and histological traumatisms remains to be demonstrated.
Objective: The aim of this work was to correlate the insertion forces recorded during cochlear implant array insertion to possible inner ear damages, and to estimate the maximal value of the force that could be applied during the insertion of lateral wall electrodes array without damaging the inner ear structures.
Methods: Twelve fresh frozen temporal bones were implanted at constant speed with the aid of a motorized insertion tool. During the insertion the forces were recorded and the following metrics were calculated: Maximal peak of force, force momentum, sudden rise of the force, and smoothness of the curve. Pre- and post-implantation cone beam CT scans were performed in order to study the cochlear anatomy and the position of the electrodes array. Anatomical parameters, position of the array and force metrics were correlated to scanning electron microscopy images and histological findings.
Results: An atraumatic insertion occurred in 6 cochlee a translocation in 5 cochlee and a basilar membrane rupture in 1 cochlea. The translocation always occurred in 150 / 180-degree area. In atraumatic insertions the profile of the forces was similar in all cases; the friction force remained low for the first half of the insertion and then progressively increased, reaching a peak of force at the end of insertion (59 ± 19.9 mN). In case of traumatic insertion different profile of forces were observed with a more irregular curve by the presence of an early peak force (30 ± 18.2 mN). This corresponded approximately to the first point of contact of the array to the lateral wall of the cochlea. The insertion force increased as a function of the advancement of the electrode into the cochlea ($r = 0.57$, $p < 0.001$). However, the two groups had different force values at the same depth of insertion ($p < 0.001$, two-way ANOVA), and different functions of the regression lines ($y = 1.34x + 0.7$for the atraumatic and $y = 3.37x + 0.84$ for traumatic insertion, $p < 0.001$, ANCOVA).
Conclusion: In the present study, the insertion force is correlated to the intracochlear trauma. The 180- / 150-degrees region represented the area at risk for the scalar translocation. Two different functions of the insertion force curves were identified for traumatic and atraumatic insertions; these values should be considered during the motorized insertion of the implant in order to modify the insertion parameters (e.g., angle, speed) and facilitate the preservation of endocochlear structures.

Submitted as: De Seta D, Torres R, Ferrary E, Kazmitcheff G, Heymann D, Amiaud J, Sterkers O, Bernardeschi D, Nguyen Y. Inner Ear Structures Damage During Cochlear Implantation. Analysis of Insertion Forces, Cone Beam CT, Scanning Electron Microscopy and Histological Findings in Temporal Bone Specimens. *Hearing Research*

6.2.1 Introduction

Over the past decade, the indications for cochlear implantation changed including not only those patients presenting with bilateral profound hearing loss, but also patients with residual hearing on low frequencies or presenting single sided deafness. As a consequence, surgery has evolved toward a low intracochlear trauma insertion in order to maintain the integrity of inner ear structures in all cochlear implants recipients, even those destined for electric-only stimulation. Indeed, the reduction of cochlear traumatism during implantation may offer several advantages. In patients with usable preimplant low-frequency hearing, minimizing the trauma can allow the preservation of the residual hearing, and thus the electric-acoustic stimulation. For the others, reducing cochlear damage may limit the fibrosis and ossification, making easier the revision surgery for device failure or upgrade. This point is of particular interest for pediatric patients having during their lifetime an increasing possibility that reimplantation will be required. Moreover, limiting injury potentially allows for the application of future technologies, such as cellular regeneration or other novel cochlear nerve stimulation technologies (Carlson et al. 2011). The concept of soft surgery has been introduced in 1993 by Lehnhardt, and since then the cochlear implant centers began to follow this surgical technique in all cochlear implantation regardless of the necessity to preserve the hearing or not. In parallel cochlear implant manufacturers modified the electrode array shape and physical characteristics making them thinner, more flexible, and in some cases shorter.

Short electrodes array are less traumatic over the inner ear structures (Lenarz et al. 2006), and the force applied during the insertion of a shorter array is lower than that for longer ones (Briggs et al. 2011). Nevertheless, a disadvantage of the use of short electrode array is the limited low-frequency stimulation, especially in case of secondary loss of the residual hearing that may require the reimplantation with a longer array (Nguyen et al. 2013). Considering the electrode array design, postimplantation hearing results after straight or precurved perimodiolar electrode array are controversial being better after straight electrode insertion (Briggs et al. 2011; Boyer et al. 2015) or similar (Doshi et al. 2015).

Controversial results have been also reported on the correlation between hearing results and the scalar location of the array. Scala tympani positioning was reported to have the better results, compared to scala vestibuli, in terms of speech recognition score (Skinner 2007, Ashendorff 2007, Holden et al., 2013), whereas other studies found no difference (Wanna et al 2011). Nevertheless, a relationship between the absence of translocation and the hearing preservation was found (Wanna et al. 2015).

In order to investigate on the inner ear structures insertion related trauma, the forces applied to the cochlea during the electrode array insertion have been studied considering different parameters such as the insertion speed, use of lubricants, design of the electrodes array, or use of insertion tools (Nguyen et al. 2015, Rohani et al. 2014, Miroir et al. 2012, Majdani et al. 2010, Roland 2005). To date, the relationship between the insertion forces and histological traumatisms remains unclear. The aim of this work was to correlate the forces during a straight electrode array insertion within the scala tympani to possible inner ear damages evidenced by histological study, and to estimate the maximal value of the force that should be applied without damaging the inner ear structures.

6.2.2 Material and methods

Twelve fresh frozen temporal bones (5 pairs from 5 subjects and 2 single temporal bones) were prepared with a simple mastoidectomy and a posterior tympanotomy. A cone beam CT scan (CBCT) was performed on the temporal bone specimens before and after the insertion. The array (Med El flex 28 array, Innsbruck, Austria) was inserted at constant speed using a motorized insertion tool, and the friction forces during the insertion were recorded. The final position of the electrodes within the cochlea was studied on CBCT images. The cochlea was extracted from the temporal bone for scanning electron microscope imaging (SEM). Histological analysis was performed to confirm the position of the array and to study the inner ear structures. Between each of these steps, the temporal bones were frozen at -18 °C to ensure preservation of the structures. Each step is detailed below.

Cone beam CT scan imaging

The CBCT images were obtained with the NewTom 5G machine (NewTom 5G, QR s.r.l. Verona, Italy). The system setup used a 200 x 25 mm flat panel detector at 650 mm from the radiation source. One 360-degree rotation of the x-ray tube took 36 seconds. The tube voltage was 110 kV, with a 19-mA charge at the terminals. Total filtrations were 2 mm, with a pitch of 125 µm; this corresponded to a field view of 12 x 7.5 cm diameter. The images were isometric voxel rendered from the 125 µm sections.

The DICOM images (Digital Imaging and Communications in Medicine) data were analyzed by Osirix (Osirix v 4.0 64-bit; Pixmeo Sarl, Bernex, Switzerland). This program allowed the multiplanar reconstructions for the measurement of the cochlear anatomy and the identification of the position of the arrays within the cochlea. The major cochlear diameter (distance A) from the middle of the round window membrane to the opposite lateral wall (Escude et al. 2006) was measured in the section perpendicular to the modiolus axis and coplanar to the basal turn named ‘cochlear view’ (Xu et al. 2000); the cochlear height was measured from the cochlear fossa to the apex of the cochlea in a reformatted mid-modiolar plane perpendicular to superior semicircular canal plane. The vertical and horizontal diameters of the cochlear lumen were measured at 180- and 360-degrees. The angle between the first and second turns of the cochlea was measured between the axes of these two turns in a slice parallel to the superior semicircular canal (Martinez-Monedero et al. 2011) (Fig 6.5A).

After the cochlear implantation, a second CBCT was performed. The angular depth of insertion was measured in a cochlear view with a slice thickness of 4 mm. A 2D curved multiplanar reconstruction allowed to straighten and follow the array along the cochlear lumen in order to evaluate the position of the electrodes with respect to the basilar membrane (Nguyen et al. 2012) (Fig 6.5B).

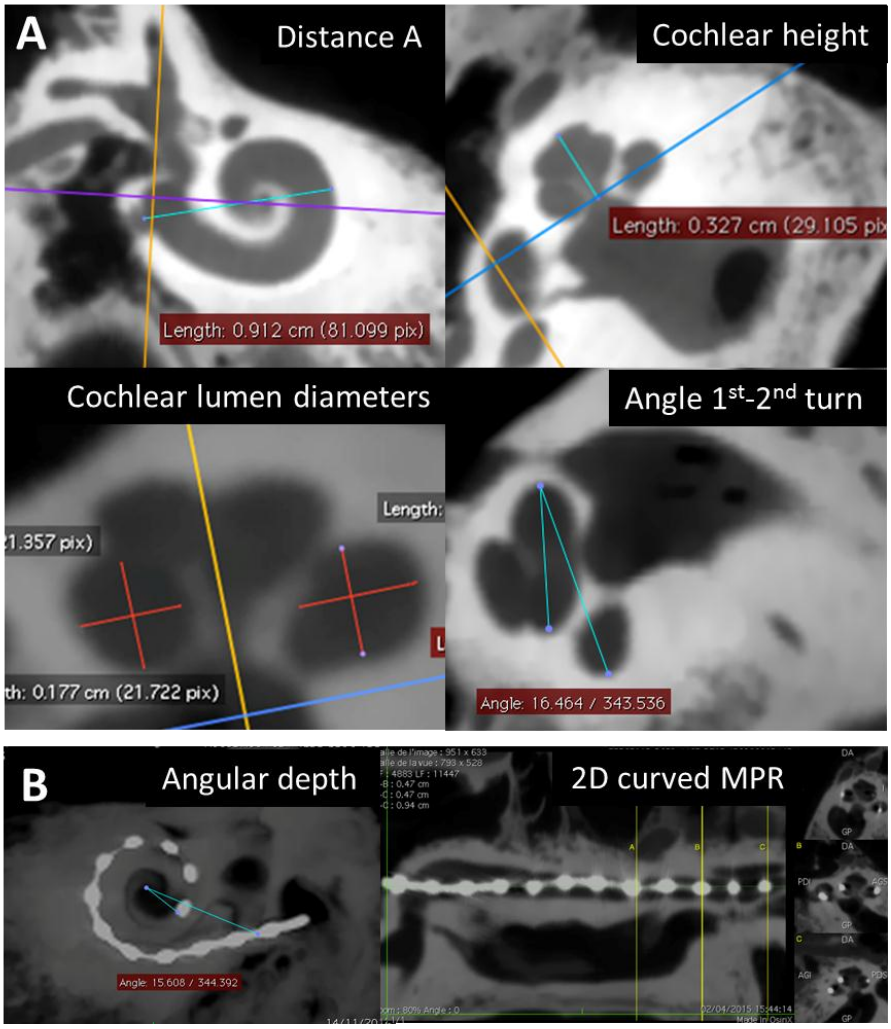

Figure 6.5. A: pre-insertion cone Beam CT measurements. The major cochlear diameter (distance A) was measured in the cochlear view plane. The cochlear height was measured in the plane perpendicular to the superior semicircular canal (SSC) passing through the modiolus in the cochlear view; the cochlear lumen diameters were measured in the mid-modiolar plane at 180- and 360-degrees; the angle between 1st-2nd turn was measured in the plane parallel to the SSC. B: post-insertion cone Beam CT analysis. The angular depth of insertion is measured in the cochlear view; the 3D curved multiplanar reconstructions (MPR) allowed to follow the trajectory of electrode array in the cochlear lumen and identify the position of the electrodes (right panels).

Cochlear implantation and insertion forces measurement

The temporal bone was fixed to an in-house made temporal bone holder that was coupled to a force sensor (ATI Nano 17, calibration type SI-12-0.12, resolution: 3 mN, Apex, NC). The electrodes array was inserted through an extended inferior round window approach using a motorized insertion tool developed in our laboratory (Miroir et al. 2012) (Fig.6.6). This tool comprised a rotary actuator (RE10CLL, MDP, Miribel, France) connected to a threaded screw that pushed a blunt pin into an insertion tube loading the array. The tool was held steady by a flexible arm. No force feedback loop between this tool and the force sensor was applied. The actuator speed was controlled via laboratory power supply (Metrix AX 503, Chauvin-Arnoux,

Paris, France) and set at 0.8 mm·s^{-1}. The round window region was irrigated with saline serum, and sodium hyaluronate (Healon, Abbott Medical Optics, Abbott Park, Illinois, USA) was applied before the electrodes array insertion. Force sensor data were recorded in real-time via the same analog to digital interface card controlling the actuator input power at a sample rate of 60 Hz. From the 6-axis sensor, insertion forces were computed only based on three linear force norms (Dx, Dy, Dz). The shape of the curve corresponding to the force versus the time was investigated. Five different metrics have been calculated: The peak of force, the total change in momentum, the number of times where forces were increased by 50% within a small time step (sudden rise), the number of occurrence where the applied forces were over an arbitrary threshold, fixed at 0.1 N, and the smoothness of the curve, studied as "jerk" variation (expressed as N·s^{-1}) (Nguyen et al. 2014).

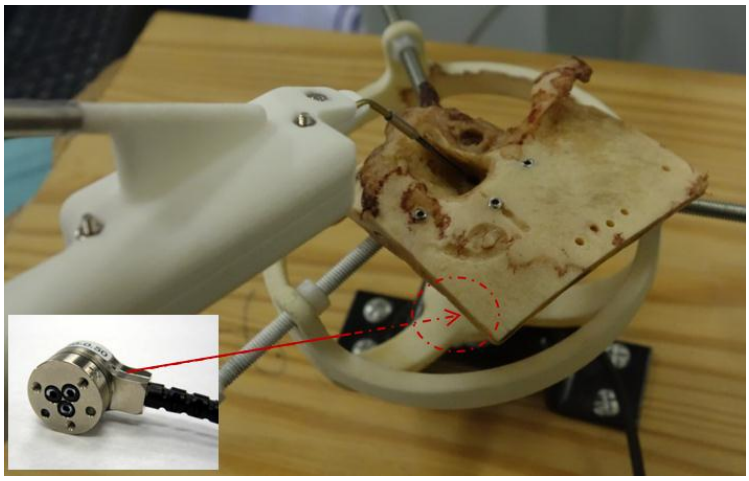

Figure 6.6. Measurement insertion forces bench. The insertion tool was fixed to a steady flexible arm, avoiding any contact with the cochlea. The insertion speed was fixed to 0.8 mm·s^{-1}. The insertion forces were measured with the 6-axes force sensor (small panel) placed under the temporal bone holder and successively analyzed.

Histological procedures

Immediately after its insertion the electrode array was fixed with cyanoacrylate glue to the round window region in order to avoid any displacement during the successive steps. Cochlea was removed from the temporal bone and was fixed in 10% buffered formalin. The specimen was successively dehydrated in graded alcohol and casted in methyl methacrylate resin (10% Polyiethylene Glycol 400, 20% Technovit 7200 VLC, Heraeus Kulzer Gmbh, Germany; 70% Methylmethacrylate) (Fig 6.7 A).

The specimen was sawed (Leica SP 1660 Saw Microtome, Nussloch GmbH, Germany, sawing speed 3) perpendicularly to the basal turn passing through the round window (Fig 6.7 B and C). An electronic microscopic scan image (Hitachi TM 3000, Tokyo, Japan) was successively obtained in order to confirm the position of the electrodes, and each face of the resin bloc was also observed under white light microscope. The half cochlea (Fig 6.7 D) was successively grinded in order to reach the apical electrode and a second acquisition with the SEM was performed. The damage to the inner ear structures was assessed using the cochlear trauma grading system (Eshraghi et al. 2015) as followed: 0 represented no observable trauma; 1, elevation of the basilar membrane; 2, rupture of basilar membrane; 3, electrode in scala vestibuli; 4, severe trauma such as fracture of the osseous spiral lamina or modiolus or

tear of stria vascularis. The location of the trauma was also evaluated: a, lower basal turn (0 to 180°), b, upper basal turn (181° to 360°), c, lower middle turn (361° to 540°), d, upper middle turn (541° to 720°); e, apex (>721°).

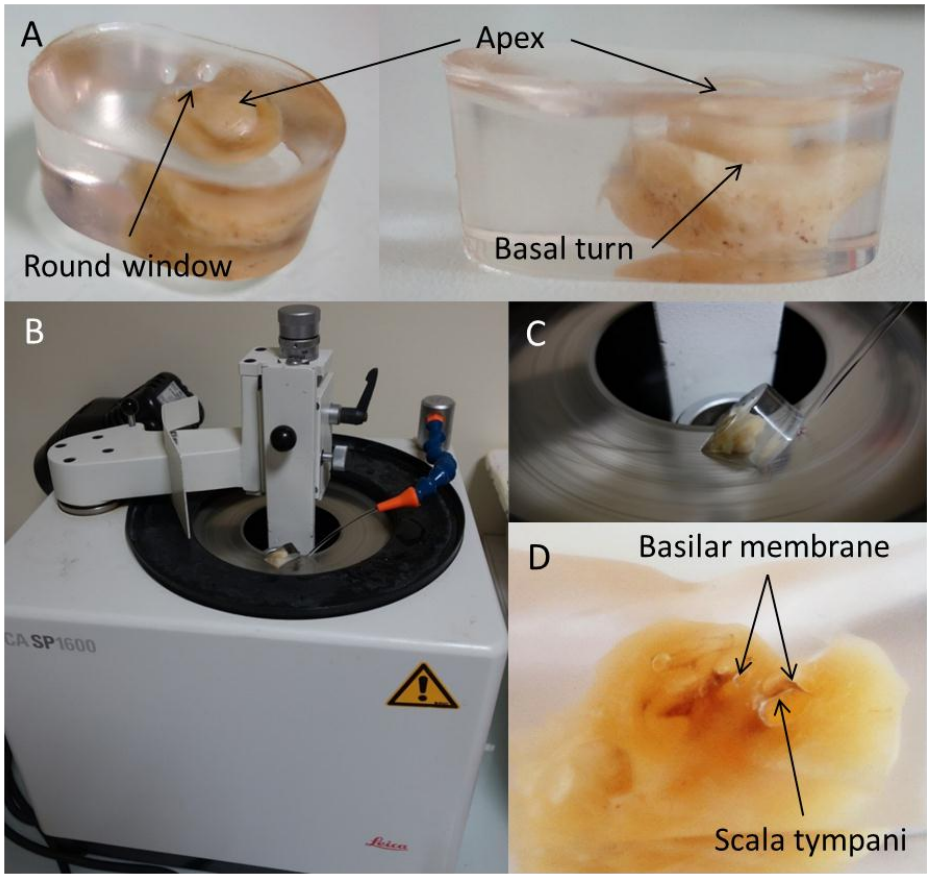

Figure 6.7. A The cochlea was drilled and the basal turn was clearly identified for allow the correct orientation during the embedding in methilmetacrilate resin. The transparent resin helped the orientation of the specimen in the successive steps. B, Leica SP 1600 saw microtome. C, detail of the sawing procedure. D, the specimen after the midmodiolar cut.

Statistical analysis

Results are expressed as mean ± standard deviation. Insertion forces graphics were generated by "R" statistical software (http://www.r-project.org/). Spearman's rho correlation coefficient was used to study the correlation where appropriated. Two-ways ANOVA [factors: traumatism (translocation, no translocation) and depth of insertion: (90-, 120-, 150-, 180-, 210-, 240-degrees)] was applied to analyze the insertion force across group and depth of insertion. The difference of the slope of the regression lines of the force for the two groups was tested by means of the analysis of covariance (ANCOVA). All statistical analyses were performed using IBM SPSS for Windows (v 22.0, SPSS Inc., Chicago, Illinois, USA). For all comparisons, $p < 0.05$ was considered as significant.

6.2.3 Results

The cochlear anatomy parameters and the insertion forces measurements are reported in Table 6.1. As expected the cochlear height was correlated with the angle between the first and second turn (r = 0.64, p=0.02, data not shown). No other anatomic correlations were found. Ten electrodes arrays were full inserted and 2 insertions were incomplete with 1 or 2 electrodes out of the cochlea. The analysis of post insertion cone-beam images identified 6 array correctly positioned in the scala tympani, 5 translocations in the 180-degrees region and 1 array in intermediate positions from the 140-degrees region until the apical electrode. The histologic images confirmed 6 atraumatic insertions, a translocation in 5 specimens, and a basilar membrane rupture without translocation in another insertion (Fig 6.8). The scalar translocation occurred in the 150- / 180-degrees region in all 5 cases, the 6 traumatic insertions occurred in 5 different subjects (Table 6.2). No correlation was found between anatomic measurements and force metrics, no differences in anatomical parameters were found between traumatic and atraumatic insertions (NS, Mann-Whitney U test) (Table 6.3).

TABLE 6.1. ANATOMICAL AND INSERTION FORCE PARAMETERS

Anatomical parameters	
Distance A (mm)	9.0±0.42
Cochlear height (mm)	3.2±0.30
Angle 1^{st}-2^{nd} turn (degrees)	14.8±1.36
Insertion force parameters	
Max Peak of force (mN)	71.3±30.3
Force momentum (N·s)	418.55±95
Jerk ($N \cdot s^{-1}$)	200.02±48
Sudden rise (No)	50.3±30

Data are means ± SD, n=12

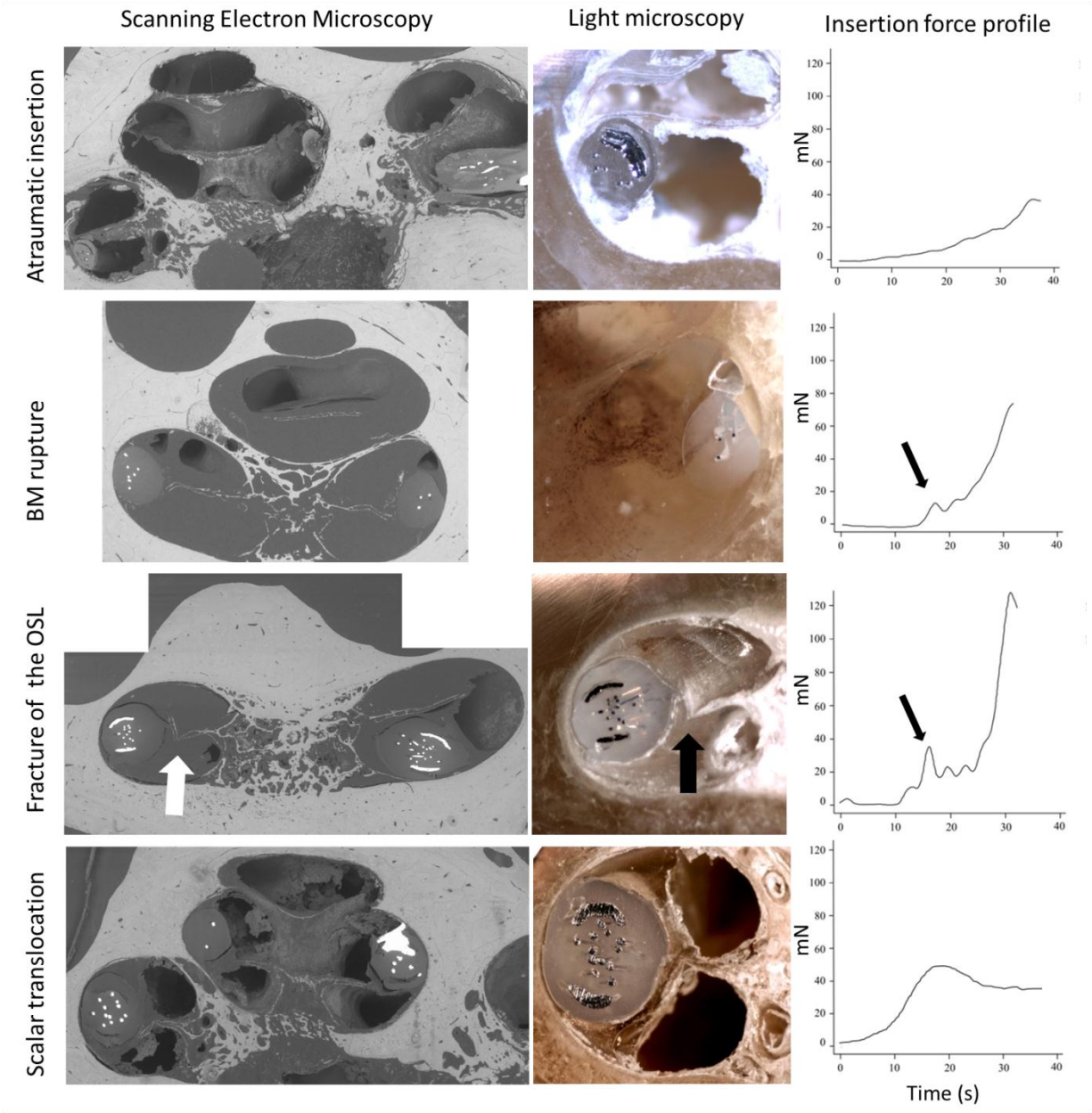

Figure 6.8 Examples of In the upper part of the figure a scanning electron microscope image, light microscope image and insertion force profile for an atraumatic insertion and three different traumatic insertions. In the lower part a traumatic insertion is represented. The fracture of the spiral osseus lamina at 160° is visible both in SEM and in light microscope image (thick arrows). A peak of force (thin arrows) is visible at 15 seconds after the beginning of the insertion, corresponding to traumatism at 160°. An early scalar translocation corresponded to an early rise of force occurred in the first part of the insertion

TABLE 6.2. TRAUMATIC INSERTIONS: HISTOLOGY

Specimen #	**Scalar translocation (degrees)**	**Transl. electrodes (n)**	**Cochlear trauma scale Location (degrees)**	
			(0-180)	**(181-360)**
R3G	-	-	2	2
R5D	190	2	2	3
R6D	180	4	3	3
R6G	160	5	4	4
R4D	150	5	3	3
R1G	150	5	4	3

Eshraghi cochlear trauma grading system (2015): 0 represented no observable trauma; 1, elevation of the basilar membrane; 2, rupture of basilar membrane; 3, electrode in scala vestibuli; and 4, severe trauma such as fracture of the osseous spiral lamina or modiolus or tear of stria vascularis

TABLE 6.3. ANATOMICAL MEASUREMENT IN TRAUMATIC AND ATRAUMATIC INSERTIONS

Distance A	Height	Angle 1^{st}-2^{nd} turn	180° diameter		360° diameter	
			Vertical	Horizontal	Vertical	Horizontal
Traumatic insertions (n=6)						
9.08±0.52	3.2±0.36	14.7±1.17	1.5±0.16	1.7±0.16	1.5±0.10	1.5±0.15
Atraumatic insertions (n=6)						
9.1±0.33	3.3±0.22	14.9±1.64	1.7±0.15	1.7±0.14	1.6±0.10	1.6±0.08

Results are presented as mean±SD. Values are in mm and degrees for the angle

Atraumatic insertions

The overall insertion force profile was similar for all temporal bones; the friction forces remained low for the first half of the insertion and then rose continuously reaching a peak of force at the end of the insertion (59.4±19.9 mN) (Fig 6.9 C). In the region at risk for translocation (150-degrees) all except one atraumatic insertion had lower friction forces than the traumatic ones (Fig 6.10).

Traumatic insertions

Analysis of the friction force profile in traumatic insertions showed in four insertion an irregular profile and the presence of a bump (peak of force: 29.56±18.2mN) around 15 seconds after the beginning of insertion corresponding approximately to the moment when the

tip of the array reached the lateral wall of the cochlea in the 150- 180-degrees region (Fig 6.9 F), another insertion presented an early rise of force. The last traumatic insertion had a smooth and regular force profile.

The insertion force profile for the first part of the insertion for all the cochleae is reported in fig 4. As clearly results from the force profile curves, the insertion force increased as function of depth of the insertion both in traumatic and in atraumatic insertions ($r = 0.57$, $p < 0.001$). Nevertheless, the two groups had difference force values at different depths of insertion ($p < 0.001$, Two-ways ANOVA), and the slope of the regression lines for the atraumatic ($y = 1.34x + 0.7$) and traumatic ($y = 3.37x + 0.84$) was different ($p < 0.001$, ANCOVA) (Fig 6.10).
Three insertions had a max peak of force superior to 0.1 N and it was always associated with scalar translocation, nevertheless no force difference was found between different grades of trauma (i.e. grade 4 vs grade 3). No other correlation was found between other force metrics and inner ear traumatism.

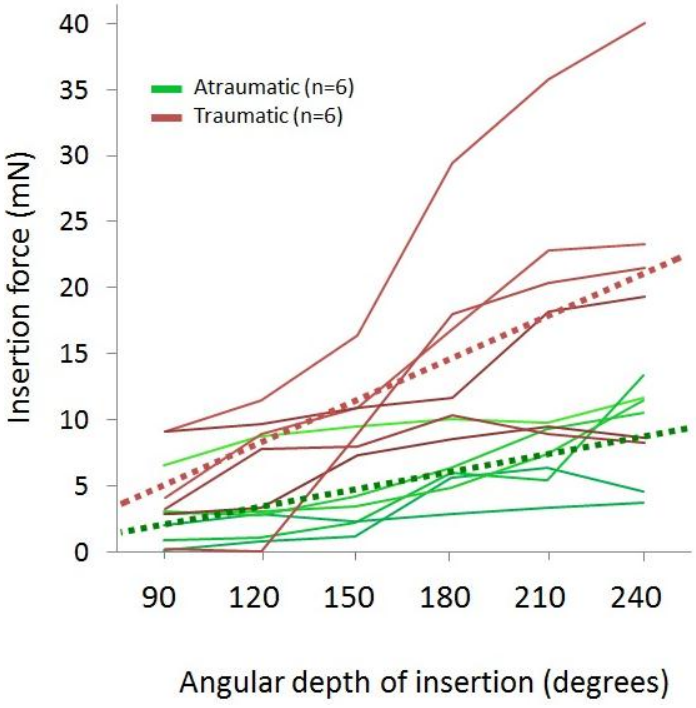

Figure 6.10. Insertion force profile of traumatic (red) and atraumatic (green) insertions in the critical region for translocation (90- 240-degrees). All the traumatism occurred between 150° and 180°. The dashed lines represent the linear regression line for traumatic ($y=3.37x +0.84$) and atraumatic ($y=1.34x +0.69$) insertion.

6.2.3 Discussion

The preservation of inner ear structures and the consequently preservation of residual hearing during cochlear implantation mainly depends by the surgical technique and by the physical characteristics of the electrodes array. In this temporal bone study, a long (28 mm) straight array was tested and a relationship between the insertion forces profile and an inner ear structures preservation has been found. To our knowledge this represents the first report showing a direct correlation between the insertion forces profile and intracochlear traumatism.

Nevertheless, our cadaveric model has some limits and intracochlear electrodes array insertions cannot be strictly compared to *in vivo* studies. The temporal bones were frozen and unfrozen multiple times (one time before the insertion); this probably interfered on the stiffness and resistance of the inner ear structures (spiral ligament, basilar membrane, spiral osseous lamina). Moreover, all the insertions were made via an extended round window approach in order to standardize the insertion and avoid contact of the array with the entry point of the cochlea; Wanna et al. (2015) report the extended round window insertion and cochleostomy to be more traumatic and prone to scalar translocation than pure round window insertion. The choice of the entry point in the cochlea should be done on the basis of the anatomical variation of the cochlea (Atturo et al. 2014) and the electrodes array should be chosen as a consequence; in any case the round window insertion should be avoided in case of perimodiolar array use (Jeyakumar et al. 2013). Although electrode insertion trauma is influenced by the array design, the occurrence of severe trauma is mainly reported in the region of 180-degrees, this is caused in part by the decrease of the scala vestibule diameter in this point (Biedron et al., 2010) and by the fact that lateral wall electrodes directly impact on that region in case of ERW or cochleostomy insertion. The traumatism and the translocation rate found in the present work were similar to other frozen temporal bone studies. Martins et al. (2015) found a higher rate of traumatism (36%) in the region 180-270 degrees than in other cochlear segments; moreover the authors didn't found any difference in terms of traumatism between anterosuperior or anteroinferior quadrant of the round window membrane.

Several studies have been published so far describing the cochlear implant insertion related trauma. The early study of Kennedy (1987), that evaluated a straight electrode array inserted through an ERW approach, reported that an insertion beyond the point of first resistance resulted in damages to the spiral ligament, the basilar membrane, and osseous spiral lamina at the junction of the first and second half of the first turn. In 1993, Welling et al. reported the results of a temporal bone study on the insertional trauma of different electrodes arrays available at that time finding damages of the lateral wall structures of the cochlea in the all the three inserted arrays, and no traumatism to the modiolar region. More recently Adunka et al. (2006) evaluated the basal trauma in temporal bone insertions of MedEl arrays of different length. Using a round window approach the rupture of spiral osseus lamina (Eshraghi grade 4) was reported in 2/8 specimens, whereas a deeper insertion (24-30 mm with a Flex soft electrode) was reported to be more traumatic. Other groups reported their experience with a different straight array, the Cochlear SRA (nowadays in the Cochlear CI422 implant). This electrode resulted atraumatic in shallow insertion (i.e. up to 20 mm) but more traumatic in deeper insertions (Skarzynski et al. 2012, Mukherjee et al. 2012). All this studies reported a subjective force measurement and suggested the insertion until the point of first resistance in case of hearing preservation procedure.

The forces necessary to determine a rupture of the inner ear stuctures has been previously studied in fresh cadaveric temporal bones. Ishii et al. (1995) isolated the basilar membrane and measured the rupture force between 29 and 39 mN, whereas for the only the membrane of Reissner isolated the authors measured a force of 4.2 mN. Schuster et al. (2014) reported the force necessary to determine a rupture of the entire system basilar membrane, Reissner's membrane and lamina spiralis ossea to be in mean 88 mN, ranging from 42 to 122 mN. In

these studies the forces applied were perpendicular to the basilar membrane; this situation was not comparable with the force applied during the electrodes array insertion being the vector of the force different, anyway the studies give useful information about the resistance of the BM-lamina spiralis. An objective measure of the forces during the CI insertion have been made by Rohani et al. (2014) that studied the insertion profile of 3 different electrodes in 6 fresh temporal bones. In this study the array was inserted through a tunnel drilled in the mastoid with a preimplantation planned linear trajectory without performing a mastoidectomy, and incomplete insertions for MedEl Standard arrays were obtained.

A previous study of our group (Nguyen et al. 2012) reported a correlation between different profile of curves and quality of insertions using a identifying a peak force of 0.5 N with a slope increase after 10 mm in the incomplete insertion and a peak force of 0.3 N and a slope rise after only 7 mm in one insertion having a folding tip; in this study the histologic analysis of the inner ear traumatism was not performed, and any correlation was reported between forces and traumatism. Several studies report the average force during the cochlear implantation (Schurzig et al., 2010, Kontorinis et al. 2011, Rohani et al. 2014). This metric depends by the duration of the insertion and results extremely low in insertions with several fits and starts and long pauses even if a high peak of force occurred during the insertion. We believe the most reasonable value to be considered should be the peak of force. Indeed, in the present study the only metrics of the insertion that resulted correlated to the insertion trauma was the peak of force. The maximal peak of force occurred in 11 out of 12 insertions at the end of the insertion and represented the friction force of the entire array with the lateral cochlear wall and inner ear structures. The force value in the region of the first contact of the tip of the array with the cochlear structures should represent the value to monitor during electrode insertion in order to detect and avoid complications. In case of elevation of the force over a defined threshold in the first contact region the insertion technique should be modified. A small rotation of the electrode or a backward and forward movement under the monitoring of the forces could be the correct attitude for avoid the structure trauma. Indeed, steerable (Zhang et al. 2010) or curvature controlled (Wu et al. 2005) electrodes array have been proposed in order to reduce the friction forces.

In our results the friction forces for traumatic and atraumatic insertion were already different at 90-degrees insertion depth, prior than the translocation and the contact of the tip of the array to the cochlear lateral wall in the region of risk for traumatism. One might suppose that other factors influence the scalar translocation. The axe of the insertion of the array that should be tangent to the basal turn of the cochlea was not controlled in our study and was determined by the position of the facial nerve in the posterior tympanotomy. The ideal insertion vector coaxial to the centerline of the scala tympani is interrupted in most of the cases by the facial nerve (Meshik et al. 2010); a preoperatory planned axis of insertion guided by a surgical navigation system could possibly improve the inner ear structures preservation aligning the electrode with the most appropriate insertion axis (Torres et al. 2015).

In conclusion, in this study the insertion forces were correlated to the inner ear damage. In the present study, a maximal peak of force superior to 0.1 N was always associated with to a traumatic insertion. Moreover, the region at 150- 180-degrees represented the region at risk for translocation and a high peak of force in this area corresponded to an inner ear damage. Two different slopes for the regression lines of traumatic and atraumatic insertion were

obtained; these values, if confirmed by further studies, could be useful for the development of future force feedback automated cochlear implant insertion tool in order to reduce the risk of insertion related damage and provide the best chance for an optimal hearing rehabilitation in cochlear implanted patients.

6.3 DISCUSSION

During the last decade with the increasing interest in electroacoustic cochlear implantation and hearing preservation, the forces during the insertion of intracochlear array have been recorded and studied with the aim to improve the design of the electrodes arrays making them thinner and less traumatic.

In order to reduce the traumatism in the point of contact with the lateral wall or the modiolar region the cochlear implant manufacturer improved the tip region of the implant making it more flexible or rounded. MedEl introduced the FLEX-tip in its latest generation of arrays (2004) providing a single electrode contact on the leading end of the array (diameter of 0.5 x 0.4 mm) to further increase mechanical flexibility. Cochlear in 2002 introduced the soft-tip, a conical shape ending of the array, the aim of this design is to minimize the pressure of the electrode tip contacting the outer wall of the scala tympani by providing the critical section that bends at relatively lower stress levels (Roland 2005). Advanced Bionics in 2013 introduced the Mid-scala electrode, a new electrodes array shape designed for an intermediate placement in the cochlear lumen, with the aim to avoid both lateral wall and modiolar structure damages typically related to straight or perimodiolar electrodes. This electrode has been tested in our laboratory, and an insertion force study in cochlear plastic model was conducted among a group of surgeons with various experiences (see Annex 1). The results of this study shows that a reduced diameter and the use of a guiding stylet with automated retraction in this pre-curved array can lead to an improvement of insertion force profiles if compared with a straight, lateral wall electrode of the same manufacturer, i.e. the 1J electrode. A recent clinical study conducted in 47 implanted patients (50 ears) showed that at 6-months postoperatively, 15% of patients had complete hearing preservation, whereas 40.0% had partial hearing preservation. At 1-year, these percentages decreased to 0% and 38.5%, respectively, close to other reports in the cochlear implant literature using different arrays (Hunter et al. 2016).

Several studies investigated on the different physical characteristics of the electrodes arrays but no correlation between the actual forces recorded during the array insertion and the intracochlear trauma was reported. Rebsher et al. (2008) measured the stiffness of different arrays in the vertical and horizontal plane measuring at 1 mm increments from the base of the array to the tip. No statistically significant relationship was seen between the mean electrode stiffness and the incidence of severe insertion trauma. However, the ratio of vertical stiffness divided by horizontal stiffness was significantly correlated with the incidence of trauma (Spearman correlation coefficient = -0.83, $p < 0.01$), i.e. proportionally greater vertical stiffness resulted in significantly less damage. Many studies were performed in cochlear plastic models (Schurzig et al. 2010, Helbig et al. 2011, Miroir et al. 2012, Nguyen et al. 2015) and obviously did not provided information about the inner ear structure damage. In a temporal bone study where the insertion forces were recorded with the same method only two insertions for each tested electrode were performed, albeit no correlation have been made with this small number of insertion a peak of force of 0.4 N with a weighted average force of 0.053 N was found in the only traumatic insertion, being the reported force values for the other 5 insertion lower (Rohani et al. 2014). In our preliminary study (Nguyen et al. 2014, Annex 2)

twenty temporal bones were implanted with the same electrodes with different insertion technique and translocation rate of 35 % of cases was found. The translocation rate has to be analyzed with precaution due to model preparation. While giving immediate information during insertion on array translocation, this kind of microdissected model has the drawback of potentially creating histological damages or weakening of the basilar membrane before array insertion. For that reason in the following studies this model was abandoned for a more clinical insertion technique in a cochlear model where we tried to preserve the structural and mechanical characteristics of the inner ear tissue. The fact that the temporal bones were not formalin fixed needed to be frozen and this may have modified the structural characteristics. Indeed, in a group of implanted patients with the same electrodes array the translocation rate was limited to 1 ear out of 9 (see chapter 4), and this results is in accordance with other reports (Boyer et al. 2015).

In our knowledge this is the first report that correlates the insertion forces to the histological trauma in a relatively large number of temporal bones using the same standardized technique The critical force value for inner ear traumatism or electrode translocation in the point of contact of the electrode array and the lateral wall structures (spiral ligament, stria vascularis, basilar membrane) still remains to be defined in patients. Our cadaveric fresh-frozen model was a good model for study the scalar translocation and the results obtained with 50 % of traumatic insertions gave us the possibility to define two different profiles of insertion forces for traumatic and atraumatic insertions. Further studies are needed to better investigate on the mechanism of the inner ear damage and the other factors involved in the insertion related traumatism. We believe that the control of the insertion forces together with a preoperatory planned axe of insertion could improve the inner ear structures preservation, and this associated with the use of navigation systems and automated or motorized force feedback controlled array insertion devices in cochlear implantation.

7 Discussion and perspectives

In this thesis we showed how the preoperative and postoperative imaging plays a fundamental role in cochlear implantation. The role of electrodes placement in the cochlea would be determinant in the first postimplantation phase, while the central adaptation would take place in the following period. In case of bilateral cochlear implantation, the cortical integration after restauration of binaural hearing by may take longer time than in unilateral implantees and protract the speech scores improvement over time. Finally, a correlation between insertion forces and intracochlear traumatism has been demonstrated and the results obtained in our temporal bone insertion model will be used for the future development of "smart" insertion tools capable to reduce the insertion related ineer ear trauma.

Speech perception scores in bilateral implanted patients continue to improve after 1 year postimplantation

Cochlear implants do not accurately replace all the normal functions of the ear. These neuroprosthetic devices activate the auditory pathways differently from what occurs in the normal ear and they do not stimulate all the components of the auditory nervous system that are normally stimulated by sound. This requires the nervous system to "learn" a new code. It has been known for a long time that expression of neural plasticity helps to regain function after trauma or insults, such as from strokes. While plasticity of sensory systems is most pronounced during infancy, when the establishment of neural architecture first occurs, plasticity is known to continue into adulthood such that neural systems remain capable of undergoing substantial reorganization in response to altered inputs due to trauma or an adaptive mechanism known as perceptual learning (Irvine and Wright, 2005). Functional imaging after cochlear implantation showed that metabolic activity in primary auditory cortex increase to near normal levels, with greater activity on the side contralateral to the implant, and the magnitude of the increase appears to be correlated with the performance of the implanted patient (Lee et al. 2007). The auditory experience plays a key role in the development of the fine organisational structure of the central auditory system, and there is no doubt that this plasticity contributes to the remarkable success of many cochlear implant subjects in achieving near-normal speech perception despite the impoverished input provided by the implant (see for review: Irvine 2007; Fallon et al. 2008). Training is a powerful method for activating neural plasticity and is a part of all cochlear implant programs. We know from previous published studies that in unilateral implanted patients the speech scores improve during the first months and until 1-year postimplantation (Lenartz et al. 2012, Holden et al. 2013). As we demonstrated in this study and confirmed by other authors, in bilateral implanted patients the improvement of the hearing perception score is protracted over the first year (Chang et al. 2010, Eapen et al. 2009, De Seta et al. 2016). The additional finding of our study was that the ears having poor results at one year postimplantation continued to improve over time reducing the difference with the better ear in speech score discrimination at 5-years. The missing speech perception assessment between the 1-year and 5-years measurement

intervals did not allow us to evaluate if the speech perception scores improved gradually or not over the follow-up period, but in any case the results should encourage both the patients and the speech terapists to continue the speech training sessions even after one year postimplantation. This would permit to the implanted ears with poor performance to continue to improve and to the good ears to not decrease over time.

Insertion tool for atraumatic intracochlear insertion

A repeatable and controllable gesture is needed to study the mechanics of the insertion and the physical characteristics of the elecrodes array and subsequently the possible damages to the inner ear structures. The manual insertion with forceps has been demonstrated to be influenced by human hand tremor and fits and starts and to have a less regular force profile that the insertions performed with both a manual and a motorized insertion tool (Nguyen et al. 2014). A motorized insertion is indispensable to provide constant progression speed of the array in order to obtain repeatable force profile curves and evaluate the factors that may influence the quality of insertion. The insertion tool we used in this study represents the last version of a device that was developed in our lab in the the last years (Miroir et al. 2012, Nguyen et al. 2014). This version of the device included a rotatory actuator that pushed the electrodes array into the scala tympani. The speed of insertion was controlled by a laboratory power supply and no force feedback loop between the tool and the force sensor was applied. This tool permitted us to standardize the insertion technique and obtain repeatable curve in plastic cochlear model and to perform the same insertion in all temporal bone specimens. A force sensor (1 axis) was integrated in the first version of our insertion device, and other authors proposed similar solution inserting a force sensor in the device (Schurzig et al. 2010, Kobler et al. 2014). The values of the force obtained in our temporal bone insertion togheter with the histological data concerning the traumatism of the inner ear will be useful in the improvement of future insertion tool that is under development in our lab. The development of reliable cochlear implant insertion device with a force feedback control would permit to modify the insertion parameters during the insertion in order to reduce the risk of insertion related damage.

Segmentation and image fusion for identification of scalar position

With this study we validated a technique to identify the intracochlear position of straight electrodes array in the cone beam CT images using the 3D curved multiplanar reconstruction tool of Osirix®.

In the last years the increasing interest in mini-invasive surgery and the evolution of indications in cochlear implantation led to the development of new softwares for the imaging analysis. The use of interactive applications, allows the delineation of anatomical region of interest by manual or automatic segmentation (Fig 7.1). The images obtained can be successively elaborated and aligned with 3D images elaborating softwares that allow for example the visualization of the cochlear implant fusioned with the preoperative CT scan or MRI of the patients in order to visualize the relationship between electrodes and basilar membrane (Fig.7.2). Some authors used create a dedicate software for the segmentation conventional CT scans using an ‘‘active shape model algorithm’’ based on cochlear micro CT scans acquired ex-vivo. The model is fitted to the partial information available in the

conventional scans and used the active shape algorithm to estimate the position of the cochlear scalae and the basilar membrane (Noble et al. 2011). This model was validated in temporal bones in a radiohistological study (Schuman et al. 2010) and used for correlate the intracochlear electrodes position and hearing outcomes in implanted patients (Wanna et al. 2011). Skinner et al. (2007) analyzed in a similar way the pre- and post-operative high resolution CT scan for determine the scalar localization of the electrode with micro computed tomography and orthogonal-plane fluorescence optical sectioning (OPFOS) microscopy based atlas. In this rigid model the anatomy is manually aligned with the image to identify electrode position. The preliminary experience in our lab with the manual segmentation of the intracochlear structures and automatic segmentation of the electrodes array permitted to identify the intracochlear positioning of the electrodes, but we found the Osirix® program and 3D curved MPR a reliable, rapid and easy tool for the preoperative cochlear anatomical measurement and for the identification of electrodes position within the cochlea lumen.

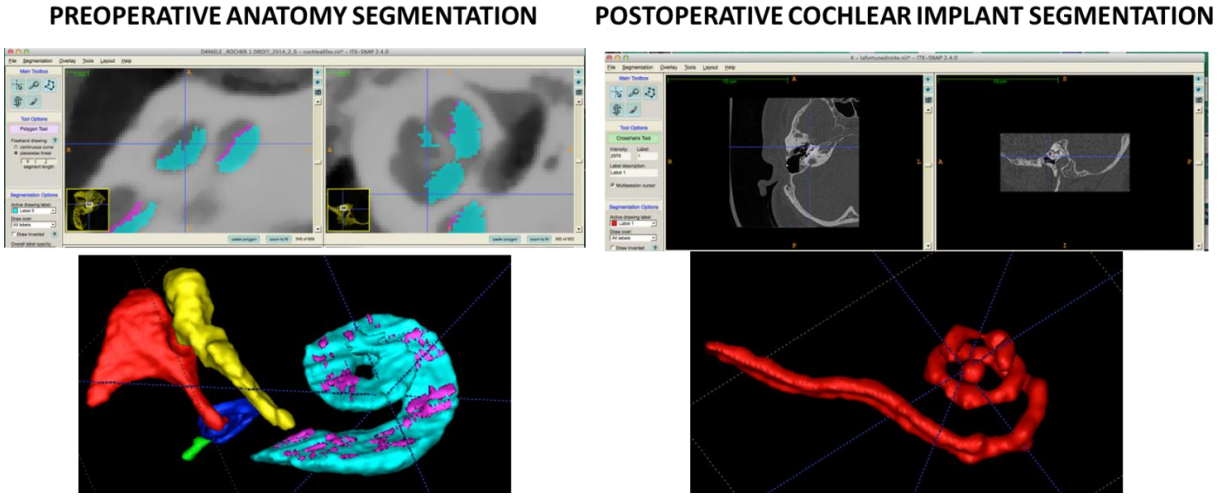

Figure 7.1 Pre- and post-operative middle and inner ear structures and the cochlear implant array by manual and automatic segmentation. The scala tympani in cyan is totally segmented, the basilar membrane (magenta) only partially in a preoperative CBCT. In red the electrode array is automatically segmented with the snake tool (right figure) in a multislice postimplantation CT scan of the same patient. The fusion of the two images can correctly assess the localization of the electrode in the cochlea and its relationship with the inner ear structures. Segmentation realized with ITK-SNAP v 3.4.0 (www.itksnap.org).

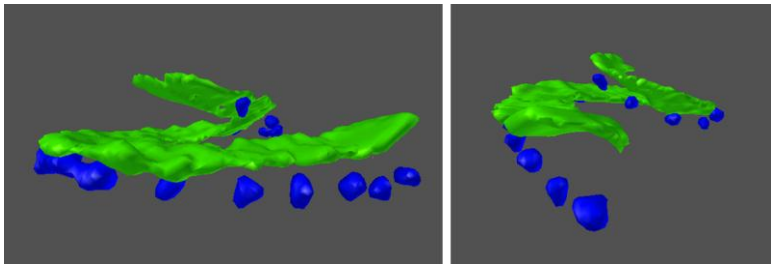

Figure 7.2 Preoperative MSCT scan and postoperative cone beam CT image alignment. The electrodes (blue) rest below the basilar membrane (green) along the entire trajectory of the array. The fusion of the two images was performed with Blender ® software.

3D models for cochlear implant insertion simulation

The development of new softwares for computational modeling represents a valid future alternative to the physical cochlear models (plastic, temporal bones specimen, animal) for test the electrodes array insertion and the estimate the traumatism to inner ear structures. In the last years, the generation of computational finite element models from biomedical data has been widely studied and applied in all surgical fields including the cochlear implantation. These 3D models permit the simulation of different implantation scenarios of a given patient changing the surgical procedure parameters. Personalization of computational models creating patient-specific cochlear finite element methods models has the potential to simulate the effect of patients' specific anatomic factors, interactions between cochlear structures or simulate the cochlear fluid dynamics during the insertion having the potential to optimize the implantation procedure. In particular, an individualized model would play a decisive role in the cochlear implantation to choose the implant design that better fits the patient's diagnosis (Mangado et al. 2015). For this purpose, a combined computational model of both patient's inner ear anatomy and implant is needed (Ceresa et al. 2013). A finite element model is produced with softwares, e.g., SOFA (Allard et al. 2007), using anatomical parameters obtained by patients' CT scans. Dynamic behavior of the model is considered through attributing physical properties (friction coefficients, stiffness, inertia, etc.) obtained via experimentation and from published literature for both the cochlear and electrodes array representations. Several surgical real-time haptic-rendered simulators of cochlear implant procedures have been proposed so far, both for surgeon training and pre-operative planning (Todd et al. 2012) and for simulate the final intracochlear position of the array and the hearing result (Mangado et al. 2015). Unfortunately these simulators do not take in consideration the possibility of scalar translocation, indeed the cochlea or the scala tympani were considered as a rigid body obviating the fact that the insertion may cause damage to the spiral ligament and basilar membrane. The insertion forces data acquired during the last years in our lab and the histological data obtained have been used for a 3D simulator model for cochlear implant that is under develpement in our lab in order to better study the inner ear structures insertion related traumatism and simulate the insertion *in silico*.

In conclusion, the cochlear anatomy has an inter-individual an intra-individual variability; this variability influences the final position in the cochlear lumen, and finally the hearing performance. An individualized and tailored cochlear implant surgery should be applied to all the cochlear implants recipients. The choice of the length, diameter, and flexibility of electrode array made on the basis of the preoperative radiological images should be accompanied by a motorized force feedback controlled insertion, where the parameters can be controlled and eventually modified in order to reduce the risk of insertion related damage and provide the best chance for an optimal hearing rehabilitation. Once the quality of insertion will be ensured by the totally atrumatic intracochlear positioning of the electrodes different coding strategies or modalities may be needed to stimulate in the best way the auditory system.

References

Adunka O, Kiefer J. Impact of electrode insertion depth on intracochlear trauma. Otolaryngol Head Neck Surg. 2006;135:374-82.

Alexiades G, Dhanasingh A, Jolly C. Method to Estimate the Complete and Two-Turn Cochlear Duct Length. Otol Neurotol. 2015;36:904-7.

Allard J, Cotin S, Faure F, Bensoussan PJ, Poyer F, Duriez C, Delingette H, Grisoni L. SOFA-an open source framework for medical simulation. Stud Health Technol Inform. 2007;125:13-8

Aschendorff A, Klenzner T, Richter B, Kubalek R, Nagursky H, Laszig R.Evaluation of the HiFocus electrode array with positioner in human temporal bones. J Laryngol Otol. 2003;117:527-31

Aschendorff A, Kromeier J, Klenzner T, Laszig R. Quality control after insertion of the nucleus contour and contour advance electrode in adults. Ear Hear. 2007;28(2 Suppl):75S-79S.

Atturo F, Barbara M, Rask-Andersen H. On the anatomy of the 'hook' region of the human cochlea and how it relates to cochlear implantation. Audiol Neurootol. 2014;19:378-85

Basura GJ, Eapen R, Buchman CA. Bilateral cochlear implantation: current concepts, indications, and results. Laryngoscope, 2009;119:2395-40.

Bernstein LR. Auditory processing of interaural timing information: new insights. J Neurosci Res. 2001;15;66:1035-46.

Berrettini S, Forli F, De Vito A, Bruschini L, Quaranta N. Cochlear implant in incomplete partition type I. Acta Otorhinolaryngol Ital. 2013;33:56-62.

Biedron S, Prescher A, Ilgner J, Westhofen M. The internal dimensions of the cochlear scalae with special reference to cochlear electrode insertion trauma. Otol Neurotol. 2010;31:731-7.

Blauert J. Binaural localization. Scand Audiol Suppl. 1982;15:7-26

Bodmer D, Shipp DB, Ostroff JM, Ng AH, Stewart S, Chen JM, Nedzelski JM. A comparison of postcochlear implantation speech scores in an adult population. Laryngoscope. 2007;117:1408-1411

Boyd PJ: Potential benefits from deeply inserted cochlear implant electrodes. Ear Hear. 2011;32:411-27

Boyer E, Karkas A, Attye A, Lefournier V, Escude B, Schmerber S. Scalar localization by cone-beam computed tomography of cochlear implant carriers: a comparative study between straight and periomodiolar precurved electrode arrays. Otol Neurotol. 2015;36:422-9

Briggs RJ, Tykocinski M, Stidham K, Roberson JB. Cochleostomy site: implications for electrode placement and hearing preservation. Acta Otolaryngol. 2005;125:870-6.

Briggs RJ, Tykocinski M, Xu J, Risi F, Svehla M, Cowan R, Stover T, Erfurt P, Lenarz T. Comparison of round window and cochleostomy approaches with a prototype hearing preservation electrode. Audiol Neurootol. 2006;11 Suppl 1:42-8.

Buchman CA, Dillon MT, King ER, Adunka MC, Adunka OF, Pillsbury HC. Influence of cochlear implant insertion depth on performance: a prospective randomized trial. Otol Neurotol, 2014;35:1773-9.

Buss E, Pillsbury HC, Buchman CA, Pillsbury CH, Clark MS, Haynes DS, Labadie RF, Amberg S, Roland PS, Kruger P, Novak MA, Wirth JA, Black JM, Peters R, Lake J, Wackym PA, Firszt JB, Wilson BS, Lawson DT, Schatzer R, D'Haese PS, Barco AL: Multicenter U.S. bilateral MED-EL cochlear implantation study: speech perception over the first year of use. Ear Hear. 2008;29:20-32.

Cabral Junior F, Pinna MH, Alves RD, Malerbi AF, Bento RF.Cochlear Implantation and Single-sided Deafness: A Systematic Review of the Literature. Int Arch Otorhinolaryngol. 2016;20:69-75.

Carlson ML, Driscoll CL, Gifford RH, Service GJ, Tombers NM, Hughes-Borst BJ, Neff BA, Beatty CW. Implications of minimizing trauma during conventional cochlear implantation. Otol Neurotol. 2011;32:962-8.

M. Ceresa, H.M. Kjer, S. Vera, N. Carranza, F. Perez, L. Barazzetti, P. Mistrik, A. Dhanasingh, M. Caversaccio, M. Stauber, M. Reyes, R. Paulsen, M. A. González-Ballester, Finite element model for patient-specific functional simulations of cochlear implants, Workshop on Mesh Processing in Medical Image Analysis, Nagoya (Japan), MICCAI 2013, September 2013.

Chang SA, Tyler RS, Dunn CC, Ji H, Witt SA, Gantz B, Hansen M: Performance over time on adults with simultaneous bilateral cochlear implants. J Am Acad Audiol 2010;21:35-43.

Chouard, C.H., Mac Leod, P. La rehabilitation des surdites totales: essai de l'implantation cochleaire d'electrodes multiples. La Nouv. Presse Medicale 1973 44, 2958.

Chouard, C.H., Mac Leod, P. Implantation of multiple intracochlear electrodes for rehabilitation of total deafness: preliminary report. Laryngoscope 1976;86:1743-1751.

Coez A, Zilbovicius M, Ferrary E Bouccara D, Mosnier I, Ambert-Dahan E, Bizaguet E, Martinot JL, Samson Y, Sterkers O: Brain voice processing with bilateral cochlear implants: a positron emission tomography study. Eur Arch Otorhinolaryngol 2014;271:3187-93.

Couloigner V, Sterkers O, Ferrary E. What's new in ion transports in the cochlea? Pflugers Arch. 2006;453:11-22.

Cox RM, Alexander GC, Gray GA. Audiometric correlates of the unaided APHAB. J Am Acad Audiol. 2003;14:361-71.

Cushing SL, Daly MJ, Treaba CG, Chan H, Irish JC, Blaser S, Gordon KA, Papsin BC High-resolution cone-beam computed tomography: a potential tool to improve atraumatic electrode design and position. Acta Otolaryngol. 2012;132:361-8.

Dahl HH, Saunders K, Kelly TM, Osborn AH, Wilcox S, Cone-Wesson B, Wunderlich JL, Du Sart D, Kamarinos M, Gardner RJ, Dennehy S, Williamson R, Vallance N, Mutton

P. Prevalence and nature of connexin 26 mutations in children with non-syndromic deafness. Med J Aust. 2001;20;175:191-4. Erratum in: Med J Aust. 2004;181:437.

Dahmani-Causse M., Marx M., Deguine O., Fraysse B., Lepage B., Escudé B. Morphologic examination of the temporal bone by cone beam computed tomography: Comparison with multislice helical computed tomography Eur Ann Otorhinolaryngol Head Neck Dis. 2011;128:230-5

De Seta D, Nguyen Y, Bonnard D, Ferrary E, Godey B, Bakhos D, Mondain M, Deguine O, Sterkers O, Bernardeschi D and Mosnier I.The Role of Electrode Placement in Bilateral Simultaneously Cochlear Implanted Adult Patients Otolaryngol Head and Neck Surg. *Accepted for publication April 1 2016*

De Seta E, Bosco E, Pichi B, Balsamo G, Filipo R. Sound localization in bilaterally implanted children. Cochlear Implants Int. 2005;6 Suppl 1:47-51.

Denoyelle F, Weil D, Maw MA, Wilcox SA, Lench NJ, Allen-Powell DR, Osborn AH, Dahl HH, Middleton A, Houseman MJ, Dodé C, Marlin S, Boulila-ElGaïed A, Grati M, Ayadi H, BenArab S, Bitoun P, Lina-Granade G, Godet J, Mustapha M, Loiselet J, El-Zir E, Aubois A, Joannard A, Levilliers J, Garabédian EN, Mueller RF, Gardner RJ, Petit C, et al. Prelingual deafness: high prevalence of a 30delG mutation in the connexin 26 gene. Hum Mol Genet. 1997;6:2173-7.

Denoyelle F, Weil D, Maw MA, Wilcox SA, Lench NJ, Allen-Powell DR, Osborn AH, Dahl HH, Middleton A, Houseman MJ, Dodé C, Marlin S, et al. Prelingual deafness: high prevalence of a 30delG mutation in the connexin 26 gene. Hum Mol Genet. 1997;6:2173-7.

Dincer D'Alessandro H, Filipo R, Ballantyne D, Attanasio G, Bosco E, Nicastri M, Mancini P. Low-frequency pitch perception in children with cochlear implants in comparison to normal hearing peers. Eur Arch Otorhinolaryngol. 2015;272:3115-22.

Diogo I, Franke N, Steinbach-Hundt S, Mandapathil M, Weiss R, Werner JA, Güldner C.Differences of radiological artefacts in cochlear implantation in temporal bone and complete head. Cochlear Implants Int. 2014;15:112-7

Doshi J, Johnson P, Mawman D, Green K, Bruce IA, Freeman S, Lloyd SK. Straight versus modiolar hugging electrodes: does one perform better than the other? Otol Neurotol. 2015;36:223-7

Dunn CC, Tyler RS, Oakley S Gantz BJ, Noble W. Comparison of speech recognition and localization performance in bilateral and unilateral cochlear implant users matched on duration of deafness and age at implantation. Ear Hear 2008;29:352-9.

Eapen RJ, Buss E, Adunka MC, Pillsbury HC 3rd, Buchman CA. Hearing-in-noise benefits after bilateral simultaneous cochlear implantation continue to improve 4 years after implantation. Otol Neurotol 2009;30:153-9

Erixon E & Rask-Andersen H. How to predict cochlear length before cochlear implantation surgery. Acta Otolaryngol. 2013;133:1258-65.

Erixon E, Högstorp H, Wadin K, Rask-Andersen H.Variational anatomy of the human cochlea: implications for cochlear implantation. Otol Neurotol, 2009;30:14-22.

Escudé B, James C, Deguine O, Cochard N, Eter E, Fraysse B. The size of the cochlea and predictions of insertion depth angles for cochlear implant electrodes. Audiol Neurootol. 2006;11 Suppl 1:27-33. Epub 2006 Oct 6.

Eshraghi AA, Lang DM, Roell J, Van De Water TR, Garnham C, Rodrigues H, Guardiola M, Gupta C, Mittal J. Mechanisms of programmed cell death signaling in hair cells and support cells post-electrode insertion trauma. Acta Otolaryngol. 2015;135:328-34.

Eshraghi AA, Yang NW, Balkany TJ. Comparative study of cochlear damage with three perimodiolar electrode designs. Laryngoscope. 2003;113:415-9.

Esquia Medina GN, Borel S, Nguyen Y, Ambert-Dahan E, Ferrary E, Sterkers O, Grayeli AB. Is electrode-modiolus distance a prognostic factor for hearing performances after cochlear implant surgery? Audiol Neurootol, 2013;18:406-13.

Fallon JB, Irvine DR, Shepherd RK Cochlear implants and brain plasticity. Hear Res. 2008;238:110-7.

Ferrary E, Bernard C, Teixeira M, Julien N, Bismuth P, Sterkers O, Amiel C. Hormonal modulation of inner ear fluids. Acta Otolaryngol. 1996;116:244-7

Finley CC, Holden TA, Holden LK, Whiting BR, Chole RA, Neely GJ, Hullar TE, Skinner MW. Role of electrode placement as a contributor to variability in cochlear implant outcomes. Otol Neurotol, 2008;29:920-8.

Franke-Trieger A, Jolly C, Darbinjan A, Zahnert T, Mürbe D. Insertion depth angles of cochlear implant arrays with varying length: a temporal bone study. Otol Neurotol, 2014;35:58-63.

Friedland DR, Venick HS, Niparko JK. Choice of ear for cochlear implantation: the effect of history and residual hearing on predicted postoperative performance. Otol Neurotol. 2003;24:582-9

Friedmann DR, Ahmed OH, McMenomey SO, Shapiro WH, Waltzman SB, Roland JT Jr. Single-sided Deafness Cochlear Implantation: Candidacy, Evaluation, and Outcomes in Children and Adults. Otol Neurotol. 2016;37:154-60.

Gantz BJ, Turner C, Gfeller KE. Acoustic plus electric speech processing: preliminary results of a multicenter clinical trial of the Iowa/Nucleus Hybrid implant. Audiol Neurootol 2006;11(Suppl 1):63-8.

Gaylor JM, Raman G, Chung M, Lee J, Rao M, Lau J, Poe DS.Cochlear implantation in adults: a systematic review and meta-analysis. JAMA Otolaryngol Head Neck Surg. 2013;139:265-72

Gourévitch B, Edeline JM, Occelli F, Eggermont JJ. Is the din really harmless? Long-term effects of non-traumatic noise on the adult auditory system. Nat Rev Neurosci. 2014;15:483-91

Gourévitch B, Edeline JM. Age-related changes in the guinea pig auditory cortex: relationship with brainstem changes and comparison with tone-induced hearing loss. Eur J Neurosci. 2011;34:1953-65.

Grantham DW, Ashmead DH, Ricketts TA Labadie RF, Haynes DS. Horizontal-plane localization of noise and speech signals by postlingually deafened adults fitted with bilateral cochlear implants. Ear Hear 2007;28:524-41.

Güldner C, Wiegand S, Weiss R, Bien S, Sesterhenn A, Teymoortash A, Diogo I. Artifacts of the electrode in cochlea implantation and limits in analysis of deep insertion in cone beam tomography (CBT). Eur Arch Otorhinolaryngol. 2012;269:767-72.

Gupta R, Bartling SH, Basu SK, Ross WR, Becker H, Pfoh A, Brady T, Curtin HD. Experimental flat-panel high-spatialresolution volume CT of the temporal bone. AJNR Am J Neuroradiol 2004;25:1417–24

Helbig S, Settevendemie C, Mack M, Baumann U, Helbig M, Stöver T. Evaluation of an electrode prototype for atraumatic cochlear implantation in hearing preservation candidates: preliminary results from a temporal bone study. Otol Neurotol. 2011;32:419-23

Henderson D, Hamernik RP. Biologic bases of noise-induced hearing loss. Occup Med. 1995;10:513-34.

Hodez C, Griffaton-Taillandier C, Bensimon I. Cone-beam imaging: applications in ENT. Eur Ann Otorhinolaryngol Head Neck Dis. 2011;128:65-78

Holden LK, Finley CC, Firszt JB, Holden TA, Brenner C, Potts LG, Gotter BD, Vanderhoof SS, Mispagel K, Heydebrand G, Skinner MW. Factors affecting open-set word recognition in adults with cochlear implants. Ear Hear 2013;34:342-60

Holm S. A simple sequentially rejective multiple test procedure. Scand J Stat 1979;6: 65–70.

House, WF, Berliner, KB, Crary, WG, Graham, M, Luckey, R, Norton, N, Selters, W, Tobin, H, Urban, J, Wexler, M. Cochlear implants. Ann. Otol. Rhinol. Laryngol. 1976;85:1-93.

House, WF, Urban, J Long term results of electrode implantation and electronic stimulation of the cochlea in man. Ann. Otol. Rhinol. Laryngol 1973;82:504-517.

Hudspeth AJ. How the ear's works work. Nature 1989;341:397–404.

Hunter JB, Gifford RH, Wanna GB, Labadie RF, Bennett ML, Haynes DS, Rivas A.Hearing Preservation Outcomes With a Mid-Scala Electrode in Cochlear Implantation. Otol Neurotol. 2016;37:235-40

Husstedt HW, Aschendorff A, Richter B, Laszig R, Schumacher M. Nondestructive three-dimensional analysis of electrode to modiolus proximity. Otol Neurotol 2002;23: 49–52.

Irvine DRF. Auditory cortical plasticity: Does it provide evidence for cognitive processing in the auditory cortex? Hearing Res 2007;229:158–170

Ishii T, Takayama M, Takahashi Y. Mechanical properties of human round window, basilar and Reissner's membranes. Acta Otolaryngol 1995;519:78-82.

Jeyakumar A, Peña SF, Brickman TM.Round window insertion of precurved electrodes is traumatic. Otol Neurotol. 2014;35:52-7.

Johnston JD, Scoffings D, Chung M, Baguley D, Donnelly NP, Axon PR, Gray RF, Tysome JR. Computed Tomography Estimation of Cochlear Duct Length Can Predict Full Insertion in Cochlear Implantation. Otol Neurotol. 2016;37:223-8.

Kennedy DW. Multichannel intracochlear electrodes: mechanism of insertion trauma. Laryngoscope. 1987;97:42-9.

Kerber S and Seeber BU: Sound localization in noise by normal-hearing listeners and cochlear implant users. Ear Hear 2012;33:445-57.

Kobler JP, Beckmann D, Rau TS, Majdani O, Ortmaier T.An automated insertion tool for cochlear implants with integrated force sensing capability. Int J Comput Assist Radiol Surg. 2014;9:481-94.

Kontorinis G, Lenarz T, Stöver T, Paasche G. Impact of the insertion speed of cochlear implant electrodes on the insertion forces. Otol Neurotol. 2011;32:565-70. a

Kontorinis G, Paasche G, Lenarz T, Stover T. The effect of different lubricants on cochlear implant electrode insertion forces. Otol Neurotol, 2011; 32:1050–1056. b

Kronenberg J, Migirov L, Dagan T. Suprameatal approach: new surgical approach for cochlear implantation. J Laryngol Otol. 2001;115:283-5.

Kurzweg T, Dalchow CV, Bremke M, Majdani O, Kureck I, Knecht R, Werner JA, Teymoortash A The value of digital volume tomography in assessing the position of cochlear implant arrays in temporal bone specimens. Ear Hear. 2010;31:413-9

Lane JI, Driscoll CL, Witte RJ, Primak A, Lindell EP. Scalar localization of the electrode array after cochlear implantation: a cadaveric validation study comparing 64-slice multidetector computed tomography with microcomputed tomography. Otol Neurotol. 2007;28:191-4.

Lazard DS, Vincent C, Venail F, Van de Heyning P, Truy E, Sterkers O, Skarzynski PH, Skarzynski H, Schauwers K, O'Leary S, Mawman D, Maat B, Kleine-Punte A, Huber AM, Green K, Govaerts PJ, Fraysse B, Dowell R, Dillier N, Burke E, Beynon A, Bergeron F, Başkent D, Artières F, Blamey PJ. Pre-, per- and postoperative factors affecting performance of postlinguistically deaf adults using cochlear implants: a new conceptual model over time PLoS One. 2012;7:e48739

Lecerf P, Bakhos D, Cottier JP, Lescanne E, Trijolet JP, Robier A.Midmodiolar reconstruction as a valuable tool to determine the exact position of the cochlear implant electrode array. Otol Neurotol. 2011;32:1075-81.

Lee HJ, Giraud AL, Kang E, Oh SH, Kang H, Kim CS, Lee DS. Cortical activity at rest predicts cochlear implantation outcome. Cereb Cortex 2007;17:909–917

Lee J, Nadol JB Jr, Eddington DK. Depth of electrode insertion and postoperative performance in humans with cochlear implants: a histopathologic study. Audiol Neurootol, 2010;15:323-31.

Lee J, Nadol JB Jr, Eddington DK. Factors associated with incomplete insertion of electrodes in cochlear implant surgery: a histopathologic study. Audiol Neurootol 2011;16:69-81

Lehnhardt E. Intracochlear placement of cochlear implant electrodes in soft surgery technique. HNO. 1993;41:356-9.

Lenarz M, Sönmez H, Joseph G, Büchner A, Lenarz T. Long-term performance of cochlear implants in postlingually deafened adults. Otolaryngol Head Neck Surg 2012;147:112-8.

Lenarz T, James C, Cuda D, Fitzgerald O'Connor A, Frachet B, Frijns JH, Klenzner T, Laszig R, Manrique M, Marx M, Merkus P, Mylanus EA, Offeciers E, Pesch J, Ramos-Macias A, Robier A, Sterkers O, Uziel A. European multi-centre study of the Nucleus Hybrid L24 cochlear implant. Int J Audiol. 2013;52:838-48.

Lenarz T, Stover T, Buechner A, Paasche G, Briggs R, Risi F, Pesch J, Battmer RD.Temporal bone results and hearing preservation with a new straight electrode. Audiol Neurootol. 2006;11 Suppl 1:34-41.

Li PM, Wang H, Northrop C, Merchant SN, Nadol JB Jr. Anatomy of the round window and hook region of the cochlea with implications for cochlear implantation and other endocochlear surgical procedures. Otol Neurotol. 2007;28:641-8

Litovsky RY, Parkinson A, Arcaroli J, Sammeth C. Simultaneous bilateral cochlear implantation in adults: a multicenter clinical study. Ear Hear 2006;27:714–731.

Litovsky RY, Parkinson A, Arcaroli J. Spatial hearing and speech intelligibility in bilateral cochlear implant users. Ear Hear 2009; 30:419-31.

Magnusson L. Comparison of the fine structure processing (FSP) strategy and the CIS strategy used in the MED-EL cochlear implant system: Speech intelligibility and music sound quality. Int J Audiol. 2011;50:279-87.

Majdani O, Schurzig D, Hussong A, Rau T, Wittkopf J, Lenarz T, Labadie RF. Force measurement of insertion of cochlear implant electrode arrays in vitro: comparison of surgeon to automated insertion tool. Acta Otolaryngol. 2010;130:31-6.

Mangado N, Ceresa M, Duchateau N, Kjer HM, Vera S, Dejea Velardo H, Mistrik P, Paulsen RR, Fagertun J, Noailly J, Piella G, González Ballester MÁ. Automatic Model Generation Framework for Computational Simulation of Cochlear Implantation. Ann Biomed Eng. 2015 Dec 29. [Epub ahead of print]

Manzoor NF, Wick CC, Wahba M, Gupta A, Piper R, Murray GS, Otteson T, Megerian CA, Semaan MT.Bilateral Sequential Cochlear Implantation in Patients With Enlarged Vestibular Aqueduct (EVA) Syndrome. Otol Neurotol. 2016;37:96-103

Martinez-Monedero R, Niparko JK, Aygun N. Cochlear coiling pattern and orientation differences in cochlear implant candidates. Otol Neurotol. 2011;32:1086-93.

Martins Gde S, Brito Neto RV, Tsuji RK, Gebrim EM, Bento RF. Evaluation of Intracochlear Trauma Caused by Insertion of Cochlear Implant Electrode Arrays through Different Quadrants of the Round Window. Biomed Res Int. 2015;2015:236364.

Marx M, Risi F, Escudé B, Durmo I, James C, Lauwers F, Deguine O, Fraysse B. Reliability of cone beam computed tomography in scalar localization of the electrode array: a radio histological study. Eur Arch Otorhinolaryngol. 2014;271:673-9.

Mertens G, De Bodt M, Van de Heyning P.Cochlear implantation as a long-term treatment for ipsilateral incapacitating tinnitus in subjects with unilateral hearing loss up to 10 years. Hear Res. 2016;331:1-6.

Mick P, Amoodi H, Shipp D, Friesen L, Symons S, Lin V, Nedzelski J, Chen J. Hearing preservation with full insertion of the FLEXsoft electrode. Otol Neurotol. 2014;35:e40-4.

Miracle AC, Mukherji SK. Conebeam CT of the head and neck, part 1: physical principles. AJNR Am J Neuroradiol. 2009;30:1088-95

Miroir M, Nguyen Y, Kazmitcheff G, Ferrary E, Sterkers O, Grayeli AB. Friction force measurement during cochlear implant insertion: application to a force-controlled insertion tool design. Otol Neurotol. 2012;33:1092-100.

Møller AR. Frequency selectivity of single auditory nerve fibers in response to broadband noise stimuli. J Acoust Soc Am 1977;62:135–142,

Moore DR. Anatomy and physiology of binaural hearing. Audiology. 1991;30:125-34.

Mori MC, & Chang KW . CT analysis demonstrates that cochlear height does not change with age. AJNR Am J Neuroradiol, 2012;33:119-23.

Mosnier I, Sterkers O, Bebear JP, Godey B, Robier A, Deguine O, Fraysse B, Bordure P, Mondain M, Bouccara D, Bozorg-Grayeli A, Borel S, Ambert-Dahan E, Ferrary E: Speech performance and sound localization in a complex noisy environment in bilaterally implanted adult patients. Audiol Neurootol. 2009;14:106-14.

Mukherjee P, Uzun-Coruhlu H, Wong CC, Curthoys IS, Jones AS, Gibson WP Assessment of intracochlear trauma caused by the insertion of a new straight research array. Cochlear Implants Int. 2012;13:156-62.

Müller J, Brill S, Hagen R, Moeltner A, Brockmeier SJ, Stark T, Helbig S, Maurer J, Zahnert T, Zierhofer C, Nopp P, Anderson I. Clinical trial results with the MED-EL fine structure processing coding strategy in experienced cochlear implant users. ORL J Otorhinolaryngol Relat Spec. 2012;74:185-98.

Müller J, Schön F, Helms J: Speech understanding in quiet and noise in bilateral users of the MED-EL COMBI 40/40+ cochlear implant system. Ear Hear 2002;23:198-206.

Nguyen Y, Bernardeschi D, Kazmitcheff G, Miroir M, Vauchel T, Ferrary E, Sterkers O.Effect of embedded dexamethasone in cochlear implant array on insertion forces in an artificial model of scala tympani. Otol Neurotol. 2015;36:354-8

Nguyen Y, Kazmitcheff G, De Seta D, Miroir M, Ferrary E, Sterkers O. Definition of metrics to evaluate cochlear array insertion forces performed with forceps, insertion tool, or motorized tool in temporal bone specimens. Biomed Res Int. 2014;2014:532570.

Nguyen Y, Miroir M, Kazmitcheff G, Sutter J, Bensidhoum M, Ferrary E, Sterkers O, Bozorg Grayeli A.Cochlear implant insertion forces in microdissected human cochlea to evaluate a prototype array. Audiol Neurootol. 2012;17:290-8.

Nguyen Y, Mosnier I, Borel S, Ambert-Dahan E, Bouccara D, Bozorg-Grayeli A, Ferrary E, Sterkers O. Evolution of electrode array diameter for hearing preservation in cochlear implantation. Acta Otolaryngol. 2013;133:116-22.

Noble JH, Labadie RF, Majdani O, Dawant BM. Automatic segmentation of intracochlear anatomy in conventional CT. IEEE Trans Biomed Eng. 2011;58:2625-32

Pelliccia P, Venail F, Bonafé A, Makeieff M, Iannetti G, Bartolomeo M, Mondain M. Cochlea size variability and implications in clinical practice. Acta Otorhinolaryngol Ital. 2014;34:42-9.

Peters BR, Litovsky R, Parkinson A, Lake J Importance of age and postimplantation experience on speech perception measures in children with sequential bilateral cochlear implants.Otol Neurotol. 2007;28:649-57.

Purcell D, Johnson J, Fischbein N, Lalwani AK. Establishment of normative cochlear and vestibular measurements to aid in the diagnosis of inner ear malformations. Otolaryngol Head Neck Surg, 2003;128:78-87.

R Core Team: R: A language and environment for statistical computing. R Foundation for Statistical Computing. Vienna, Austria; 2015. http://www.R-project.org/.

Raphael Y, Altschuler RA. Structure and innervation of the cochlea. Brain Res Bull. 2003;60:397-422.

Rask-Andersen H, Liu W, Erixon E, Kinnefors A, Pfaller K, Schrott-Fischer A, Glueckert R. Human cochlea: anatomical characteristics and their relevance for cochlear implantation. Anat Rec (Hoboken). 2012;295:1791-811.

Rayess HM, Weng C, Murray GS, Megerian CA, Semaan MT. Predictive factors and outcomes of cochlear implantation in patients with connexin 26 mutation: a comparative study. Am J Otolaryngol. 2015;36:7-12.

Rebscher SJ, Hetherington A, Bonham B, Wardrop P, Whinney D and Leake PA Considerations for the design of future cochlear implant electrode arrays: Electrode array stiffness, size and depth of insertion J Rehabil Res Dev. 2008;45: 731–748.

Reiss LA, Turner CW, Karsten SA, Gantz BJ Plasticity in human pitch perception induced by tonotopically mismatched electro-acoustic stimulation. Neuroscience. 2014;3;256:43-52.

Rhode WS. J Acoust Soc Am. 1980;67:1696-703. Cochlear partition vibration--recent views.

Ricketts TA, Grantham DW, Ashmead DH Haynes DS, Labadie RF: Speech recognition for unilateral and bilateral cochlear implant modes in the presence of uncorrelated noise sources. Ear Hear 2006;27:763-73.

Riss D, Hamzavi JS, Blineder M, Honeder C, Ehrenreich I, Kaider A, Baumgartner WD, Gstoettner W, Arnoldner C FS4, FS4-p, and FSP: a 4-month crossover study of 3 fine structure sound-coding strategies. Ear Hear. 2014;35:e272-81

Riss D, Hamzavi JS, Selberherr A, Kaider A, Blineder M, Starlinger V, Gstoettner W, Arnoldner C.Envelope versus fine structure speech coding strategy: a crossover study. Otol Neurotol. 2011;32:1094-101.

Rohani P, Pile J, Kahrs LA, Balachandran R, Blachon GS, Simaan N, Labadie RF. Forces and trauma associated with minimally invasive image-guided cochlear implantation. Otolaryngol Head Neck Surg. 2014;150:638-45.

Roland JT Jr, Gantz BJ, Waltzman SB, Parkinson AJ. Multicenter Clinical Trial Group. United States multicenter clinical trial of the cochlear nucleus hybrid implant system. Laryngoscope. 2016;126:175-81.

Roland JT Jr. A model for cochlear implant electrode insertion and force evaluation: results with a new electrode design and insertion technique. Laryngoscope. 2005;115:1325-39.

Ruivo J, Mermuys K, Bacher K, Kuhweide R, Offeciers E, Casselman JW. Cone beam computed tomography, a low-dose imaging technique in the postoperative assessment of cochlear implantation. Otol Neurotol. 2009;30:299-303

Sachs MB and Young ED. Encoding of steady-state vowels in the auditory nerve: Representation in terms of discharge rate. J Acoust Soc Am 66: 470–479, 1979.

Saeed SR, Selvadurai D, Beale T, Biggs N, Murray B, Gibson P, Risi F, Boyd P The use of cone-beam computed tomography to determine cochlear implant electrode position in human temporal bones. Otol Neurotol. 2014;35:1338-44.

Salvi RJ, Wang J, Ding D. Auditory plasticity and hyperactivity following cochlear damage. Hear Res. 2000;147:261-74.

Schulze R, Heil U, Gross D, Bruellmann DD, Dranischnikow E, Schwanecke U, Schoemer E.Artefacts in CBCT: a review. Dentomaxillofac Radiol. 2011;40:265-73

Schuster D, Kratchman LB, Labadie RF.Characterization of intracochlear rupture forces in fresh human cadaveric cochleae. Otol Neurotol. 2015;36:657-61

Shepherd RK, Hatsushika S, Clark GM. Electrical stimulation of the auditory nerve: the effect of electrode position on neural excitation. Hear Res. 1993;66:108-20

Singla A, Sahni D, Gupta AK Aggarwal A, Gupta T. Surgical Anatomy of the Basal Turn of the Human Cochlea as Pertaining to Cochlear Implantation. Otol Neurotol. 2015;36:323-8

Skarzynski H, Lorens A, Matusiak M, Porowski M, Skarzynski PH, James CJ. Cochlear Implantation With the Nucleus Slim Straight Electrode in Subjects With Residual Low-Frequency Hearing. 2014;35:e33-43.

Skarzynski H, Lorens A, Matusiak M, Porowski M, Skarzynski PH, James CJ. Partial deafness treatment with the nucleus straight research array cochlear implant. Audiol Neurootol. 2012;17:82-91

Skinner MW, Holden TA, Whiting BR, Voie AH, Brunsden B, Neely JG, Saxon EA, Hullar TE, Finley CC. In vivo estimates of the position of advanced bionics electrode arrays in the human cochlea. Ann Otol Rhinol Laryngol Suppl. 2007;197:2-24.

Sparreboom M, van Schoonhoven J, van Zanten BG, Scholten RJ, Mylanus EA, Grolman W, Maat B.The effectiveness of bilateral cochlear implants for severe-to-profound deafness in children: a systematic review. Otol Neurotol. 2010;31:1062-71.

Sterkers O, Ferrary E, Amiel C. Production of inner ear fluids. Physiol Rev 1988;68:1083–1128

Tamir S, Ferrary E, Borel S, Sterkers O, Bozorg Grayeli A Hearing preservation after cochlear implantation using deeply inserted flex atraumatic electrode arrays. Audiol Neurootol. 2012;17:331-7.

Todd CA and Naghdy F. Real-time Modeling and Simulation for Cochlear Implantation; Visualization and Force Rendering during Virtual Prosthetic Insertions. Int J Modeling and Optimization. 2012;2:518-523.

Torres R, Kazmitcheff G, Bernardeschi D, De Seta D, Bensimon JL, Ferrary E, Sterkers O, Nguyen Y. Variability of the mental representation of the cochlear anatomy during cochlear implantation Eur Arch Otorhinolaryngol. 2015 Sep 1. DOI 10.1007/s00405-015-3763-x

Trieger A, Schulze A, Schneider M, Zahnert T, Mürbe D. In vivo measurements of the insertion depth of cochlear implant arrays using flat-panel volume computed tomography. Otol Neurotol. 2011;32:152-7.

Tyler RS, Dunn CC, Witt SA Noble WG. Speech perception and localization with adults with bilateral sequential cochlear implants. Ear Hear 2007;28:86S-90S.

van der Marel KS, Briaire JJ, Wolterbeek R. Diversity in cochlear morphology and its influence on cochlear implant electrode position. Ear Hear, 2014;35:9-20.

van Schoonhoven J, Sparreboom M, van Zanten BG, Scholten RJ, Mylanus EA, Dreschler WA, Grolman W, Maat B. The effectiveness of bilateral cochlear implants for severe-to-profound deafness in adults: a systematic review. Otol Neurotol. 2013;34:190-8

Verbist BM, Ferrarini L, Briaire JJ, Zarowski A, Admiraal-Behloul F, Olofsen H, Reiber JH, Frijns JH.Anatomic considerations of cochlear morphology and its implications for insertion trauma in cochlear implant surgery. Otol Neurotol. 2009;30:471-7.

Verbist BM, Skinner MW, Cohen LT, Leake PA, James C, Boëx C, Holden TA, Finley CC, Roland PS, Roland JT Jr, Haller M, Patrick JF, Jolly CN, Faltys MA, Briaire JJ, Frijns JH Consensus panel on a cochlear coordinate system applicable in histologic, physiologic, and radiologic studies of the human cochlea. Otol Neurotol. 2010;31:722-30.

Viccaro M, Covelli E, De Seta E, Balsamo G, Filipo R. The importance of intra-operative imaging during cochlear implant surgery. Cochlear Implants Int. 2009;10:198-202.

von Békésy G. Travelling waves as frequency analysers in the cochlea. Nature 1970:28:1207-9

Waltzman SB and Roland JT Jr. Cochlear Implant Candidates in Cochlear Implants. ThiermeMedical Publishers, New York, NY, USA, 2006

Wanna GB, Noble JH, Carlson ML, Gifford RH, Dietrich MS, Haynes DS, Dawant BM, Labadie RF. Impact of electrode design and surgical approach on scalar location and cochlear implant outcomes. Laryngoscope. 2014;124 Suppl 6:S1-7

Wanna GB, Noble JH, Gifford RH, Dietrich MS, Sweeney AD, Zhang D, Dawant BM, Rivas A, Labadie RF. Impact of Intrascalar Electrode Location, Electrode Type, and Angular Insertion Depth on Residual Hearing in Cochlear Implant Patients: Preliminary Results. Otol Neurotol. 2015;36:1343-8.

Wanna GB, Noble JH, McRackan TR, Dawant BM, Dietrich MS, Watkins LD, Rivas A, Schuman TA, Labadie RF. Assessment of electrode placement and audiological outcomes in bilateral cochlear implantation. Otol Neurotol. 2011;32:428-32.

Wardrop P, Whinney D, Rebscher SJ, Luxford W, Leake P. A temporal bone study of insertion trauma and intracochlear position of cochlear implant electrodes. II: Comparison of Spiral Clarion and HiFocus II electrodes. Hear Res. 2005;203:68-79. (b)

Wardrop P, Whinney D, Rebscher SJ, Roland JT Jr, Luxford W, Leake PA. A temporal bone study of insertion trauma and intracochlear position of cochlear implant electrodes. I: Comparison of Nucleus banded and Nucleus Contour electrodes. Hear Res. 2005;203:54-67. (a)

Welling DB, Hinojosa R, Gantz BJ, Lee JT Insertional trauma of multichannel cochlear implants. Laryngoscope. 1993;103:995-1001.

Wouters J, McDermott HJ, Francart T. Sound coding in cochlear implants: from electric pulses to hearing. IEEE Signal Processing Magazine 2015;32:67-80

Xu J, Xu SA, Cohen LT, Clark GM. Cochlear view: postoperative radiography for cochlear implantation. Am J Otol. 2000;21:49-56.

Young ED and Sachs MB. Representation of steady-state vowels in the temporal aspects of the discharge patterns of populations of auditory nerve fibers. J Acoust Soc Am 1979;66:1381–1403,.

Yuan YY, Song YS, Chai CM, Shen WD, Han WJ, Liu J, Wang GJ, Dong TX, Han DY, Dai P. Intraoperative CT-guided cochlear implantation in congenital ear deformity. Acta Otolaryngol 2012;132:951-958

Yukawa K, Cohen L, Blamey P, Pyman B, Tungvachirakul V, O'Leary S. Effects of insertion depth of cochlear implant electrodes upon speech perception. Audiol Neurootol, 2004;9:163–172

Zhang J, Wei W, Ding J, Roland JT Jr, Manolidis S, Simaan N. In roads toward robot-assisted cochlear implant surgery using steerable electrode arrays. Otol Neurotol. 2010;31:1199-206

ANNEX 1

Presented by Daniele De Seta: Poster at ARO Midwinter Meeting. February 24-26 2016, San Diego CA, USA
Podium presentation at the Congress of the French Society of Otolaryngology October 10-12 2015, Paris
Podium presentation at 14th International Conference on Cochlear Implants May 11-14, 2016, Toronto, Canada

Influence of Cochlear Array Design on Insertion Forces among 28 Surgeons of Various Experiences in a Synthetic Model of Scala Tympani.

Yann Nguyen [1,2,3]; Guillaume Kazmitcheff [1,2,3]; Renato Torres1,2,3; Daniele De Seta [1,2,3,4]; Elisabeth Mamelle [1,2,3]; Evelyne Ferrary [1,2,3]; Olivier Sterkers [1,2,3]; Daniele Bernardeschi [1,2,3]

1 Hospital Pitié Salpêtrière; 2 Sorbonne University, UPMC Univ Paris 06, UMR S 1159; 3 INSERM, UMR S 1163; 4 Sapienza University of Rome

Research Background

It has been shown that array design could influence insertion forces of cochlear implants (CI) when array comparison is performed with reproducible motorized insertion tools. Manual insertion is subject to intra- and interindividual variations thus affecting the results of an improved array design. The goal of the study was to compare two array designs among a large group of surgeons with various experiences.

Material and methods

Twenty eight surgeons with various experiences (no experience in CI to 300 surgeries achieved) were enrolled in the study during two instructions course for CI. An artificial model of scala tympani was mounted on a 6-axis force sensor in order to measure insertion forces. After a training session, participants were asked to insert Hi-Focus 1J (lateral wall array, 1J) and Hi-Focus Mid-Scala (pre-curved array design with stylet, MS) arrays (Advanced Bionics, Valencia, USA) (Fig 1).

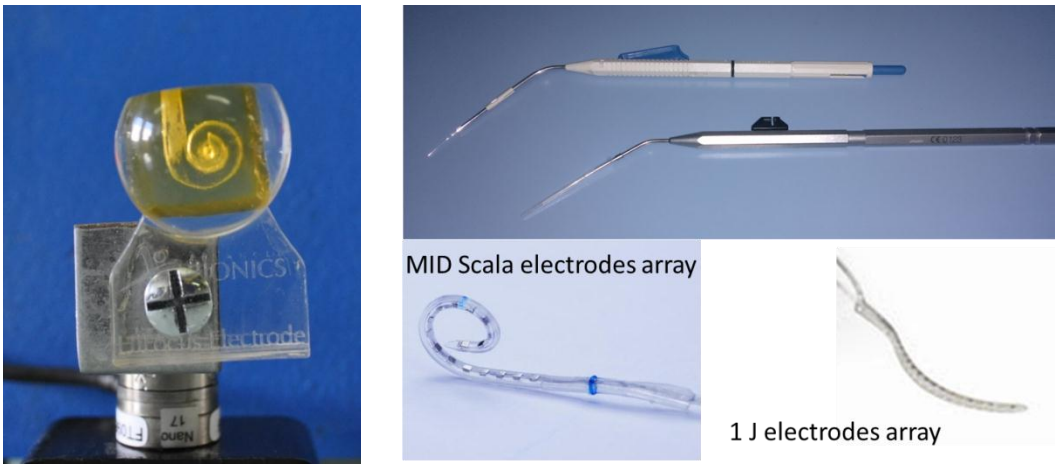

Fig 1 the artificial scala tympani model and the two different arrays with the respectives insertion tools

The following metrics were used to compare, (Student paired test p-value One side) the insertions force profiles: peak of force applied during the insertion (in N), the total change in momentum , number of occurrence where the applied forces were over 0.1 N, number of time where forces were increased by 50% during 0.1 s (sudden rise), and smoothness of the curve, studied as 'jerk' variation (in N.s-1) (Fig 2).

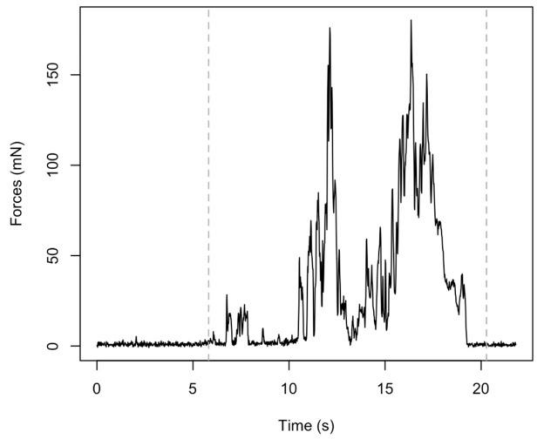

Figure 2 Example of insertion forces profile of 1J electrodes array

Results

A better result has been observed for MS array compared to 1J array for 24/28 surgeons for the peak of force (0.30+/- 0.191N vs 0.15+/-0.181N ; 1J vs MS; $p<0.001$, mean gain 42%), for 24/28 surgeons for the total change in momentum (1.03+/- 0.802Ns vs 0.54+/-1.086Ns, 1J vs MS; $p<0.001$; mean gain 40%). The number of occurrence where the applied forces were over 0.1 N was reduced for 26/28 surgeons (3+/-2.7 vs 1+/-1.6 times; 1J vs MS; $p<0.001$; mean gain 61%) The number sudden rises was improved for 21/28 surgeons (21+/-14.7 vs 13+/-16.0 times, 1J vs MS; $p<0.001$ mean gain de 11%). The'jerk' variation was improved for 22/28 surgeons (0.19+/- 0.134 vs 0.11+/-0.096 N.s -1; 1J vs MS; $p<0.01$ mean gain 33% (Fig 3).

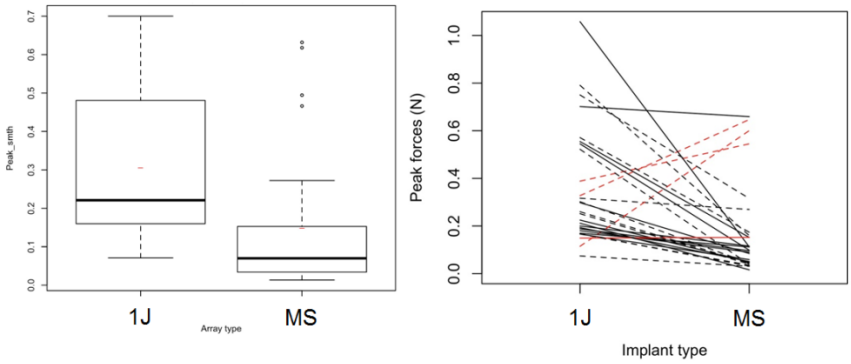

Figure 2 Peak force was decreased by 42% with the midscala array (MS). Individual representation of surgeons results for peak forces with the two devices (n=28) are represented in the right panel

Conclusion

This study shows that a reduced diameter and the use of a guiding stylet with automated retraction in a pre-curved array can lead to an improvement of force profiles among a group of surgeons with various experiences

Hindawi Publishing Corporation
BioMed Research International
Volume 2014, Article ID 532570, 9 pages
http://dx.doi.org/10.1155/2014/532570

ANNEX 2

Research Article

Definition of Metrics to Evaluate Cochlear Array Insertion Forces Performed with Forceps, Insertion Tool, or Motorized Tool in Temporal Bone Specimens

Yann Nguyen,[1,2,3] Guillaume Kazmitcheff,[2,3] Daniele De Seta,[2,3,4] Mathieu Miroir,[2,3] Evelyne Ferrary,[1,2,3] and Olivier Sterkers[1,2,3]

[1] *Otolaryngology Department, Unit of Otology, Auditory Implants and Skull Base Surgery, Hospital Pitié Salpêtrière, 47-83 Boulevard de l'Hôpital, Cedex 13, 75651 Paris, France*
[2] *Sorbonne University, "Minimally Invasive Robot-Based Hearing Rehabilitation", UPMC Univ Paris 06, UMR S 1159, 75005 Paris, France*
[3] *INSERM, "Minimally Invasive Robot-Based Hearing Rehabilitation", UMR S 1159, 75018 Paris, France*
[4] *Sensory Organs Department, Sapienza University of Rome, 00100 Rome, Italy*

Correspondence should be addressed to Yann Nguyen; yann.nguyen@inserm.fr

Received 14 February 2014; Accepted 17 June 2014; Published 15 July 2014

Academic Editor: Peter Brett

Introduction. In order to achieve a minimal trauma to the inner ear structures during array insertion, it would be suitable to control insertion forces. The aim of this work was to compare the insertion forces of an array insertion into anatomical specimens with three different insertion techniques: with forceps, with a commercial tool, and with a motorized tool. *Materials and Methods*. Temporal bones have been mounted on a 6-axis force sensor to record insertion forces. Each temporal bone has been inserted, with a lateral wall electrode array, in random order, with each of the 3 techniques. *Results*. Forceps manual and commercial tool insertions generated multiple jerks during whole length insertion related to fits and starts. On the contrary, insertion force with the motorized tool only rose at the end of the insertion. Overall force momentum was 1.16 ± 0.505 N (mean ± SD, $n = 10$), 1.337 ± 0.408 N ($n = 8$), and 1.573 ± 0.764 N ($n = 8$) for manual insertion with forceps and commercial and motorized tools, respectively. *Conclusion*. Considering force momentum, no difference between the three techniques was observed. Nevertheless, a more predictable force profile could be observed with the motorized tool with a smoother rise of insertion forces.

1. Introduction

Cochlear implant is a neural prosthesis that is inserted within the cochlea into the scala tympani in order to electrically stimulate spiral ganglion fibers from the auditory nerve. It has become the most efficient device to rehabilitate patients suffering from severe to profound deafness [1]. Three critical steps can be identified in the cochlear implantation procedure: approach to cochlea, cochlea opening, and array insertion. Minimizing trauma during the cochlear implantation procedure is critical to preserve residual hearing in case of acoustic electric stimulation or remaining inner ear structures in case of electric stimulation only [2]. Even though multiple approaches can be performed to access cochlea such as suprameatal, transcanal, or minimally invasive key-hole access, the routine exposure of the cochlea in a vast majority of cochlear implant centers is mastoidectomy followed by posterior tympanotomy [3]. The cochlea opening through the round window membrane, a cochleostomy, or an extended round window approach remains a current debate frequently discussed [4]. These two first steps determine the axis and the entry point of the array into the cochlea. Considering solutions to reduce trauma during the array insertion, most studies compared array designs [5] and evaluated histological trauma [6] or insertion forces [7]. Even though the insertion technique remains critical for inner ear structure

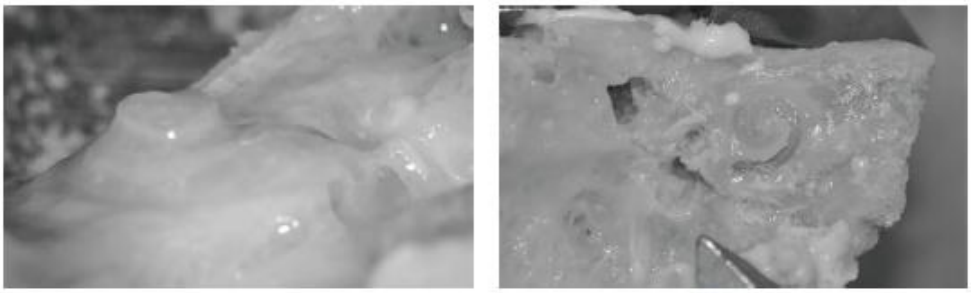

(a) (b)

FIGURE 1: Microdissected cochlea model. (a) A wide canal wall down mastoidectomy is performed to expose the cochlea. The otic capsule is then thinned with a diamond burr (left cochlea). (b) The scalae vestibuli and media are then carefully opened to expose the basilar membrane leaving the scala tympani intact (right cochlea).

preservation to achieve insertion with minimal trauma, it is seldom studied. The insertion technique will be influenced by tremor, insertion speed, and duration and possibilities of insertion axis modification including torque around the array body. It is usually performed manually using forceps, microforceps, or a dedicated tool depending on the array design. Arrays including a stylet can offer various insertion techniques depending on stylet removal timing [8]. Speed of insertion or use of lubricant have also been studied and have been shown to influence frictions forces [9, 10]. Manual insertion with forceps has been compared to robotic insertion [11] but has never been compared to the insertion with other technique with specific tool. Motorization of the tool could also be employed to reduce fits and start inherent to manual insertion as it is hard to insert the array in a single move with forceps grasping. The goal of the present work was to compare cochlear array insertion forces performed by forceps, an insertion tool, or a motorized tool in temporal bone specimens with the same array design.

FIGURE 2: Insertion force measurement setup. A plastic temporal bone holder was screwed on a 6-axis force sensor (ATI Nano 17, Apex, NC) to record array insertion forces into a temporal bone.

2. Material and Methods

2.1. Human Temporal Bone Preparation. Twenty human temporal bones have been prepared. The cochlea has been exposed through a canal wall down mastoidectomy. A large approach has been chosen to ease bony otic capsule drilling and avoid direct contact of the forceps, insertion tool, or motorized tool with the temporal bone. The bony otic capsule has been thinned using diamond burrs under microscope (Figure 1(a)). The scala vestibuli and the scala media have then been carefully opened taking care to respect the basilar membrane integrity from the round window to the apex (Figure 1(b)). This allowed visualization of the array progression during its insertion by transparency through the basilar membrane. This also allowed checking basilar membrane integrity and the lack of scalae translocation during insertion. An extended round window cochleostomy has then been drilled in the inferior rim of the round window. Temporal bones were then mounted on an in-house made temporal bone holder that could be fixed to a force sensor (Figure 2). The temporal bones specimens, fixed on the force sensor, have been oriented to align the array insertion axis, the scala tympani midline, and the D_z axis of the 6-axis force sensor. Cochleostomy was irrigated with saline serum before each insertion.

2.2. Electrode Array. Hifocus 1J arrays (Advanced Bionics, Valencia, CA) have been used in this study. 1J array is a lateral wall positioning array bearing 16 electrodes. A silicon jog is placed at its base in order to push the array with an insertion tool. This jog slides into the insertion tube and serves as the contact point for array propulsion inside the insertion tube by a rod. The array has a total length of 25 mm from the jog to the tip, an active length of 17 mm, a proximal diameter of 0.8 mm, and a distal diameter of 0.4 mm. Each array was used for two insertions and then discarded.

2.3. Insertion Protocol and Insertion Force Measurements. Frictions forces between the array and the cochlea have been recorded with a 6-axis force sensor (ATI Nano 17, calibration type SI-12-0.12, resolution: 3 mN, Apex, NC). Sensor data have been recorded in real-time via the same analog to digital interface card controlling the actuator input power at

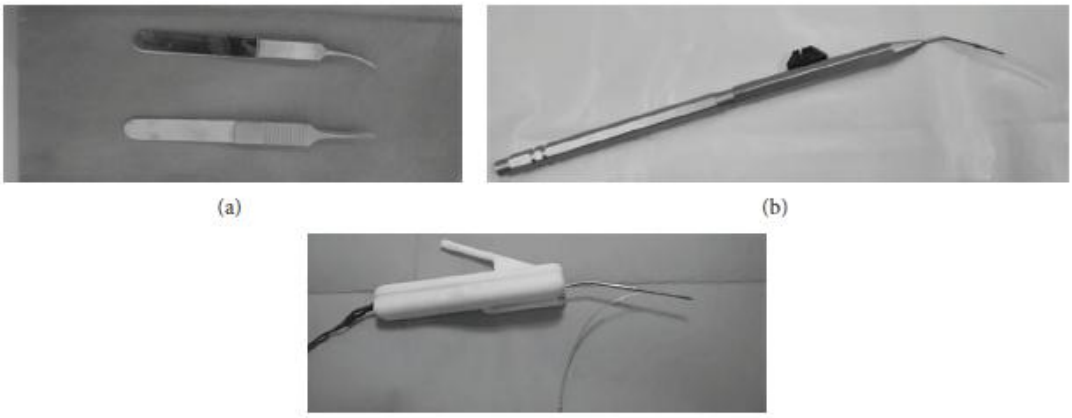

FIGURE 3: Tools and devices used in this study to insert array on temporal bones. (a) Microforceps claws, (b) Hifocus 1J tool (Advanced Bionincs, Valencia, USA), and (c) insertion with an in-house motorized tool.

a sample rate of 100 Hz. From the 6-axis sensor, insertion forces were computed only based on linear force norms (D_x, D_y, D_z).

Three insertion tools and techniques were randomly tested:

(i) manual insertion using two microforceps claws (Figure 3(a));

(ii) insertion with the Hifocus 1J electrode insertion tool (Figure 3(b)), a commercially available tool distributed with Hifocus 1J and helix array; it is composed of a handle comprising a flexible shaft connected to a slide that can eject out of an insertion tube the array by pushing its silicon jog. We have been using the metal insertion tube (AB-6135, Advanced bionics, Valencia, CA) in this study. This tool was held manually during insertion;

(iii) insertion with an in-house made motorized insertion tool (Figure 3(c)). This tool comprised a rotary actuator (RE10CLL, MDP, Miribel, France) connected to a threaded screw that pushed a blunt pin into an insertion tube loading the array. The tool was held steady by a flexible arm. No force feedback loop between this tool and the force sensor was applied. The actuator speed was controlled via laboratory power supply and set at 0.8 mm·s^{-1}.

During each insertion, a particular attention was made to avoid touching directly the temporal bone with forceps or insertions tools in order to avoid artefact recording of the force sensor. For the manual and commercial tool techniques, the operator's hands were supported on a flexible arm with a metal bar similarly to a Yasargil bar as it has been shown that supporting the wrists significantly decreases the amplitude of the tremor [12]. Force measurement was coupled to video recording through the microscope to collect force data from the beginning to the end of the insertion only.

Each temporal bone was inserted three times with the three different insertions techniques in an order that was randomized. If a basilar membrane perforation occurred during insertion, the temporal bone was excluded for analysis.

2.4. Metrics Analysis. We investigated the shape of the curve corresponding to the force versus the time. In order to do so, we have built different metrics.

(i) The peak of force applied during the insertion: this metric quantifies a potential damage of the cochlea if an excessive force is applied. Thus, the study of the peak of force allows us to identify if an insertion method may guaranty a lower maximal force.

(ii) The total change in momentum (I, in Ns) was produced during the insertion, measured by $I = \int F(t)dt$.

(iii) The number of occurrence (Th) where the applied forces were over an arbitrary threshold, fixed at 0.1 N that may yield to severe damage of anatomical structure within the cochlea: this threshold value corresponds to the peak force at the end of a complete insertion of array in temporal bones from previously published data [7].

(iv) The number of times (G) where forces (F) were increased by 50% (sudden rise) within a small time step $h = t - (t - 1) = 0.1$ s: it corresponded to the number of local discontinuities of the applied forces and possibly to the number of potential local damages into the cochlea. Consider

$$G_t = \begin{cases} G_t - 1 + 1, & \text{if } \dfrac{F_t}{F_t - 1} \geq 2, \\ G_t - 1, & \text{otherwise.} \end{cases} \quad (1)$$

(v) The smoothness of the curve, studied as "jerk" variation (J) (expressed as N·s^{-1}): it is obtained from the derivative of the force over the time. A root mean

square (RMS) function was used to analyze the jerk variation. Consider

$$\text{RMS} = \sqrt{\frac{1}{n}\sum_{i=0}^{n-1} J_i^2}, \quad \text{with } J = \frac{dF}{dt}. \tag{2}$$

2.5. Statistical Analysis. Results are expressed as mean ± standard deviation. Data were analyzed and graphics were generated by "R" statistical software (http://www.r-project.org/). Comparisons between different insertions conditions were tested by ANOVA and results are presented with the associated P value for significant data.

3. Results

3.1. Data Collection. A basilar membrane perforation occurred in 7 temporal bones (35%) out of 20. This occurred once with a forceps insertion, 3 times with the Hifocus 1J electrode insertion tool, and 3 times with the motorized insertion. The translocation rate has to be analyzed with precaution due to model preparation. While giving immediate information during insertion on array translocation, this kind of microdissected model has the drawback of potentially creating histological damages or weakening of the basilar membrane before array insertion [7].

Thus, the implants were inserted three times in the same cochlea in 13 temporal bones (39 insertions). We investigate the possible lesions of the cochlea undergone during the first insertions, in order to determine the presence of a systematic diminution of forces for the second or the third insertions. We found that force peaks of the motorized insertion on third position were significantly different compared to measurement of first and second insertion ($P = 0.0362$). Thus, third insertion could not be used for analysis and all data collected during the third insertion were discarded in all temporal bones. Consequently, insertions forces data were used for analysis in 10 manual insertions, 8 Hifocus 1J electrode insertion tool insertions, and 8 motorized insertions.

3.2. Insertion Force Profiles. Insertion force profiles had a similar shape from one temporal bone to another depending on the insertion technique. With manual forceps insertion technique (Figure 4(a1)), insertion forces remained low in the first half of the insertions with some peaks corresponding to fits and starts when the array was grasped and released multiple times from distal to proximal parts. The amplitude of these peaks rose towards the end of the insertion.

With motorized tool technique, insertion forces remained also low in the first half of the insertion (Figure 4(c1)). It rises slowly afterwards continuously without peak and reached a maximum at the end of the insertion. A plot using force versus angle representing insertions with the motorized tool is represented on Figure 5.

With the Hifocus 1J electrode insertion tool technique (Figure 4(b1)), a mix between the two previously described force profiles was observed with small amplitude peaks distributed along a force profile curve that slowly rises from the second part of the insertion toward the end.

3.3. Metric Analysis. The results from metric analysis are reported in Figure 6 and Table 1. Considering the peak force at the end of the insertion, the Hifocus 1J electrode insertion tool had higher values than techniques with forceps and motorized tool. The momentum was the same for the three techniques. There was less threshold crossing over 0.1 N with the motorized tool compared to Hifocus 1J electrode insertion tool and the forceps manual technique. Sudden rises and jerks happened also less frequently with the motorized tool compared to manual insertion and Hifocus 1J electrode insertion tool (Figures 4(a2), 4(b2), and 4(c2)).

4. Discussion

In this study, we compared cochlear array insertion forces performed manually with forceps, an insertion tool, or a motorized tool in temporal bone specimens with the same array design. We have shown that there was no difference between the three techniques for peak force and total force value. A more predictable insertion force curve with less peak and rises was seen with the motorized tool compared to the two other insertion tools.

4.1. Advantages and Drawbacks of the Three Insertion Techniques. Each of the three techniques has advantages and drawbacks. Manual insertion with forceps is commonly used because it is compatible with most of the clinically available array device, especially straight arrays. One claw forceps is used to push the array while the other is used to guide the insertion axis. Depending on array length and stiffness, full insertion of the array cannot always be performed in single step and may require multiples grasps to insert the whole array, segment after segment. These fits and starts during the insertion procedure might generate multiple short peak forces during insertion as we observed in the present study. Resistance feedback can be perceived once a physiological threshold is reached. The force feedback sensitiveness depends on wearing gloves and is clearly subject to variability between surgeons. Furthermore this technique is subject to human limitation in terms of accuracy and tremor [13].

Insertion with the Hifocus 1J electrode insertion tool is only possible with 1J and Helix arrays because it requires a silicon jog on the array. It offers an increased stability as the insertion tube can be leant on the posterior part of the posterior tympanotomy during array insertion. The tool only requires one hand to function, thus the second hand can be used as a stabilizer to further reduce tremor. Drawbacks are represented by a lack of resistance feedback feeling because friction forces within the tool and insertion tube might interfere with surgeon sensitiveness on friction forces within the cochlea [14]. Furthermore, due to insertion tube diameter, vision of the cochleostomy or round window can be reduced a little compared to a manual forceps technique. At last the stroke of the slide of the tool can require a two-step push

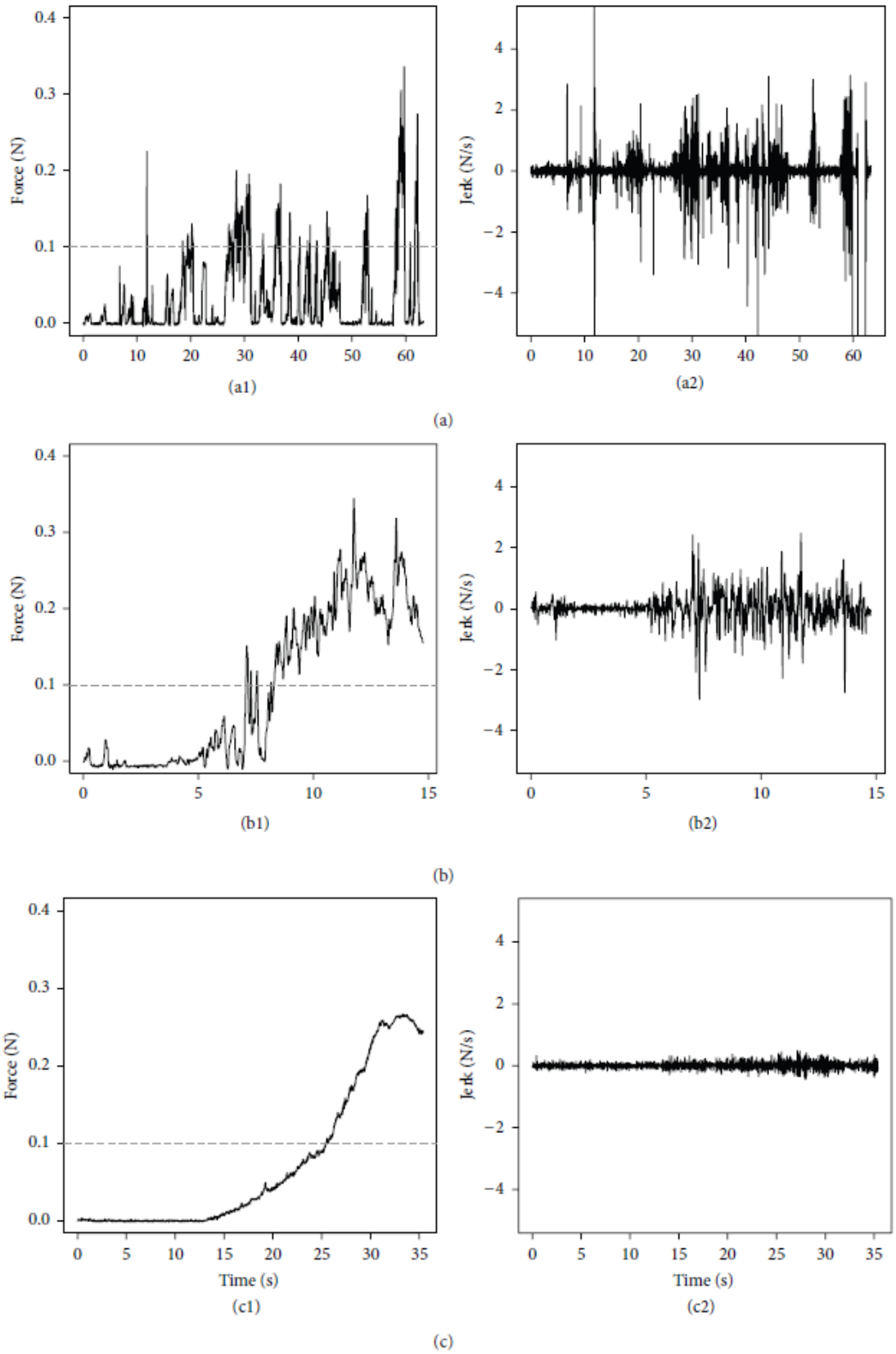

FIGURE 4: Insertion force profile and jerk of a 1J array with 3 different insertion techniques in the same temporal bone. (a) Manual insertion with microforceps claws tool, (b) insertion with Hifocus 1J electrode insertion tool, and (c) insertion with an in-house motorized tool. Left pictures ((a1), (b1), and (c1)): insertion forces profiles. Dashed line represents 0.1 N threshold. Peak forces were around 0.3 N for the three insertion techniques. Right pictures ((a2), (b2), and (c2)): jerk. Hifocus 1J electrode insertion tool provided smoother insertion with little jerk compared to manual insertion with forceps. This benefit is even more increased with a motorized tool.

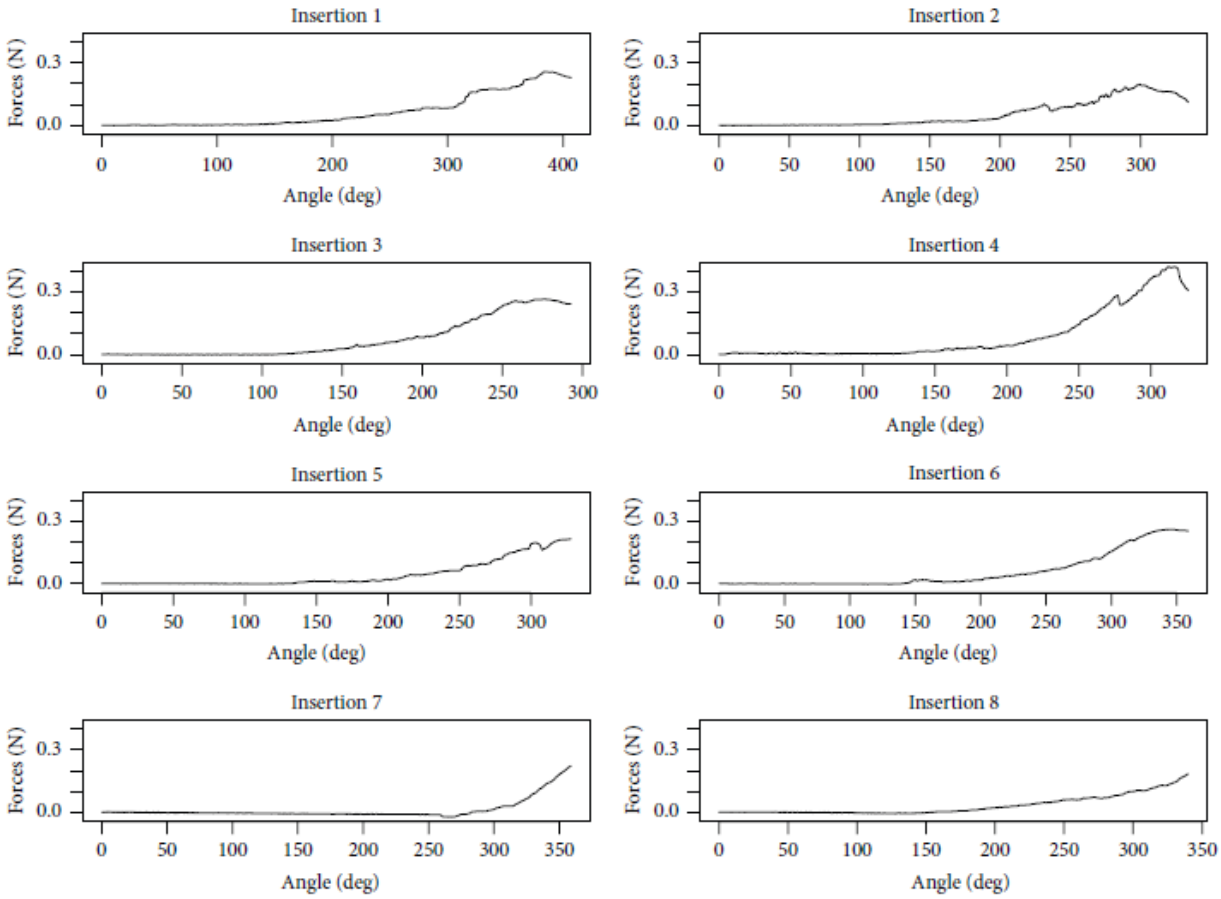

FIGURE 5: Plot using force versus angle representing insertions with the motorized tool. Insertion forces remain low in the first half on the insertion and then slowly rise with no peak and reach a maximum at the end of the insertion.

TABLE 1: Metric values recorded during of the cochlear implantation with three different insertion techniques.

Metric	Insertion technique	Mean ± SD	n	P
Peak (N)	Forceps	0.256 ± 0.061	10	NA
	Hifocus tool	0.327 ± 0.055	8	0.028
	Motorized	0.255 ± 0.075	8	NS
Momentum (Ns)	Forceps	1.16 ± 0.505	10	NA
	Hifocus tool	1.337 ± 0.408	8	NS
	Motorized	1.573 ± 0.764	8	NS
Over threshold >0.1 N	Forceps	21.00 ± 12.552	10	NA
	Hifocus tool	7.00 ± 4.036	8	0.002
	Motorized	3.38 ± 3.113	8	0.0002
Sudden rise	Forceps	90.60 ± 46.569	10	NA
	Hifocus tool	28.25 ± 15.872	8	0.0003
	Motorized	14.00 ± 6.949	8	0.00003
Jerk ($N \cdot s^{-1}$)	Forceps	0.467 ± 0.116	10	NA
	Hifocus tool	0.515 ± 0.206	8	NS
	Motorized	0.1553 ± 0.05	8	0.00008

Values are expressed as mean ± SD of n insertion. NA: not applicable; NS: not significant. "Forceps" stands for manual insertion with forceps technique, "Hifocus tool" stands for Hifocus 1J electrode insertion tool technique, and "motorized" stands for our in-house motorized insertion tool technique. Statistical analysis was performed by analysis of variance. Each technique was compared against the manual insertion with forceps technique.

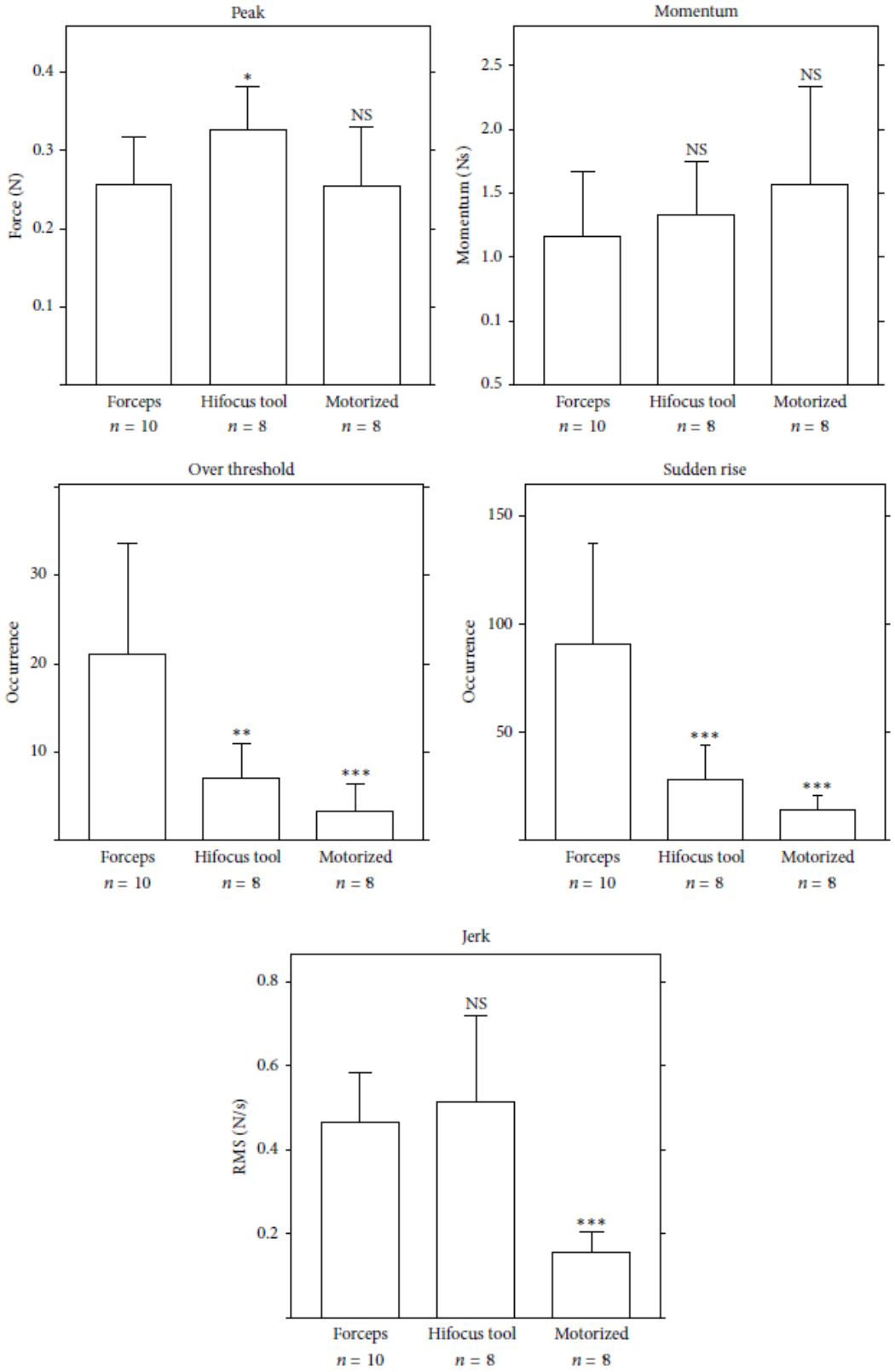

FIGURE 6: Comparison of insertion forces of cochlear implantation with 5 metrics. Bars represent mean ± SD of n insertions. NS: not significant. "Forceps" stands for manual insertion with forceps technique, "Hifocus tool" stands for Hifocus 1J electrode insertion tool technique, and "motorized" stands for our in-house motorized insertion tool technique. Statistical analysis was performed by analysis of variance. Each technique was compared against the manual insertion with forceps technique.

depending on the finger (thumb or forefinger) that is used to push the slide thus generating a fit and start during insertion.

Insertion with our current version of in-house motorized tool is only possible with 1J and helix because it requires a jog on the device to push the array. It provides a smooth and low speed insertion. Complete insertion can be achieved in a single step. Human hand tremor is removed as the tool is held by a flexible arm. However, force feedback is completely impaired and surgeon can only rely on visual control at the cochleostomy to detect a blockage within the cochlea that will lead to array bending at its proximal part outside the cochlea. Vision is also impaired just as with the tool from the second technique.

4.2. Previous Work on Insertion Technique Comparison and Definition of New Metrics to Study Insertion Forces. Majdani et al. had compared robotic to manual insertion with array using an advance off stylet technique in an artificial model of scala tympani [11]. It has been shown that a greater variability of frictions forces could be observed with a manual array insertion technique with more peaks compared to a robot-based insertion technique. The average force was also compared showing increased force for the robotic insertion compared to manual insertions.

We decided to define new metrics to study and compare insertion forces profiles because average force seems hard to interpret. For example manual insertion with a long duration will necessarily have a lower average force since during pauses for the duration of insertion, there is no effort on the cochlea. We could have compared the technique using forces in Newton versus angle or length of insertion. These data are easy to collect with a constant speed insertion such as the motorized tool but hard to collect with manual and Hifocus 1J electrode insertion tool because the array progression cannot be visualized through the basilar membrane as well as a transparent artificial model of scale tympani and the insertion speed during array progression with manual technique is difficult to collect. One of the limitations of this study is that we were not able to control or measure the insertion speed when using the manual or commercial tool technique.

No force sensor was mounted on the motorized insertion tool. Thus insertions with this tool were not force feedback controlled. Frictions of the array within the insertion tube of the commercial tool could impair surgeon's force feedback feeling. Thus, force feedback could only be perceived with the manual technique. This might account for the different basilar membrane perforation rates among the three techniques.

The new metrics that we have defined can help forces profiles analyses by giving absolute values such as the peak force or the forces momentum but also information on sudden forces changes or rises.

5. Conclusion and Perspectives

We have validated the use of metrics such as peak force, momentum of the force, threshold crossing over 0.1 N, sudden rises, and jerks that could be indicators of the quality of surgical gesture during cochlear implantation. The analysis of these metrics in insertion allows demonstrating that the Hifocus 1J electrode insertion with a commercial guided tool has less threshold crossing over 0.1 N and sudden rises compared to a manual insertion performed with forceps. These drawbacks are even more reduced with a motorized tool leading to a smoother insertion. Next step will be to introduce a force feedback control loop between the motorized tool and the force sensor in order to reduce the insertion peaks (in amplitude and in duration) and to stop the insertion in case of abnormal force sudden rise. If those parameters can be controlled, it should be possible to enhance the safety of cochlear implantation.

Conflict of Interests

The authors declare that there is no conflict of interests regarding the publication of this paper.

Acknowledgment

Authors would like to thank Advanced Bionics (Valencia, USA) for providing 1J Arrays, Hifocus 1J electrode insertion tools, and financial support to UMR-S 1159 for this study.

References

[1] B. S. Wilson and M. F. Dorman, "Cochlear implants: a remarkable past and a brilliant future," *Hearing Research*, vol. 242, no. 1-2, pp. 3–21, 2008.

[2] M. L. Carlson, C. L. Driscoll, R. H. Gifford et al., "Implications of minimizing trauma during conventional cochlear implantation," *Otology & Neurotology*, vol. 32, no. 6, pp. 962–968, 2011.

[3] M. E. Zernotti, A. Suárez, V. Slavutsky, L. Nicenboim, M. F. Di Gregorio, and J. A. Soto, "Comparison of complications by technique used in cochlear implants," *Acta Otorrinolaringologica Espanola*, vol. 63, no. 5, pp. 327–331, 2012.

[4] S. Havenith, M. J. W. Lammers, R. A. Tange et al., "Hearing preservation surgery: cochleostomy or round window approach? A systematic review," *Otology and Neurotology*, vol. 34, no. 4, pp. 667–674, 2013.

[5] Y. Nguyen, I. Mosnier, S. Borel et al., "Evolution of electrode array diameter for hearing preservation in cochlear implantation," *Acta Oto-Laryngologica*, vol. 133, no. 2, pp. 116–122, 2013.

[6] A. A. Eshraghi, N. W. Yang, and T. J. Balkany, "Comparative study of cochlear damage with three perimodiolar electrode designs," *Laryngoscope*, vol. 113, no. 3, pp. 415–419, 2003.

[7] Y. Nguyen, M. Miroir, G. Kazmitcheff et al., "Cochlear implant insertion forces in microdissected human cochlea to evaluate a prototype array," *Audiology and Neurotology*, vol. 17, no. 5, pp. 290–298, 2012.

[8] D. Schurzig, R. J. Webster, M. S. Dietrich, and R. F. Labadie, "Force of cochlear implant electrode insertion performed by a robotic insertion tool: comparison of traditional versus advance off-stylet techniques," *Otology & Neurotology*, vol. 31, no. 8, pp. 1207–1210, 2010.

[9] G. Kontorinis, T. Lenarz, T. Stöver, and G. Paasche, "Impact of the insertion speed of cochlear implant electrodes on the insertion forces," *Otology and Neurotology*, vol. 32, no. 4, pp. 565–570, 2011.

[10] G. Kontorinis, G. Paasche, T. Lenarz, and T. Stöver, "The effect of different lubricants on cochlear implant electrode insertion forces," *Otology and Neurotology*, vol. 32, no. 7, pp. 1050–1056, 2011.

[11] O. Majdani, D. Schurzig, A. Hussong et al., "Force measurement of insertion of cochlear implant electrode arrays in vitro: comparison of surgeon to automated insertion tool," *Acta Oto-Laryngologica*, vol. 130, no. 1, pp. 31–36, 2010.

[12] C. J. Coulson, P. S. Slack, and X. Ma, "The effect of supporting a surgeon's wrist on their hand tremor," *Microsurgery*, vol. 30, no. 7, pp. 565–568, 2010.

[13] D. Mürbe, K.-B. Hüttenbrink, T. Zahnert et al., "Tremor in otosurgery: influence of physical strain on hand steadiness," *Otology and Neurotology*, vol. 22, no. 5, pp. 672–677, 2001.

[14] M. Miroir, Y. Nguyen, G. Kazmitcheff, E. Ferrary, O. Sterkers, and A. B. Grayeli, "Friction force measurement during cochlear implant insertion: application to a force-controlled insertion tool design," *Otology and Neurotology*, vol. 33, no. 6, pp. 1092–1100, 2012.